

# **QCD at Hadron Colliders**

## **Introduction and Perspectives**

H. Jung 

April 4, 2024



# Contents

<b>1 Overview</b>	<b>7</b>
1.1 Introduction	7
<p>These notes aim to introduce the basic principles of Quantum Chromo Dynamics (QCD) in high energy particle colliders. The Monte Carlo technique is introduced to calculate integrals and to generate variables according to different distributions. The main focus will lie on collinear and Transverse Momentum Dependent (TMD) parton distribution functions and how they can be obtained from a solution of the evolution equations. Practical exercises based on jupyter-notebook after some chapters will lead finally to a simplified calculation of the transverse momentum spectrum of Z and Higgs - bosons. The discussion is completed with an extension of collinear and TMD parton density functions for all Standard Model fermions and bosons, including <math>\gamma</math> and W, Z bosons.</p>	
1.2 Science For Peace	7
1.3 Thanks	9
<b>2 Monte Carlo methods</b>	<b>11</b>
<p>The basics of pseudo random number generators and the Monte Carlo technique is described. The method can be used to generate random numbers according to different distributions. The Monte Carlo technique is essential for the calculation of complicated integrals. In the exercises the Monte Carlo technique is applied.</p>	
2.1 Random Numbers	11
2.2 Statistics and Probabilities	14
2.3 Random Numbers from arbitrary distributions	17
2.4 Law of Large Numbers and Central Limit Theorem	19
2.5 Monte Carlo Integration	20
2.6 Exercises: Monte Carlo technique	24
2.7 Exercise Solutions: Monte Carlo technique	25
2.7.1 Constructing a random number generator	25
2.7.2 Constructing a gauss random number generator, by adding several random numbers.	26
2.7.3 Testing Monte Carlo integration I	29
2.7.4 Testing Monte Carlo integration II	29
2.7.5 Testing Monte Carlo integration III.	30
<b>3 Probing the Structure of Matter</b>	<b>31</b>
<p>The Quark-Parton Model is introduced, together with order <math>\alpha_s</math> corrections</p>	
3.1 The Quark Parton Model	31
3.2 Cross Section in DIS	36
3.3 The photon-proton cross section	39

3.4	$\mathcal{O}(\alpha_s)$ contribution to DIS	40
3.4.1	QCDC process	41
3.4.2	BGF process	43
<b>4</b>	<b>Parton evolution equation</b>	<b>45</b>
The DGLAP evolution equation for parton densities is derived, and collinear factorization is introduced. Methods to solve the integer-differential evolution equation are discussed. The solution of the DGLAP equation with the Monte Carlo method is described.		
4.1	Conservation and Sum Rules	46
4.1.1	Flavor Conservation	47
4.1.2	Conservation Rules of Splitting Functions	49
4.2	Collinear factorization	50
4.2.1	Factorization Schemes	51
4.3	Solution of DGLAP equations	51
4.3.1	Double Leading Log approximation for small $x$	52
4.3.2	From evolution equation to parton branching	54
4.3.3	Ordering conditions	57
4.4	Solution of evolution equation with Monte Carlo method	61
4.5	Exercises: Parton Evolution	63
4.6	Exercise: Parton Evolution	64
4.6.1	Sudakov form factor and Monte Carlo integration.	64
4.7	Sudakov form factor and Monte Carlo integration.	64
4.7.1	Demonstration of the parton evolution using MC method	66
<b>5</b>	<b>The Parton Branching Method</b>	<b>71</b>
The Parton Branching Method allows to solve the DGLAP evolution equation for collinear parton densities but also to determine Transverse Momentum Dependent (TMD) parton densities. The derivation of the PB method is described and a comparison with standard solutions of the DGLAP equation are shown. The importance of soft gluons is discussed in terms of collinear as well as TMD distributions.		
5.1	The Parton Branching solution of the DGLAP equation	71
5.1.1	The Momentum Sum Rule and the Sudakov form factor	72
5.1.2	The limit $z_M$	73
5.2	Determination of Parton Densities using the Parton-Branching Method	75
5.2.1	Connection of parton density with Cross Section	76
<b>6</b>	<b>Transverse Momentum Dependent parton distributions</b>	<b>79</b>
Transverse Momentum Dependent (TMD) parton densities are introduced. Based on the Parton Branching method a simple approach to TMD parton densities is given. Methods for the calculation of TMD parton densities are described.		
6.1	Why are transverse momenta important for the evolution ?	79
6.2	Transverse Momentum Dependent parton densities: Parton Branching TMD	81
6.2.1	The PB-TMD evolution equation	82
<b>7</b>	<b>Drell-Yan production in Hadron-Hadron scattering</b>	<b>85</b>
7.1	Inclusive Drell-Yan production in $pp$	85
7.1.1	Factorization of production and decay in Drell Yan processes	88
7.1.2	Factorization of transverse momenta in Drell Yan processes	89
7.1.3	$\mathcal{O}(\alpha_s)$ contributions to Drell Yan production	90

7.2	The $p_t$ spectrum of Drell Yan production . . . . .	92
7.2.1	The DY cross section and PB TMD distributions . . . . .	95
7.3	Exercises: Boson Production . . . . .	97
7.4	Exercise: Boson Production - Solutions . . . . .	98
7.4.1	Calculate the x-section for $p p \rightarrow \text{Higgs} + X$ . . . . .	98
7.4.2	Calculation of the Higgs cross section using Monte Carlo integration. . . . .	102
<b>8</b>	<b>Generalization of Splitting Functions for all Standard Model particles</b>	<b>109</b>
<p>The evolution equations of QCD partons are extended to include all Standard Model constituents (bosons and fermions), including parton densities for the photon, the <math>W</math> and <math>Z</math> bosons as well as for the Higgs boson. The evolution equations are solved with the Parton Branching method, leading to a complete set of collinear and TMD parton distributions.</p>		
8.1	Extraction of General Splitting Functions . . . . .	109
8.2	Photon and Heavy Boson Parton Densities . . . . .	111
8.2.1	Photon densities . . . . .	111
8.2.2	Heavy Boson densities . . . . .	111
<b>A</b>	<b>Kinematics and Cross Section definition</b>	<b>115</b>
A.1	Four-Vector Kinematics . . . . .	115
A.2	Light Cone Variables . . . . .	116
A.3	Cross Section definition . . . . .	117
A.4	Kinematics for DIS and $pp$ . . . . .	118
A.4.1	$ep$ - case . . . . .	118
A.4.2	$pp$ - case . . . . .	118
A.5	Calculation of transverse momentum of Drell Yan pair . . . . .	119



# Chapter 1

## Overview

### 1.1 Introduction

The aim of the lecture series *QCD and Monte Carlo techniques* is to introduce the basic concepts of Quantum Chromodynamics (QCD) and how this can be used for comparison with measurements at past and present high energy particle colliders, HERA and the LHC. Since events produced at high energy collisions contain many particles, most of the calculations cannot be performed analytically. Even for the calculation of integrals, numerical methods have to be applied and for complicated multidimensional integrals the Monte Carlo method is best suited. While the basic concepts and methods did not change in the last few years, the experimental results and the interest to understand the measurements has changed: HERA and the LHC have provided a large number of measurements and challenge the theoretical predictions. Calculations at higher order in the expansion of the strong coupling  $\alpha_s$  were needed and new methods to perform calculations were developed.

In recent years, with the development of the *Parton Branching Method*, a direct correspondence of the solution of the evolution equations, parton density functions and their extension to include transverse momentum effects (TMDs) was established. In many measurements obtained from LHC experiments, but also for studies foreseen at future colliders at the EIC, fixed order calculations are found to be not sufficient and a resummation to all orders is needed. Some of the measurements at the LHC which are of particular interest for QCD studies will be discussed.

A warning is needed here: although the lecture will cover Monte Carlo methods, it will not be a description how to run a given Monte Carlo event generator, nor it will describe the detailed implementation of QCD processes in Monte Carlo generators. The lectures will provide the basics to understand the principles of Monte Carlo event simulation and basic QCD calculations.

### 1.2 Science For Peace

In the aftermath of World War II, nations came together and formed the United Nations (UN) with the purpose, as stated in the first article of the UN charter [1], "... to take effective collective measures for the prevention and removal of threats to the peace". With more than 100 ongoing wars and military conflicts, we are further away than ever from this ideal.

In a similar spirit as the UN, CERN was founded in 1954 to bring nations together through peaceful scientific collaboration. Remarkably, just one year after its foundation, cooperation between CERN and Soviet scientists began via the Joint Institute for Nuclear Research in Dubna [2]. In

2014, on the occasion of CERN's 60th anniversary, the then Director-General Rolf Heuer wrote that "CERN has more than fulfilled the hopes and dreams of advancing science for peace". One of CERN's missions is *Science for Peace* [3].

A very nice example of the Science4Peace idea is the transformation of military equipment for the use in a particle collider, here the CMS Hadronic Calorimeter (HCAL). In the CMS book it is written [4]: *In Russian military storage there were thousands of shells made of brass that would fit such stringent requirements – all 50 years old, made by the Navy and designed to stand internal high stress and sea storage aboard a 1940s Navy Vessel. The shells could be melted for use in the HCAL. The first hurdle involved obtaining permission of the Commander of the Navy, never easy, but who in fact agreed fairly quickly. Fifteen navy arsenals began recycling their shells, many being off-loaded from battleships in Murmansk to begin their new scientific life as absorber plates within CMS.*



Figure 1.1: Using Russian navy shells (from [4]).

*First the shells were sent to a plant in the North of Russia to be disarmed of their explosive contents. The shell casings were then stored at JSC Krasnyj Vyborzhets in St. Petersburg before being melted down and rolled into plates, a difficult process given that the brass was already semi-processed.*

*Over a million World War II brass shell casings were melted down to make the detector components. But when even this fell short of the massive 600 tonnes of brass needed to make the endcaps, the US agreed to provide a further 1 million in copper (brass being an alloy of copper and zinc) to complete the endcaps. As an example of the international cooperation and mutual trust fostered through this work, even this deal was agreed to on an amicable "handshake" basis.*

*In Minsk, Belarus, the brass was machined into absorber plates and finally pre assembled into parts of the endcaps, weighing 300 tonnes each, before being sent to CERN. Dollezhal Research and Development Institute of Power Engineering (NIKIET) coordinated the efforts of the Northern Navy and the companies involved, and ran 1400 tests to ensure the material was of high quality and suitable for constructing the endcap HCALs. The shells and additional copper became a total of 1296 brass pieces, which were delivered to CERN in 2002 and 2003 and have since been installed and tested within CMS. This project was part of an international agreement to convert Russian military industry into peaceful technology. The recycling of stocks of ship artillery into materials for fundamental research was also symbolic; instead of being used to destroy, the weapons could actively benefit humankind through their contribution to enhanced knowledge and technology.*

In an article to the CERN courier in 2022 [5] H. Schopper (director of CERN from 1981 to 1988) argued very clearly and strongly for the Science4Peace idea.

Limiting international scientific collaboration is against the advancement of knowledge, which is not just a global public good but a powerful instrument for intercultural dialogue and peace – especially during times of crisis [6–8].



## 1.3 Thanks

These lecture notes developed over the years, starting with lectures on *QCD and collider physics* at the University of Hamburg in 2005-2007 over lectures on *QCD and Monte Carlo* from 2008 - 2015 in Antwerp to block-courses at the University of Aachen in 2022 and 2024.

Especially the exercises developed from plain C-based exercises with the need to link to ROOT [9] to jupyter-notebook exercises which only need small extensions like *numpy* and *matlab*. The exercises were significantly improved by contributions from S. Taheri Monfared, P.L.S Connor and R. Zlebcik.



## Chapter 2

# Monte Carlo methods

The general case of a process  $A + B \rightarrow$  anything to be calculated is given in fig. 2.1. A more detailed figure of the process to be studied is shown in fig 2.2, where on the left side is shown the lowest order process for jet production in hadron hadron collisions and on the right side the process is shown including multiparton radiation, which is the subject of this lecture.

It becomes clear, that with many partons<sup>1</sup> involved in the calculation this cannot be done analytically, and numerical methods are needed, one of them is the Monte Carlo method.

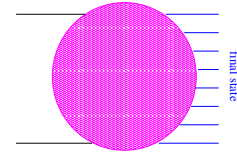


Figure 2.1: General case of scattering  $A + B \rightarrow$  anything

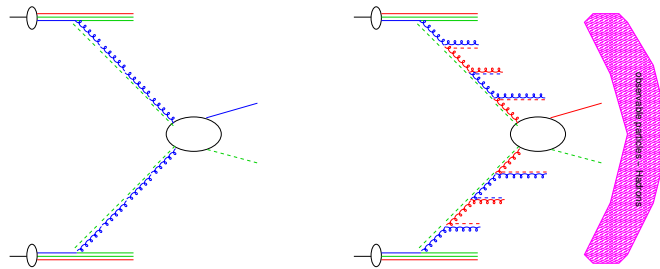


Figure 2.2: Left: lowest order process for jet production in hadron hadron collisions. Right: Process for jet production including multiparton radiation and hadronization

## 2.1 Random Numbers

Monte Carlo method refers to any procedure, which makes use of random numbers and uses probability statistics to solve the problem<sup>2</sup>. The Monte Carlo method was invented and developed in the 1930's for the calculation of nuclear decays, but nowadays it is widely used in any calculation of complicated processes for the simulation of natural phenomena, simulation of the experimental

<sup>1</sup>Partons are used as a generic name for quarks and gluons

<sup>2</sup>The name comes from a saga, that the first true random numbers were obtained by recording the results of the roulette game in the casino of Monte Carlo.

apparatus, simulation of the underlying physics process but also in economy for risk analysis etc. Even more, the Monte Carlo method is a precise method for the calculation of integrals, and it is applied in all calculations of cross sections nowadays. The Monte Carlo method is a mathematically precise method for estimating integrals. The basic theorems are the *central limit theorem* and the *limit of large numbers* which guarantees that a Monte Carlo estimate of an integral converges to the true value of the integral.

Monte Carlo methods make use of random numbers. An example of a random number is 3 or 4. There is nothing like a *random number*. Any number can appear to be random. Only if we have a sequence of numbers, where each number has nothing to do with the other numbers in the series, we can say the numbers appear to be random.

In the following we consider random numbers always only in the interval  $[0, 1]$ . In a uniform distribution of random numbers in this interval  $[0, 1]$  all numbers have the same chance to appear, note that 0.00000034 has the same chance to appear as 0.5.

Random numbers can be obtained by several methods:

- using a truly chaotic system like roulette, lotto or 6-49
- using a process which is inherently random
- generating "random numbers" on a computer

Examples for random numbers obtained from chaotic processes are using atmospheric noise [10] or using quantum physics which is intrinsically random [11].

Random numbers generated on a computer are never really random, since they always are determined according to some algorithm [12]. They may appear random to someone, who does not know the algorithm. The randomness of random numbers can be checked by several tests, which will be discussed later. Random numbers, which are generated on a computer are called *pseudo-random numbers*. In contrast, *quasi-random numbers* are random numbers which are by intention not random but are designed to be as uniform as possible in order to minimize the uncertainties in integration procedures.

A simple random number generator (so called *multiplicative congruential linear random number generator*) can be built as follows [13][p 40ff] and [14][Vol II,p 9]. From an initial number  $I_0$  we generate a series of random numbers  $R_j$  according to:

$$\begin{aligned} I_j &= \text{mod}(aI_{j-1} + c, m) \\ R_j &= \frac{I_j}{m} \end{aligned} \tag{2.1}$$

with  $a$  being an multiplicative and  $c$  a additive constant and  $m$  the modulus<sup>3</sup>. With this procedure one obtains a series of number  $R_j$  in the interval  $(0, 1)$  (note that the values 0 and 1 are excluded). This random number generator will be tested in the exercise. In fig 2.3 the correlation of 2 random numbers is shown on the left side. The right side shows the same correlation for another random number generator RANLUX [15–17], which will be used later in the calculations. It is obvious, that the *multiplicative congruential linear random number generator* produces random numbers, which show correlations and does therefore not satisfy quality criteria for a good random number generator; the RANLUX generator seems to be better. Similar distributions are obtained

<sup>3</sup>the modulus function is defined as  $\text{mod}(i_1, i_2) = i_1 - \text{INT}(i_1/i_2) \cdot i_2$

with the PCG random number generator [18], which is a sophisticated congruential generator. This generator is available in python numpy.

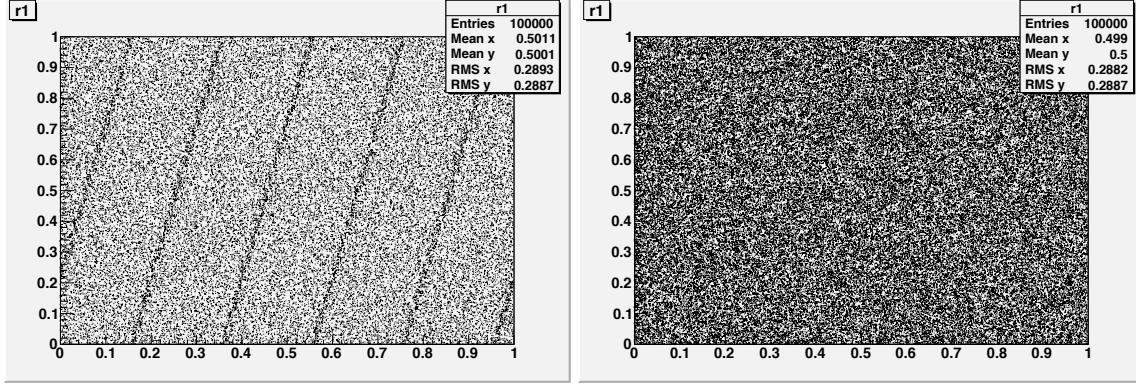


Figure 2.3: Left: correlation of two successive random numbers obtained according to 2.1. Right: correlation of two random numbers obtained with RANLUX [17]

Several criteria on the randomness of a series of *pseudo random numbers* can be applied to test the quality of the random number generator [14][Vol II,p 59]:

- **statistical test** (test uniformity of distributions, frequency test, equi-distribution test)  
Divide the interval  $(0, 1)$  into  $k$ -subintervals with length  $1/k$ . Count how many random numbers fall into the  $k$ 's interval [19]. Calculate:

$$\chi^2 = \sum_{i=1}^k \frac{(N_i - N/k)^2}{N/k} \quad (2.2)$$

with  $N$  random numbers  $R_i$ . If the random numbers are uniformly distributed, then Eq. 2.2 is a  $\chi^2$  distribution with  $k - 1$  degrees of freedom and should give  $\chi^2/(ndf) \sim 1$ , with  $ndf$  being the number of degrees of freedom.

- **serial test** (pairs of successive random numbers should be distributed in an independent way (see fig. 2.3)). *The sun comes up just about as often as it goes down, in the long run, but this does not make its motion random* [14][Vol II,p 60].  
Count pairs of random numbers  $(Y_{2j}, Y_{2j+1}) = (q, r)$  for any  $0 \leq j \leq n$  and apply a  $\chi^2$  test as above.
- **sequence up-down test**  
Count the number of runs, where the random numbers are increasing  $Y_{j+1} > Y_j$ . Example: take the sequence 1298536704 and insert vertical lines for  $Y_{j+1} > Y_j$ , resulting in |129|8|5|367|0|4|. Count the number of runs-up with length  $k$ . The number of runs-up and the number of runs-down should be similar, but they should not be adjacent: often a long run will be followed by a short one.
- **gap test**  
Choose two numbers  $\alpha, \beta$  with  $0 \leq \alpha < \beta \leq 1$ . Generate  $r + 1$  random numbers. The probability that the first  $r$  random numbers are outside  $(\alpha, \beta)$  is  $P_r = p(1-p)^r$  with  $p = \beta - \alpha$  being the probability for the  $r + 1$  event to be inside  $(\alpha, \beta)$ .
- **Random walk test**  
Choose  $0 \leq \alpha \leq 1$  and generate a large number of random variables  $R_i$ . Count how often

$R_i < \alpha$  and call it  $r$ . We expect a binominal distribution for  $r$  with  $p = \alpha$ . The same test can be performed for  $R_i > (1 - \alpha)$ .

Practical criteria for random numbers can be formulated as follows [12]:

- **Long period**
- **Repeatability**  
for testing and development one needs to repeat calculations. Repeatability also allows to repeat only part of the job, without re-doing the whole.
- **Long disjoint sequences**  
for long procedures one needs to be able to perform independent sub-calculations which can be added later.
- **Portability**  
not only the code should be portable but also the results should be the same, independent on which platform the calculations are done.
- **Efficiency**  
generation of random numbers should be fast.

To test a random number generator, a series of tests have to be performed. Even if a Random Number generator passes all  $n$ -tests, one cannot assume that it also passes the  $n + 1$ -test.

## 2.2 Statistics and Probabilities

A very good overview on statistics and probabilities is given in [13, 20], which was used for the discussion in this chapter. In an experiment where the outcome depends on a single variable  $x$  one can ask what is the probability to find values of  $x$  in the interval  $[x, x + dx]$ . This is given by  $f(x)dx$  with  $f(x)$  being the probability density function *p.d.f* (not to be confused with the pdf which is used for the parton density function to be discussed later). Since we assume, there is an experiment with some outcome, the probability to find  $x$  anywhere must be unity, that is:

$$\int_{-\infty}^{\infty} f(x)dx = 1 \quad (2.3)$$

The *p.d.f* has to satisfy in addition:

$$f(\infty) = f(-\infty) = 0 \quad (2.4)$$

The expectation value (mean values or average value) of a function  $h(x)$  is defined as:

$$E[h] = \int_{-\infty}^{+\infty} h(x)f(x)dx = \int h(x)dG(x) = \frac{1}{b-a} \int h(x)dx \quad (2.5)$$

with  $f(x)$  being the probability density function. In the right part of the equation we used the special case  $dG(x) = dx/(b - a)$  for a uniform distribution. In case of discrete distributions we have:

$$E[h] = \sum_i^{\infty} h(x_i)f(x_i) \quad (2.6)$$

A special case is the expectation value of  $x$  (or the mean on the distribution)

$$E[x] = \int_{-\infty}^{+\infty} f(x)x dx \stackrel{\text{def}}{=} \langle x \rangle \quad (2.7)$$

From the definition of the expectation value we see that  $E[h]$  is a **linear operator**:

$$\begin{aligned} E[cg(x) + h(x)] &= \int (cg(x) + h(x)) f(x) dx \\ &= c \int g(x) dx + \int h(x) f(x) dx \\ &= cE[g] + E[h] \end{aligned} \quad (2.8)$$

with  $c$  being a constant. Similarly we can see that the expectation value of the expectation value  $E[E[g]]$  is simply  $E[g]$ :

$$\begin{aligned} E[E[g(x)]] &= \int \left( \int g(x) f(x) dx \right) f(x') dx' \\ &= E[g(x)] \int f(x') dx' \\ &= E[g(x)] \end{aligned} \quad (2.9)$$

because  $\int f(x') dx' = 1$  by definition of the *p.d.f*

The variance  $\sigma^2$  measures the spread of a distribution and can be defined as the mean quadratic deviation from the mean value. The square-root of  $\sigma^2$  is also called the *standard deviation*. The variance  $V[h]$  is defined as:

$$V[h] = \sigma^2 = E[(h(x) - E[h(x)])^2] = \int (h(x) - E[h(x)])^2 f(x) dx \quad (2.10)$$

From the definition, the variance  $V[cg(x) + h(x)]$  can be calculated:

$$\begin{aligned} V[cg(x) + h(x)] &= \int (cg(x) + h(x) - E[cg(x) + h(x)])^2 f(x) dx \\ &= \int (cg(x) + h(x) - cE[g(x)] - E[h(x)])^2 f(x) dx \\ &= \int ((c(g - E[g]) + (h - E[h]))^2 f(x) dx \\ &= \int (c^2(g - E[g])^2 + 2c(g - E[g])(h - E[h]) + (h - E[h])^2) f(x) dx \\ &= c^2V[g] + 2cE[(g - E[g])(h - E[h])] + V[h] \\ &= c^2V[g] + V[h] + 2cE[g \cdot h - gE[h] - hE[g] + E[g]E[h]] \\ &= c^2V[g] + V[h] + 2c(E[g \cdot h] - E[g]E[h] - E[h]E[g] + E[g]E[h]) \\ V[cg(x) + h(x)] &= c^2V[g] + V[h] + 2c(E[g \cdot h] - E[g]E[h]) \end{aligned} \quad (2.11)$$

In the case that  $g(x)$  and  $h(x)$  are uncorrelated, we have  $E[g \cdot h] = E[g]E[h]$  and the expression simplifies to:

$$V[cg(x) + h(x)] = c^2V[g] + V[h] \quad (2.12)$$

A special case is the variance of  $x$ :

$$\begin{aligned}
 V[x] &= E((x - \langle x \rangle)^2) = \int (x - E[x])^2 f(x) dx \\
 &= E[x^2 - 2x\langle x \rangle + \langle x \rangle^2] \\
 &= E[x^2] - 2E[x]\langle x \rangle + \langle x \rangle^2 \\
 V[x] &= E[x^2] - \langle x \rangle^2 \\
 V[x] &= E[x^2] - E[x]^2
 \end{aligned} \tag{2.13}$$

where the relation  $E[x] = \langle x \rangle$  has been applied.

Consider independent random numbers  $x_1$  and  $x_2$  with variances  $V[x_1] = \sigma_1^2$  and  $V[x_2] = \sigma_2^2$  and mean values  $\mu_1$  and  $\mu_2$ . The expectation value of the sum of  $x_1$  and  $x_2$  is:

$$\begin{aligned}
 E[x_1 + x_2] &= E[x_1] + E[x_2] \\
 &= \mu_1 + \mu_2
 \end{aligned} \tag{2.14}$$

The variance of the sum is (using  $x = x_1 + x_2$ ):

$$\begin{aligned}
 \sigma^2 &= \langle (x - \langle x \rangle)^2 \rangle \\
 &= E[(x - \langle x \rangle)^2] \\
 &= E[(x - \mu_1 - \mu_2)^2] \\
 &= E[(x - \mu_1 + x_2 - \mu_2)^2] \\
 &= E[\underbrace{(x_1 - \mu_1)^2}_{\sigma_1^2} + 2\underbrace{(x_1 - \mu_1)(x_2 - \mu_2)}_0 + \underbrace{(x_2 - \mu_2)^2}_{\sigma_2^2}] \\
 \sigma^2 &= \sigma_1^2 + \sigma_2^2
 \end{aligned} \tag{2.15}$$

because  $E[x_1] = \mu_1$ , since  $x_1$  and  $x_2$  are independent. The general form is then:

$$\sigma^2 = \sum_{i=1}^N \sigma_i^2 \tag{2.16}$$

Consider now a sample of  $x_i$  where all  $x_i$  follow the same probability density function  $f(x)$ , having the same variance  $\sigma^2$  and the same  $\mu$ . The mean of the sample is defined as:

$$\bar{x} = \frac{1}{N} \sum_{i=1}^N x_i \tag{2.17}$$

The expectation value  $E[\bar{x}]$  is given by:

$$\begin{aligned}
 E[\bar{x}] &= E\left[\frac{1}{N} \sum_{i=1}^N x_i\right] \\
 &= \frac{1}{N} E\left[\sum_{i=1}^N x_i\right] \\
 &= \frac{1}{N} N E[x_i] \\
 E[\bar{x}] &= E[x] = \langle x \rangle
 \end{aligned} \tag{2.18}$$



resulting in the expectation value of the mean being the mean itself. To obtain above, the features of the linearity of the operator are applied.

The variance of the mean is:

$$\begin{aligned}
 V[\bar{x}] &= V\left[\frac{1}{N} \sum_{i=1}^N x_i\right] \\
 &= \frac{1}{N^2} V\left[\sum x_i\right] \\
 &= \frac{1}{N^2} \sum \sigma_i^2 \\
 &= \frac{1}{N^2} N \sigma^2 \\
 V[\bar{x}] &= \frac{1}{N} \sigma^2
 \end{aligned} \tag{2.19}$$

or in the familiar form as the standard deviation of the mean:

$$\sigma_N = \frac{\sigma}{\sqrt{N}} \tag{2.20}$$

## 2.3 Random Numbers from arbitrary distributions

Given a sequence of random numbers uniformly distributed in  $[0, 1]$  the next step is to determine a sequence of random numbers  $x_1, x_2 \dots$  distributed according to a probability density function *p.d.f.*

The task is to find a suitable function  $x(r)$  which gives the same sequence of random numbers when evaluated with uniformly distributed values  $r$ .

The probability to obtain a value  $r$  in the interval  $[r, r + dr]$  is  $u(r)dr$  and this should be equal to the probability to find  $x$  in  $[x, x + dx]$  which is  $f(x)dx$  (see fig 2.4):

$$\begin{aligned}
 u(r')dr' &= f(x')dx' \\
 \int_{-\infty}^r u(r')dr' &= \int_{-\infty}^x f(x')dx'
 \end{aligned} \tag{2.21}$$

Using a random number  $R$  uniform in  $[0, 1]$  with  $R = \int_{-\infty}^r u(r')dr'$  we obtain:

$$R = \int_{-\infty}^x f(x')dx' = F(x)$$

with  $f(x) = \frac{dF(x)}{dx}$  being the probability density function *p.d.f.* (as defined before) with:

$$\begin{aligned}
 \int_{-\infty}^{\infty} f(x)dx &= 1 \\
 f(\infty) &= f(-\infty) = 0
 \end{aligned}$$

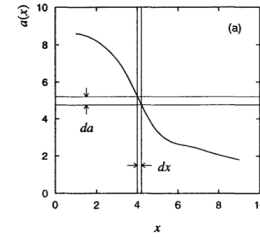


Figure 2.4: Illustration of  $a(r)dr = f(x)dx$ . Picture from [13] [p14]

Examples (assuming we have random numbers  $R_j$  uniformly distributed in  $[0, 1]$ ):

- **linear p.d.f:**  $f(x) = 2x$ .

The primitive function  $F(x)$  is:

$$\begin{aligned} F(x) &= \int_0^x f(t)dt = \int_0^x 2t dt = x^2 \\ R &= F(x) = x^2 \\ x_j &= \sqrt{R_j} \end{aligned}$$

For any uniformly distributed random numbers  $R_j$ , the  $x_j$  values are distributed according to the function  $f(x) = 2x$ , when calculated as  $x_j = \sqrt{R_j}$

- **exponential p.d.f:**  $f(x, \lambda) = \lambda \exp(-\lambda x)$ .

The primitive function  $F(x)$  is:

$$\begin{aligned} F(x) &= \int_0^x f(t)dt = \int_0^x \lambda e^{(-\lambda t)} dt = \lambda \left. \frac{-1}{\lambda} e^{(-\lambda t)} \right|_0^x \\ &= 1 - e^{-\lambda x} \\ -R + 1 &= e^{-\lambda x} \\ \log(1 - R) &= -\lambda x \\ x_j &= \frac{-1}{\lambda} \log(R_j) \end{aligned}$$

The values  $x_j$  can be generated from a uniform distribution of random numbers  $R_j$  with  $x_j = \frac{-1}{\lambda} \log(1 - R_j) = \frac{-1}{\lambda} \log(R_j)$  since for a uniform distribution the probability of occurrence of  $1 - R_j$  is the same as for  $R_j$

- **p.d.f:**  $f'(x) = 1/x$  in the range  $[x_{min}, x_{max}]$

The normalization integral is:

$$\int_{x_{min}}^{x_{max}} \frac{1}{t} dt = \log \frac{x_{max}}{x_{min}} \quad (2.22)$$

Since this function  $f'(x)$  is not normalized to unity, the normalization factor has to be included:

$$f(x) = \frac{f'(x)}{\log \frac{x_{max}}{x_{min}}} = \frac{1}{x} \frac{1}{\log \frac{x_{max}}{x_{min}}} \quad (2.23)$$

The primitive function  $F(x)$  is then:

$$\begin{aligned} F(x) &= \int_{x_{min}}^x f(t)dt \\ &= \frac{1}{\log \frac{x_{max}}{x_{min}}} \int_{x_{min}}^x \frac{1}{t} dt = \frac{1}{\log \frac{x_{max}}{x_{min}}} \log \frac{x}{x_{min}} \\ R &= \frac{\log \frac{x}{x_{min}}}{\log \frac{x_{max}}{x_{min}}} \\ \log \left( \frac{x_{max}}{x_{min}} \right)^R &= \log \left( \frac{x}{x_{min}} \right) \end{aligned} \quad (2.24)$$

The values  $x_j$  can be generated from a uniform distribution of random numbers  $R_j$  with  $x_j = x_{min} \left( \frac{x_{max}}{x_{min}} \right)^{R_j}$ .

- **brute force or hit and miss method:**

If there is no easy way to find an analytically integrable function, which can be inverted, one can use the *hit-and-miss* method. Assume we want to generate random numbers according to a function  $f(x)$  in the interval  $[a, b]$ . The procedure is then the following: determine the maximum value, the function  $f(x)$  can reach in  $[a, b]$ , which is  $f_{max}$ . Then select  $x_i$  uniformly in the range  $[a, b]$  with  $x_i = a + (b - a)R_i$  with  $R_i$  in  $(0, 1)$ . Use another random variable  $R_j$  also in  $(0, 1)$ . Decide according to the following, if the pair  $R_i, R_j$  of random numbers is accepted or rejected.

$$\begin{aligned} \text{if } f(x_i) < R_j \cdot f_{max} &\rightsquigarrow \text{ reject} \\ \text{if } f(x_i) > R_j \cdot f_{max} &\rightsquigarrow \text{ accept} \end{aligned}$$

The accepted random numbers  $x_i$  follow then exactly the distribution of the function  $f(x)$ . The only disadvantage of this method is, that depending on the function  $f(x)$ , it can be rather inefficient.

- **improvements of the *hit and miss method*.**

Find a function  $g(x)$  which is similar to  $f(x)$  but which is integrable and invertible, i.e.  $G(x) = \int g(x)dx$  and  $G^{-1}(x)$  must exist. Then choose a constant such that always  $c \cdot g(x) > f(x)$  for all  $x$ . Generate  $x$  according to the function  $g(x)$  with the methods described above. Generate another random variable  $R_j$  and apply the *hit and miss method* as above:

$$\begin{aligned} \text{if } f(x_i) < R_j \cdot c \cdot g(x) &\rightsquigarrow \text{ reject} \\ \text{if } f(x_i) > R_j \cdot c \cdot g(x) &\rightsquigarrow \text{ accept} \end{aligned}$$

The accepted distribution of variables  $x_i$  will follow the original function  $f(x)$ .

## 2.4 Law of Large Numbers and Central Limit Theorem

The law of large numbers is fundamental for all the considerations above [13,20,21]. The law says, that for uniformly distributed random values  $u_i$  in the interval  $[a, b]$ , the sum of the probability density functions converges to the true estimate of the mean of the function  $f(x)$ :

$$\frac{1}{N} \sum_{i=1}^N f(u_i) \rightsquigarrow \frac{1}{b-a} \int_a^b f(u) du \quad (2.25)$$

The law of large numbers has been applied in the sections before implicitly. The function  $f(x)$  must satisfy certain conditions: it must be integrable, and it must be finite in the whole range of  $[a, b]$ . The left hand side of eq.(2.25) is a Monte Carlo estimate of the integral on the right hand side and the law of large numbers says that the Monte Carlo estimate of the integral is a consistent estimate of the true integral as the size of the random sample becomes large. At this stage, nothing is said, how large "large" has to be.

The law of large numbers tells that for infinitely large numbers the Monte Carlo estimate of the integral converges to the true estimate of the integral. The Central Limit Theorem tells us how the convergence goes for finite number of  $N$ . The Central Limit Theorem says that the sum of a large number of random variables follows a normal distribution (i.e. the sum of random variables is Gauss distributed), no matter according from which *p.d.f* the individual random variables were generated, only the number  $N$  must be large enough and the random variables must have finite

expectation values and variances. An example of the application of the Central Limit Theorem is the construction of a Random Number generator for Gaussian distributed random numbers, which will be done in the exercises:

- take a sum of uniformly distributed random numbers  $R_i$ :

$$R_n = \sum_{i=1}^n R_i$$

The expectation value and the variance are calculated according to the rules in eq.(2.8,2.11):

$$\begin{aligned} E[R_1] &= \int u du = \frac{1}{2} \\ V[R_1] &= \int \left(u - \frac{1}{2}\right)^2 du = \frac{1}{12} \\ E[R_n] &= \frac{n}{2} \\ V[R_n] &= \frac{n}{12} \end{aligned}$$

According to the Central Limit Theorem the sum of random values is Gauss distributed. To obtain a distribution centered around 0 with  $\sigma = 1$  we take:

$$\frac{\sum_i x_i - \sum_i \mu_i}{\sqrt{\sum_i \sigma_i^2}} \rightarrow \mathcal{N}(0, 1)$$

For example, if we sum  $n = 12$  random numbers (many times  $N \rightarrow \infty$ ), we obtain a "normal" (Gauss) distribution  $\mathcal{N}$  [21]:

$$\mathcal{N}(0, 1) \rightarrow \frac{R_n - n/2}{\sqrt{n/12}} = R_{12} - 6$$

## 2.5 Monte Carlo Integration

Already in the previous sections we had to deal with the problem to obtain a reliable estimate of the true value of an integral [19]:

$$I = \int_a^b f(x) dx$$

The integral  $I$  is directly connected to the expectation value of the function  $f(x)$  with the  $x$  values distributed according to a probability density function  $g(x)$ .

$$E[f] = \int_{-\infty}^{\infty} f(x) g(x) dx$$

where the *p.d.f.*  $g(x)$  must be defined such, that it vanishes outside the range of  $(a, b)$ . In the case of uniformly distributed  $x$  this reduces to  $g(x) = 1/(b - a)$  for  $a < x < b$  (and  $g(x) = 0$  otherwise) which gives:

$$E[f] = \int_{-\infty}^{\infty} f(x) g(x) dx = \frac{1}{b - a} \int_a^b f(x) dx$$

The Monte Carlo estimate of the integral is then:

$$I \approx I_{MC} = (b - a) \frac{1}{N} \sum_{i=1}^N f(x_i) \quad (2.26)$$

and the variance is:

$$V[I_{MC}] = \sigma_I^2 = V \left[ (b - a) \frac{1}{N} \sum_{i=1}^N f(x_i) \right] \quad (2.27)$$

$$= \frac{(b - a)^2}{N^2} V \left[ \sum_{i=1}^N f(x_i) \right] \quad (2.28)$$

$$= \frac{(b - a)^2}{N} V[f] \quad (2.29)$$

The variance depends on the number of times the integrand is evaluated, but also on the variance of  $f$ :  $V[f]$ .

Applying the definition of the variance eq.(2.11), the variance  $V[f]$  becomes (with  $\bar{f} = \int f dx = 1/N \sum f_i$  and assuming  $g(x)$  being uniform):

$$V[f] = \int (f - \bar{f})^2 g dx = \int (f^2 - 2f\bar{f} + \bar{f}^2) g dx \quad (2.30)$$

$$= \int f^2 g dx - \bar{f}^2 \quad (2.31)$$

$$= \sum \frac{f_i^2}{N} - \left( \frac{\sum f_i}{N} \right)^2 \quad (2.32)$$

$$(2.33)$$

Then the  $V[I]$  becomes:

$$V[I] = \frac{1}{N} (b - a)^2 \left( \frac{1}{N} \sum f_i^2 - \left( \frac{\sum f_i}{N} \right)^2 \right)$$

With this we can estimate the uncertainty of a Monte Carlo integration (use this in the exercises).

The Monte Carlo integration gives a probabilistic uncertainty band: we can only give a probability that the MC estimate lies within a certain range of the true values [12].

To further improve the accuracy of the Monte Carlo integration, several approaches exist:

- **importance sampling**

If an approximate function  $g(x)$  exists then the integral  $I$  can be estimated to:

$$\begin{aligned} I = \int_a^b f(x) dx &= \int_a^b \frac{f(x)}{g(x)} g(x) dx \\ &= \int h(x) g(x) dx \\ &= E \left[ \frac{f(x)}{g(x)} \right] \end{aligned}$$

provided  $g(x)$  is normalized and integrable in  $[a, b]$ . Thus the integration reduces to calculating the expectation value of  $E[f/g]$ , if the values of  $x$  are distributed according the *p.d.f*  $g(x)$ . The values of  $x$  can be generated according to the methods discussed in the previous sections and we obtain:

$$I = \frac{1}{N} \sum \frac{f(x_i)}{g(x_i)} \quad (2.34)$$

We assume that  $g(x)$  is a *p.d.f* normalized to 1 in the integration range. For example using  $g(x) = (1/x)1/\log\left(\frac{x_{max}}{x_{min}}\right)$  (see eq.(2.23)) gives then:

$$I = \frac{\log\left(\frac{x_{max}}{x_{min}}\right)}{N} \sum \frac{f(x_i)}{\frac{1}{x_i}}. \quad (2.35)$$

The variance is then given by:

$$V\left[\frac{f(x)}{g(x)}\right] = E\left[\left(\frac{f(x)}{g(x)} - E\left[\frac{f(x)}{g(x)}\right]\right)^2\right] \quad (2.36)$$

A danger in this method is when  $g(x)$  becomes zero or approaches zero quickly [12].

- **subtraction method (control variates)** [12]

Find a function  $g(x)$  which is close to the true function  $f(x)$ :

$$\int_a^b f(x)dx = \int_a^b g(x)dx + \int_a^b (f(x) - g(x)) dx$$

This method also reduces the variances and is especially successful if the function  $f(x)$  has a divergent part. This method is often used in next-to-leading order (NLO) QCD calculations.

- **stratified sampling**

divide the integration region into subintervals:

$$\int_a^b f(x)dx = \int_a^c f(x)dx + \int_c^b f(x)dx \quad (2.37)$$

Then the integral is:

$$I = \frac{c-a}{n/2} \sum_1 f_i + \frac{b-c}{n/2} \sum_2 f_i \quad (2.38)$$

with the variance (if we take  $c-a = b-c = (a-b)/2$ ):

$$\begin{aligned} V[I] &= V[I_1] + V[I_2] \\ &= \frac{(b-a)^2}{N} \left( \frac{\sum_1 f_i^2}{N} + \frac{\sum_2 f_i^2}{N} - 2 \left[ \left( \frac{\sum_1 f_i}{N} \right)^2 + \left( \frac{\sum_2 f_i}{N} \right)^2 \right] \right) \end{aligned}$$

We obtain a smaller variance, since the fluctuations in each interval are smaller.

- **brute force method**

The accept-reject method also works for MC integration. Defining  $I_0$  as the area in  $[a, b]$  and  $f_{max}$  as the maximum of the function  $f(x)$  in this range. With a random number  $R_i$  we

generate  $x_i$  and another random number  $R_j$  is used to accept or reject the pair of random numbers  $i, j$  according to:

$$\begin{aligned} \text{if } f(x_i) < R_j \cdot f_{max} &\leadsto \text{reject} \\ \text{if } f(x_i) > R_j \cdot f_{max} &\leadsto \text{accept} \end{aligned}$$

We count the number of trails with  $N_0$  and the number of accepted events with  $N$ . Then we obtain:

$$\begin{aligned} I &= \int_a^b f(x) dx \\ &= I_0 \frac{N}{N_0} \end{aligned}$$

The variance  $V[r] = (\delta(N))^2 = \sigma^2$  is (using binomial statistics with  $V[r] = N_0\epsilon(1 - \epsilon)$  with  $\epsilon = N/N_0$ ):

$$V[r] = N(1 - \epsilon)$$

With this we can calculate the uncertainty of the integral estimate  $\delta(I)$  as:

$$\frac{\delta I}{I} = \frac{I_0 \sigma / N_0}{I_0 N / N_0} = \sqrt{\frac{N(1 - \epsilon)}{N^2}} = \sqrt{\frac{(1 - \epsilon)}{N}}$$

## 2.6 Exercises: Monte Carlo technique

1. construct a uniform random number generator from the congruential method:

$$I_{i+1} = \text{mod}(a \cdot I_i + c, m)$$

$$R_{i+1} = \frac{I_{i+1}}{m}$$

with  $I_0 = 4711$ ,  $a = 205$ ,  $c = 29573$  and  $m = 139968$

Compare the correlation of 2 random numbers. Compare this with RANDOM.

2. construct a Gaussian random number generator from a uniform random number generator
3. write a small program that integrates (with Monte Carlo method) the function  $f(x) = 3x^2$  for  $\int_0^1 f(x)dx$ , and calculate the uncertainty.
4. write a small program that integrates (with Monte Carlo method)  $\int_0^1 \int_0^x dx dy$  with  $0 < x, y < 1$ .
5. write a small program to integrate a simple function in one dimension:  $\int_{x_{min}}^1 g(x)dx = \int_{x_{min}}^1 (1-x)^5 \frac{dx}{x}$ , using Monte Carlo integration, with  $x_{min} = 0.0001$   
Improve the above integration by using importance sampling.



## 2.7 Exercise Solutions: Monte Carlo technique

### 2.7.1 Constructing a random number generator

```
[1]: import numpy as np
import matplotlib.pyplot as plt
```

#### Define the congruential random number generator

```
[2]: def randCon():
    # construct random numbers according the formula in exercise 1
    im = 139968
    ia = 205
    ic = 29573
    randCon.r = (ia*randCon.r+ic) % im #get next random number
    # print("R=", randCon.r)
    return float(randCon.r) / im #return normalized one
```

```
[3]: last = 4711
randCon.r = last #Starting value (seed)
```

Number of points to be generated

```
[4]: npoints = 1000000
```

Use RANDOM from numpy

```
[5]: rng1 = np.random.default_rng(1234)
```

Set the arrays

```
[6]: xC, yC, xR, yR = [], [], [], []
```

Generate random numbers from congruential generator

```
[7]: for n in range(npoints):
    # fill the 2 random numbers into a scatter plot to compare the correlation
    xC_val = randCon()
    yC_val = randCon()
    xC.append(xC_val)
    yC.append(yC_val)
hCongruent, xedges, yedges = np.histogram2d(xC, yC, bins=100, range=[[0, 1], [0, 1]])
```

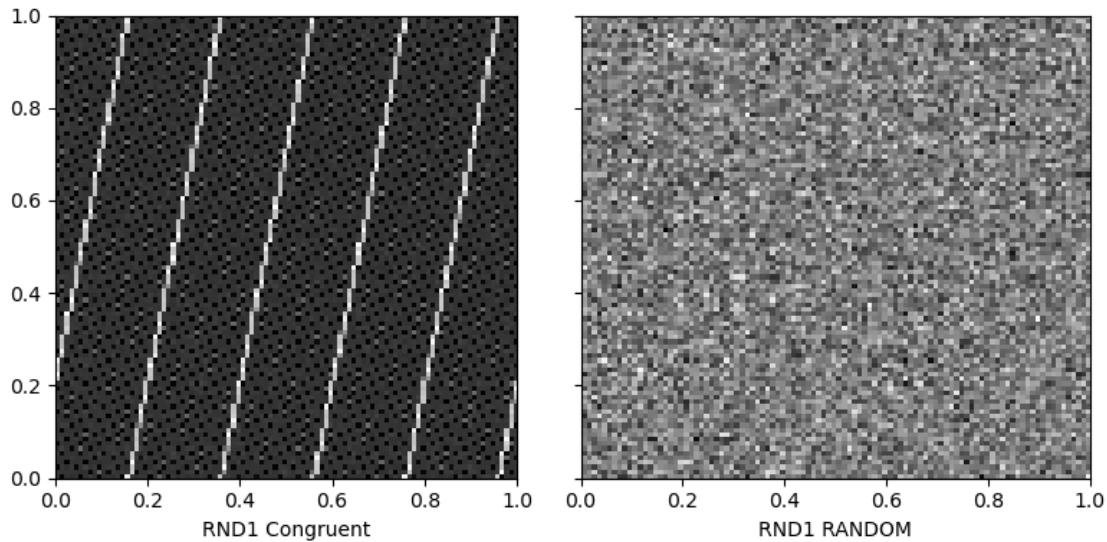
next use the ranlux generator and compare also the 2 random numbers (here we use the numpi implementation of RANDOM)

```
[8]: for n in range(npoints):
    xR_val = rng1.random()
    yR_val = rng1.random()
    xR.append(xR_val)
    yR.append(yR_val)
hRANDOM, xedges, yedges = np.histogram2d(xR, yR, bins=100, range=[[0, 1], [0, 1]])
```

Plotting the results for our own random number generator

```
[9]: fig, axs = plt.subplots(figsize=(8, 4),nrows=1, ncols=2,sharey=True, tight_layout=True)
#fig, ax1 = plt.subplots()
# Set aspect ratio for rectangular shape
axs[0].set_aspect('auto')
axs[0].imshow(hCongruent.T, origin='lower', extent=[0, 1, 0, 1], cmap='gray')
axs[0].set_xlabel("RND1 Congruent")
#axs[0].set_ylabel("RND2 Congruent")
axs[1].imshow(hRANDOM.T, origin='lower', extent=[0, 1, 0, 1], cmap='gray')
# Set aspect ratio for rectangular shape
axs[1].set_aspect('auto')
axs[1].set_xlabel("RND1 RANDOM")
#axs[1].set_ylabel("RND2 RANDOM")
```

```
[9]: Text(0.5, 0, 'RND1 RANDOM')
```



## 2.7.2 Constructing a gauss random number generator, by adding several random numbers.

First import what is needed

```
[1]: import numpy as np
import matplotlib.pyplot as plt
from math import sqrt
```

Define histograms with sum of random numbers

```
[2]: pointsA = [1, 2, 3, 6, 12, 20, 40, 60]
#pointsA = [1]
bins = 100
```

```
[3]: rng = np.random.default_rng(1234) # initialise random number generator PCG-64
print(rng)
```

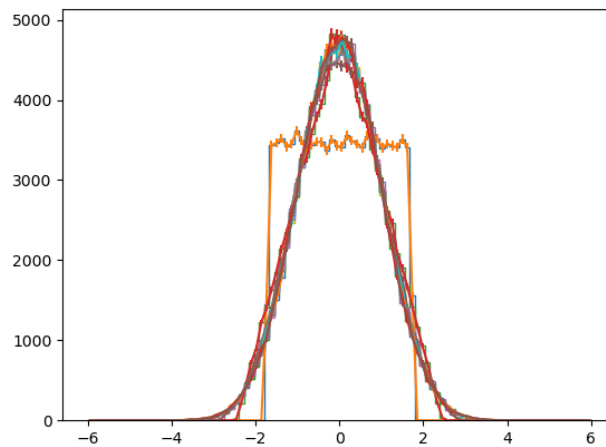
Generator(PCG64)

Fill the histograms with random numbers here calculate the sum over the random numbers and fill them into the histograms calculate it for the sum over 1,3,6,10,12,20,40 random numbers in root then fit the distribution and determine the mean and sigma

Plot normalized into single Graph

```
[4]: # calculate it for the sum over 1,3,6,10,12,20,40 random numbers
Ntrials=100000
errors=[]
histo=[]
bin_edge = []
xcenters = []
histo={}
print (" Gauss Random number generator - in one graph")
for p in pointsA:
    xval=[]
    for n in range(Ntrials):
        x = 0.
        for n2 in range(p):
            x += rng.random()
        xval.append((x - p/2.)/sqrt(p/12.))
    histo[p] = xval
# plot all in one
# to get histogram normalized, set density=True
histogram, bin_edge = np.histogram(xval, bins=bins, range=[-6, 6], density=False)
errors = np.sqrt(histogram)
plt.hist(xval, bins=bins, range=[-6, 6], density=False, histtype='step')
xcenters = (bin_edge[:-1] + bin_edge[1:]) / 2
plt.errorbar(xcenters, histogram, yerr=errors)
```

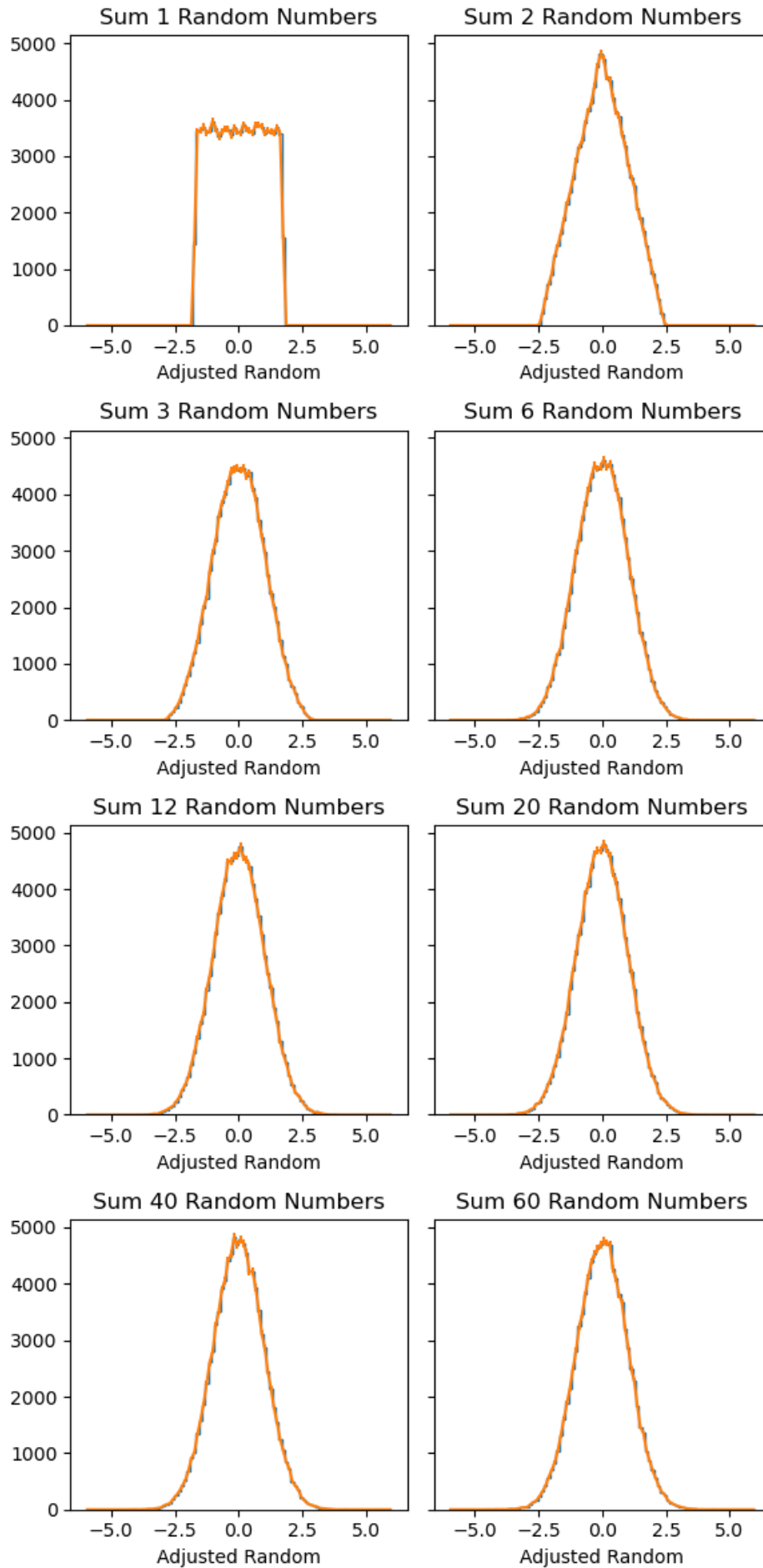
Gauss Random number generator - in one graph



Plot all Histos separately

```
[6]: icount=0
icol=-1
fig, axs = plt.subplots(figsize=(6, 12),nrows=4, ncols=2,sharey=True, tight_layout=False)
for p in pointsA:
    histogram, bin_edge = np.histogram(histo[p], bins=bins, range=[-6, 6],density=False)
    errors = np.sqrt(histogram)
    icol=icol+1
    if (icol > 1 ):
        icol=0
        icount=icount+1

    text = "Sum "+str(p) + " Random Numbers"
    axs[icount,icol].hist(histo[p], bins=bins, range=[-6, 6],density=False, histtype='step')
    axs[icount,icol].set_xlabel("Adjusted Random")
    axs[icount,icol].set_title(text )
    xcenters = (bin_edge[:-1] + bin_edge[1:]) / 2
    axs[icount,icol].errorbar(xcenters, histogram, yerr=errors)
```



### 2.7.3 Testing Monte Carlo integration I

We have a test function:  $g_0 = 3x^2$  We weight the histo with the function value. It is integrated over the region from 0 to 1.

We calculate the result and its error.

Define function which we want to integrate

```
[1]: import numpy as np
import matplotlib.pyplot as plt
from math import sqrt
```

```
[2]: def g0(z):
return 3*z*z;
```

```
[3]: rng = np.random.default_rng(1234) # initialise random number generator PCG-64
print(rng)
```

Generator(PCG64)

Calculate the sum and sum2 of the function values at the random points

```
[4]: xg0 = xg00 = 0
npoints = 1000000
for n in range(npoints):
    x0 = rng.random()
    f = g0(x0)
    xg0 += f
    xg00 += f**2
```

Calculate average and average to the squared values

```
[5]: avg = xg0 / npoints
avg2 = xg00 / npoints

sigma2 = avg2 - avg*avg # Get the average deviation squared
error = sqrt(sigma2/npoints) # error behaves as 1/sqrt(npoints)
```

Finally the result

```
[6]: print (" integral for 3x**2 is: ", avg, "+/-", error)
print (" true integral for 3x**2 is : 1.0 ")
```

```
integral for 3x**2 is:  1.0003948829353004 +/- 0.0008947753106679922
true integral for 3x**2 is : 1.0
```

### 2.7.4 Testing Monte Carlo integration II

We calculate the integral  $\int_0^x \int_0^1 dx dy$  and its error.

Import what is needed

```
[1]: import numpy as np
import matplotlib.pyplot as plt
from math import sqrt
```

Loop over random points in the 2D space

```
[2]: npoints = 2000000
```

initialise random number generator:

```
[3]: rng = np.random.default_rng(1234) # initialise random number generator PCG-64
print(rng)
```

Generator(PCG64)

```
[4]: nhit = 0

for n in range(npoints):
    x,y = rng.random(), rng.random()
    # insert here the values for x,y and the rejection condition
    # accept if y < x
    if y < x:
        nhit += 1
```

```
[5]: # Calculate the integral
      Int = float(nhit)/npoints
```

```
[6]: # the uncertainty is calculated from a Binominal distribution

      sigma2 = (1. - Int)/nhit
      error = sqrt(sigma2)*Int
```

```
[7]: print (" integral for is: ", Int, "+/-", error)
      print (" true integral is : 0.5 ")

      integral for is: 0.50021 +/- 0.00035355335940986336
      true integral is : 0.5
```

## 2.7.5 Testing Monte Carlo integration III.

We have a test function:  $g_0 = (1 - x)^5/x$  We weight the histo with the function value. It is integrated over the region from  $x_{min}$  to 1.

We calculate the result and its error.

Import what is needed

```
[1]: import numpy as np
      import matplotlib.pyplot as plt
      from math import sqrt, log
```

```
[2]: def g0(z):
      return (1 - z)**5 / z
```

```
[3]: npoints = 100000 # Loop over random points in the 2D space
```

```
[4]: rng = np.random.default_rng(1234) # initialise random number generator PCG-64
      print(rng)
```

Generator(PCG64)

```
[5]: # The lower limit of the integration, the upper is 1
      xmin = 1e-4
```

```
[6]: xg0 = xg00 = 0
      for n1 in range(npoints):
          # here do the calculation with importance sampling
          x0 = xmin*rng.random()
          weight = x0*log(1/xmin)
          # here do the calculation using linear sampling
          # x0 = xmin+(1-xmin)*rng.random()
          # weight = 1-xmin
          f = g0(x0)
          ff = weight*f
          xg0 += ff
          xg00 += ff**2
```

Calculate the integral

```
[7]: xg0 /= npoints
      xg00 /= npoints
      sigma2 = xg00 - xg0*xg0
      error = sqrt(sigma2/npoints)
```

Show the results

```
[8]: print (" integral for g(x) = (1-x)**5/x is: ", xg0, "+/-", error)

      integral for g(x) = (1-x)**5/x is: 6.931074361607794 +/- 0.00992428090524805
```

## Chapter 3

# Probing the Structure of Matter

The force that keeps matter together is the strong force which is described by the theory of Quantum Chromo Dynamics (QCD). Basically everything is included in the QCD Lagrangian, which describes the non-abelian nature of QCD.

Probing the structure of matter is in analogy to optics: to resolve objects the wavelength  $\lambda$  of the probe has to be smaller than the size  $d$  of the target:  $\lambda < d$ . In all calculations below we assume *natural units*:  $\hbar = c = 1$ .

An introduction to kinematics in High Energy Physics (HEP), the definition of light-cone vectors and the cross-section can be found in Appendix A.

For an introduction to the standard model see [22]. Calculations of QCD processes (including many the details for the calculation) are described nicely in [23]. A theoretical description and a discussion on parton showers and Monte Carlo generators is given in the *Pink Book* [24]. A detailed discussion on parton evolution is given in [25].

### 3.1 The Quark Parton Model

In analogy to optics, photons can be used to probe the structure of matter. In quantum theory every particle has a particular wave-length, so any particle with a small enough wave-length can be used as a probe to measure the structure of a target: photons from electron or muons,  $W/Z$  bosons and also jets produced in high energy collisions can be used to extract information on the colliding hadrons.

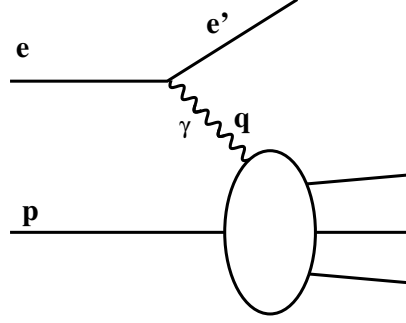
In the following the structure of the proton as tested in Deep Inelastic Scattering (DIS) of electrons (or muons) on a proton target (fig. 3.1) will be discussed. The following invariant quantities can be defined (here the electron four-vector is denoted with  $e$ , the scattered electron with  $e'$  and the proton four vector with  $p$ ):

$$s = (e + p)^2 \quad (3.1)$$

$$q^2 = (e - e')^2 \stackrel{\text{def}}{=} -Q^2 \quad (3.2)$$

$$y = \frac{p \cdot q}{p \cdot e} \quad (3.3)$$

$$x_{Bj} = \frac{Q^2}{2p \cdot q} \quad (3.4)$$

Figure 3.1: General diagram for DIS scattering  $e + p \rightarrow e' + X$ 

If we neglect the electron and proton masses, then we obtain:

$$Q^2 = x \cdot y \cdot s \quad (3.5)$$

$$\begin{aligned} W^2 &= (q + p)^2 = -Q^2 + 2q \cdot p \\ &= -Q^2 + y s = -Q^2 + \frac{Q^2}{x} \end{aligned} \quad (3.6)$$

with  $q$  being the photon- $(\gamma)$  four-vector. The "invariant mass" (or virtuality) of the photon is given by  $Q^2 = -q^2$ , the "energy" of the photon is given by  $y$  which reduces to  $y = 1 - E'/E$  in the proton rest frame with  $E$  ( $E'$ ) being the energy of the electron (scattered electron) in the proton rest frame. The quantity  $x_{Bj}$  is called *x-Bjorken* after its inventor James Bjorken in 1969 [26]. In the quark parton model (QPM) (and only there)  $x_{Bj}$  can be associated with the momentum fraction the quark takes from the proton momentum (as we will discuss later). This interpretation is only true in the QPM in DIS, but not if higher orders are included nor in hadron-hadron scattering.

Deep inelastic scattering is defined by:

$$\begin{aligned} Q^2 &\gg m_p^2 && \text{deep} \\ W^2 &\gg m_p^2 && \text{inelastic} \end{aligned}$$

where  $m_p$  is the proton mass.

The general form of the cross section in DIS is given by (see [22, 24]):

$$d\sigma \sim L_{\mu\nu}^e W^{\mu\nu} \quad (3.7)$$

with the leptonic  $L_e^{\mu\nu}$  and hadronic  $W^{\mu\nu}$  tensors given by:

$$L_e^{\mu\nu} = \frac{1}{2} \text{Tr}((\not{\epsilon}' + m)\gamma^\mu(\not{\epsilon} + m)\gamma^\nu) \quad (3.8)$$

$$W^{\mu\nu} = -W_1 g^{\mu\nu} + \frac{W_2}{M^2} p^\mu p^\nu + \frac{W_4}{M^2} q^\mu q^\nu + \frac{W_5}{M^2} (p^\mu q^\nu + q^\mu p^\nu) \quad (3.9)$$

where the structure functions  $W_i$  are introduced to parametrize our ignorance about the details of the structure of the proton. On very general grounds, assuming current conservation and symmetries only two out of the five structure functions  $W$  are independent (for unpolarized scattering). After a bit of algebra and rewriting using  $W_1 = F_1$  and  $\nu W_2 = F_2$  with  $\nu = \frac{Q^2 + W^2 - M^2}{2M}$ , we obtain



the master formula for DIS scattering [24][p 89] :

$$\begin{aligned}\frac{d\sigma}{dx dQ^2} &= \frac{4\pi\alpha^2}{Q^4} \left[ (1 + (1-y)^2) F_1 + \frac{(1-y)}{x} (F_2 - 2xF_1) \right] \\ &= \frac{2\pi\alpha^2}{xQ^4} \left[ (1 + (1-y)^2) F_2 - \frac{y^2}{2} F_L \right]\end{aligned}\quad (3.10)$$

where in the second line the longitudinal structure function  $F_L = F_2 - 2xF_1$  is introduced. In case of purely transverse polarized photon interactions the *Callan-Cross* relation gives  $F_2 = 2xF_1$ . The structure functions  $F_1$ ,  $F_2$  and  $F_L$  are what can be measured in experiment and what will be the subject in the following sections.

The early measurements of Deep Inelastic Scattering led to the interpretation of the structure function  $F_2$  in terms of the quark-parton model (QPM) where the proton is seen as composed of objects, the quarks and gluons (generically called partons). Inelastic scattering is interpreted as an incoherent superposition of scatterings on the individual partons. These partons (quarks) are supposed to be quasi-free such that any interaction between them can be neglected. A very nice and understandable discussion of this is in the original article by J. Bjorken and E. Paschos [26].

Whether the partons can be regarded as free during the interaction can be estimated by calculating the interaction and fluctuation time in DIS scattering (as done in the original paper [26]). If the interaction time  $\tau_i$  is small compared to the fluctuation time  $\tau_f$  in which a particle can fluctuate into partons, then the partons can be considered as free.

Assume scattering at large energies in the center-of-mass frame of the electron-proton system, where the electron mass can be neglected (see fig 3.2).

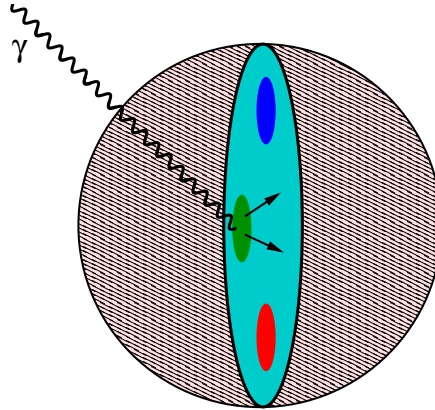


Figure 3.2: The proton in the high energy center-of-mass frame (or in the infinite momentum frame) looks like a pancake. The interaction time is small compared to the time where a parton can fluctuate into others ( $qq$ ).

As an example, we let the proton split into two partons  $q_1$  and  $q_2$  with momentum fractions  $x$  of the proton momentum  $P = (E_p, \vec{p})$ :

$$\begin{aligned}q_1 &= xP \\ q_2 &= (1-x)P\end{aligned}$$

The electron has four-momentum  $e = (E_p, \vec{p})$  and the photon has momentum  $q = e - e'$  with  $e'$  being the four momentum of the scattered electron. We now calculate the interaction time  $\tau_i = 1/\Delta E_{electron} = 1/E_\gamma$ . From energy momentum conservation we get  $e' = e - q$  and

$$e'^2 = (e - q)^2 = e^2 - 2e \cdot q + q^2$$

Since  $e^2 = e'^2 = m_e^2 \rightarrow 0$ , we obtain with  $Q^2 = -q^2$

$$0 = -2e \cdot q - Q^2$$

and

$$Q^2 = -2e \cdot q = -2(E_\gamma E_p + \vec{p}_p \vec{q}) \quad (3.11)$$

where we have used the relations  $E_e = E_p$  (for  $m_p = m_0 = 0$ ) and  $\vec{p}_p = -\vec{p}_e$  valid in the center-of-mass frame. Using  $x = Q^2/(2p \cdot q)$  together with  $p \cdot q = E_\gamma E_p - \vec{p}_p \vec{q}$  we can write:

$$\begin{aligned} \frac{Q^2}{2x} &= E_\gamma E_p - \vec{p}_p \vec{q} \\ \vec{p}_p \vec{q} &= -\frac{Q^2}{2x} + E_\gamma E_p \end{aligned}$$

Inserting this into eq.(3.11) we obtain:

$$Q^2 = -2E_\gamma E_p + \frac{2Q^2}{2x} - 2E_\gamma E_p \quad (3.12)$$

$$\rightsquigarrow Q^2 \left(1 - \frac{1}{x}\right) = -4E_\gamma E_p \quad (3.13)$$

$$\rightsquigarrow E_\gamma = -\frac{Q^2 \left(1 - \frac{1}{x}\right)}{4E_p} \quad (3.14)$$

The next step is to calculate the fluctuation time  $\Delta E_{qq}$  which is the energy of the  $qq$  pair.

$$\Delta E_{qq} = E_1 + E_2 - E_p$$

With  $q_1 = (E_1, \vec{k}_T, xE_p)$  and  $q_2 = (E_2, -\vec{k}_T, (1-x)E_p)$  using  $\sqrt{1+x} \approx 1 + (1/2)x + \dots$  we obtain:

$$\begin{aligned} E_1 &= \sqrt{(xE_p)^2 + k_T^2} = xE_p \sqrt{1 + \frac{k_T^2}{(xE_p)^2}} \\ &\approx xE_p \left(1 + \frac{1}{2} \frac{k_T^2}{(xE_p)^2} + \dots\right) \\ E_2 &= \sqrt{((1-x)E_p)^2 + k_T^2} = (1-x)E_p \sqrt{1 + \frac{k_T^2}{((1-x)E_p)^2}} \\ &\approx (1-x)E_p \left(1 + \frac{1}{2} \frac{k_T^2}{((1-x)E_p)^2} + \dots\right) \end{aligned}$$

Inserting the above into the expression for  $\Delta E_{qq}$

$$\begin{aligned}
 \Delta E_{qq} &= E_1 + E_2 - E_p \\
 &= xP + \frac{1}{2} \frac{k_T^2}{xE_p} + (1-x)E_p + \frac{1}{2} \frac{k_T^2}{(1-x)E_p} - E_p \\
 &= \frac{1}{2} \frac{(1-x)k_T^2 + xk_T^2}{x(1-x)E_p} \\
 &= \frac{1}{2} \frac{k_T^2}{x(1-x)E_p}
 \end{aligned}$$

With

$$\tau_f = \frac{1}{\Delta E_{qq}} = \frac{2x(1-x)E_p}{k_T^2} \approx \frac{2xE_p}{k_T^2} \quad (3.15)$$

$$\tau_i = \frac{1}{\Delta E_{ee'}} = \frac{1}{E_\gamma} = \frac{4E_p}{Q^2 \left(\frac{1-x}{x}\right)} \approx \frac{4xE_p}{Q^2} \quad (3.16)$$

where the last approximation is done for  $x \ll 1$ . We now have:

$$\frac{\tau_{interaction}}{\tau_{fluctuation}} \approx \frac{4xP}{Q^2} \frac{k_T^2}{2xE_p} = \frac{2k_T^2}{Q^2} \quad (3.17)$$

Thus, for small  $k_T$  ( $k_T^2 \ll Q^2$ ) the interaction time is much smaller than the fluctuation time, and the partons can be considered as frozen and therefore behave as free partons.

### 3.2 Cross Section in DIS

In the previous section we have seen that the partons inside the proton can be considered free as long as transverse momentum squared  $k_T^2$  is small compared to  $Q^2$ .

In the following we calculate the cross section for  $eP \rightarrow e'X$  from the partonic cross section  $ep_q \rightarrow e'p'_q$  with  $p_q$  being the four-momentum of any type of quark with momentum fraction  $\xi$  such that  $p_q = \xi P$ . The Mandelstam variables are then:

$$\hat{s} = (e + p_q)^2 = 2e \cdot p_q \quad (3.18)$$

$$\hat{u} = (p_q - e')^2 = -2p_q \cdot e' \quad (3.19)$$

$$\hat{t} = (e - e')^2 = -Q^2 \quad (3.20)$$

$$(3.21)$$

The matrix element squared for  $ep_q \rightarrow e'p'_q$  is [22][p 124]:

$$|\mathcal{M}|^2 = 2e_q^2(4\pi\alpha)^2 \frac{\hat{s}^2 + \hat{u}^2}{\hat{t}^2} \quad (3.22)$$

with  $e_q$  being the electric charge of the parton. Using the DIS variables (see eq.(3.1)) with  $q = e - e'$  gives:

$$y = \frac{q \cdot P}{e \cdot P} = \frac{q \cdot p_q}{e \cdot p_q} = 1 - \frac{e' \cdot p_q}{e \cdot p_q} = 1 + \frac{\hat{u}}{\hat{s}} \quad (3.23)$$

The matrix element can then be expressed as:

$$|\mathcal{M}|^2 = 2e_q^2(4\pi\alpha)^2 \frac{1}{Q^4} (\hat{s}^2 + \hat{s}^2(y-1)^2) \quad (3.24)$$

$$= 2e_q^2(4\pi\alpha)^2 \frac{\hat{s}^2}{Q^4} (1 + (1-y)^2) \quad (3.25)$$

With this we obtain the cross section:

$$\frac{d\sigma}{d\hat{t}} = \frac{d\sigma}{dQ^2} = \frac{1}{16\pi\hat{s}^2} |\mathcal{M}|^2 \quad (3.26)$$

$$= \frac{2e_q^2(4\pi\alpha)^2 \hat{s}^2}{16\pi\hat{s}^2} \frac{1}{Q^4} (1 + (1-y)^2) \quad (3.27)$$

$$= (2\pi\alpha^2 e_q^2) \frac{1}{Q^4} (1 + (1-y)^2) \quad (3.28)$$

Before we compare this expression to the cross section for DIS of eq.(3.10) we investigate the meaning of  $\xi$ . Using the mass-shell condition (the quarks are assumed to be massless) we obtain:

$$p_q'^2 = (p_q + q)^2 = q^2 + 2p_q \cdot q + p_q^2 \quad (3.29)$$

$$= -Q^2 + 2p_q \cdot q = -Q^2 + 2\xi P \cdot q \quad (3.30)$$

$$= -2P \cdot q \cdot x + 2\xi P \cdot q \quad (3.31)$$

$$= -2P \cdot q(x - \xi) \quad (3.32)$$

thus, we find  $x = \xi$  for massless partons  $p_q^2 = p_q'^2 = 0$ . Using

$$\int dx \delta(x - \xi) = 1$$

we can rewrite eq.(3.28) as:

$$\frac{d\sigma^2}{dx dQ^2} = (4\pi\alpha^2) \frac{1}{Q^4} (1 + (1 - y)^2) e_q^2 \frac{1}{2} \delta(x - \xi) \quad (3.33)$$

Now we can compare eq.(3.33) with eq.(3.10) and find:

$$\hat{F}_1 = \frac{1}{2} e_q^2 \delta(x - \xi) \quad (3.34)$$

$$\hat{F}_2 = 2x \hat{F}_1 = x e_q^2 \delta(x - \xi) \quad (3.35)$$

Thus the structure function  $\hat{F}_2$  gives the probability to find a quark with momentum fraction  $x = \xi$ .

However, measurements have shown that the structure function  $F_2$  is not a  $\delta$ -function but rather a distribution, telling that the partons inside the proton carry a range of momentum fractions. Thus we are forced to introduce a distribution  $q(\xi)d\xi$  which represents the probability to find a quark carrying a momentum fraction  $\xi$  in the range  $\xi$  and  $\xi + d\xi$  within  $0 \leq \xi \leq 1$ .

The proton structure functions  $F_i$  are obtained by weighting the quark structure functions  $\hat{F}_i$  with the probability density functions  $q(\xi)$ :

$$F_2(x) = 2x F_1(x) = \sum_{q, \bar{q}} \int d\xi q(\xi) x \cdot e_q^2 \delta(x - \xi) \quad (3.36)$$

$$= \sum_{q, \bar{q}} e_q^2 x q(x) \quad (3.37)$$

Since there are different quark species in the proton, the electromagnetic structure function as obtained by scattering a charged lepton on a proton is:

$$F_2^{em}(x) = x \left[ \frac{4}{9} (u + \bar{u} + c + \bar{c}) + \frac{1}{9} (d + \bar{d} + s + \bar{s} + b + \bar{b}) \right] \quad (3.38)$$

with  $u, \bar{u}, \dots$  being the quark (antiquark) density functions.

Since the proton is build from two  $u_v$ -type and one  $d_v$ -type valence quarks, one can define the following number sum rules:

$$\int_0^1 dx u_v(x) = 2 \quad (3.39)$$

$$\int_0^1 dx d_v(x) = 1 \quad (3.40)$$

However it was found from experiment that the momentum sum over all quarks gives only about 50 % of the proton momentum:  $\int_0^1 dx x \sum_i q_i(x) \sim 0.5$  (note the relation to expectation values as

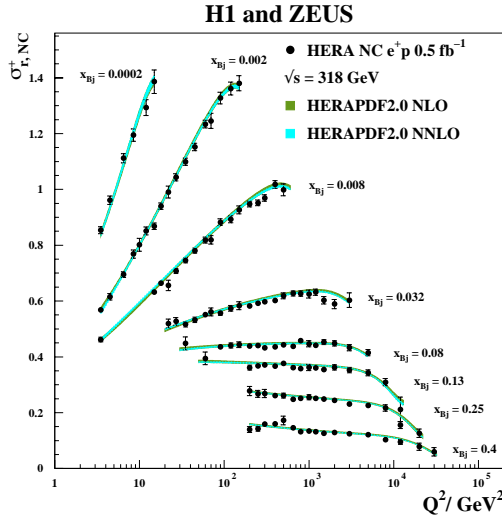


Figure 3.3: The photon-proton cross section as a function of  $Q^2$  for different values of  $x$  extracted from DIS scattering  $e + p \rightarrow e' + X$  at HERA [27].

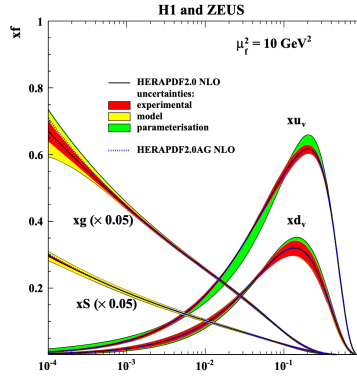


Figure 3.4: The parton density functions as a function of  $x$  extracted from DIS scattering  $e + p \rightarrow e' + X$  at HERA [27].

discussed in the first chapter). If the QPM picture is correct, the remaining 50 % of the proton momentum is carried by partons other than the quarks, namely the gluons, such that

$$\int_0^1 dx \, x [\text{all pdfs}] = 1 \quad (3.41)$$

The momentum sum rules are subject of the exercises.

In fig. 3.3 the measurement of  $F_2(x, Q^2)$  as a function of  $Q^2$  obtained at HERA [27] is shown. In fig. 3.4 the parton density functions for quarks and gluons as obtained from the measurement of  $F_2(x, Q^2)$  is shown. The measurements show, that the structure function  $F_2$  depends also on  $Q^2$ , which is not predicted in the simple QPM. These *scaling violations* are subject of the next sections.

### 3.3 The photon-proton cross section

The cross section for  $e + p_q \rightarrow e' + p'_q$  can be separated into two parts: the part at the lepton vertex and the part at the quark vertex. In the following we calculate the cross section for  $\gamma^* p_q \rightarrow p'_q$ . The matrix element for  $\gamma^* p_q \rightarrow p'_q$  can be found in [22][section 10.2]:

$$\begin{aligned} |\mathcal{M}|^2 &= 2e_q^2 e^2 p_q \cdot q \\ &= 8\pi\alpha e_q^2 p_q \cdot q \end{aligned}$$

with  $\alpha = e^2/(4\pi)$ . We introduce

$$z = \frac{Q^2}{2q \cdot p_q} \quad (3.42)$$

The cross section is then:

$$\sigma = \int \frac{1}{flux} dLips |\mathcal{M}|^2 \quad (3.43)$$

$$= 2\pi\alpha e_q^2 \cdot 2\pi\delta((p_q + q)^2) \quad (3.44)$$

$$= 2\pi\alpha e_q^2 \cdot 2\pi\delta(2p_q \cdot q(1 - z)) \quad (3.45)$$

$$= \frac{4\pi^2\alpha}{2p_q \cdot q} e_q^2 \delta(1 - z) \quad (3.46)$$

where we have used  $z = Q^2/(2q \cdot p_q)$  and for the *flux*:

$$flux = 4\sqrt{(p_q \cdot q)^2 - m_1^2 m_2^2} \quad (3.47)$$

$$= 4p_q \cdot q \quad (3.48)$$

and for *dLips* using  $(q + p_q)^2 = -Q^2 + Q^2/z$ :

$$\int dLips = (2\pi)^4 \int \delta^4(-p_q - q + p'_q) \frac{d^4 p'_q}{(2\pi)^3} \delta(p_q'^2 - m_q'^2) \quad (3.49)$$

$$= 2\pi\delta(p_q'^2) \quad (3.50)$$

$$= 2\pi\delta((p_q + q)^2) \quad (3.51)$$

We now compare the full expression for  $e + p_q \rightarrow e' + p'_q$  as given in eq.(3.33) with the cross section for  $\gamma^* p_q \rightarrow p'_q$  of eq.(3.46):

$$\frac{d\sigma^2}{dx dQ^2} = (4\pi\alpha^2) \frac{1}{Q^4} (1 + (1 - y)^2) e_q^2 \frac{1}{2} \delta(x - \xi) \quad (3.52)$$

$$= \frac{\alpha}{2\pi Q^2} (1 + (1 - y)^2) \frac{4\pi^2\alpha}{Q^2} e_q^2 \frac{1}{\xi} \delta\left(\frac{x}{\xi} - 1\right) \quad (3.53)$$

$$= \frac{\alpha}{2\pi Q^2} (1 + (1 - y)^2) \frac{4\pi^2\alpha}{Q^2} e_q^2 \frac{z}{x} \delta(z - 1) \quad (3.54)$$

$$= \frac{\alpha}{2\pi Q^2 x} (1 + (1 - y)^2) \frac{4\pi^2\alpha}{2p_q \cdot q} e_q^2 \delta(1 - z) \quad (3.55)$$

$$= \frac{\alpha}{2\pi Q^2 x} (1 + (1 - y)^2) \sigma_0(z) e_q^2 \delta(1 - z) \quad (3.56)$$

where we have used  $z\xi = x$  with  $x = Q^2/(ys)$ . With the Jacobean  $\frac{dx}{dy} = \frac{x}{y}$  we obtain:

$$\frac{d\sigma^2}{dydQ^2} = \frac{d\sigma^2}{dx dQ^2} \frac{dx}{dy} = \frac{\alpha}{2\pi Q^2 y} (1 + (1-y)^2) \sigma_0(z) e_q^2 \delta(1-z) \quad (3.57)$$

We can now separate the photon flux  $F_\gamma(y, Q^2)$  from the hadronic interaction. This is also called the *equivalent photon approximation*:

$$\begin{aligned} \frac{d\sigma^2}{dydQ^2} &= F_\gamma(y, Q^2) \frac{4\pi^2\alpha}{Q^2} e_q^2 F_2 \\ F_\gamma(y, Q^2) &= \frac{\alpha}{2\pi Q^2 y} (1 + (1-y)^2) \end{aligned} \quad (3.58)$$

The photon flux 3.58 can be also expressed in terms of the so-called splitting function  $P_{ee}(z) = (1+z^2)/(1-z)$  with  $y = 1-z$

$$F_\gamma(y, Q^2) = \frac{1}{Q^2} \frac{\alpha}{2\pi} P_{ee}(y) \quad (3.59)$$

### 3.4 $\mathcal{O}(\alpha_s)$ contribution to DIS

We can apply now the method of factorizing the photon flux from the hadronic part to calculate the  $\mathcal{O}(\alpha_s)$  contributions to the total DIS cross section. We have to consider the QCD Compton (QCDC)  $e + q \rightarrow e' + q' + g$  and the boson-gluon fusion (BGF)  $e + g \rightarrow e' + q + \bar{q}$  processes. By separating the lepton vertex from the hadron vertex, the calculations can be significantly simplified, since instead of a  $2 \rightarrow 3$  process we just need to calculate the  $2 \rightarrow 2$  subprocess (Fig. 3.5).

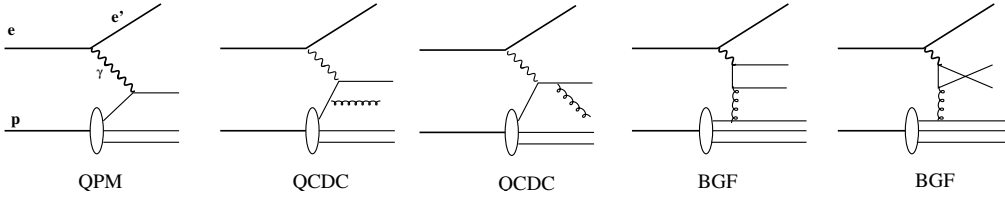


Figure 3.5: The  $\mathcal{O}(\alpha_s)$  contributions to  $e + p \rightarrow e' X$ .

The matrix elements for both QCDC and BGF are singular in  $\hat{t}$ . Since we are interested in the dominant contribution to the cross section, we can take the limit of  $\hat{t} \rightarrow 0$ . We express  $\hat{t}$  with the transverse momentum  $k_T$ . After some algebra we obtain (the explicit calculation is shown in the Appendix A.4):

$$k_T^2 = \frac{\hat{t}\hat{u}\hat{s}}{(\hat{s} + Q^2)^2} \quad (3.60)$$

using  $z = Q^2/(2q \cdot p_2)$  where  $q$  ( $p_2$ ) are the photon (parton) four-momenta, we obtain in the limit of small  $\hat{t}$  (with  $\hat{u} = -Q^2 - \hat{s}$ ):

$$k_T^2 = -\hat{t}(1-z) \quad (3.61)$$

The cross section is then given by (for  $k_T \rightarrow 0$ ):

$$\frac{d\sigma}{dk_T^2} = \frac{1}{16\pi} \frac{1}{\hat{s} + Q^2} \frac{1}{\hat{s}} \frac{1}{1-z} |M|^2 \quad (3.62)$$



### 3.4.1 QCD process

The matrix element for the QCD Compton process is given in [22][section 10.4]. Here we concentrate isolating the dominant part of the matrix element (small  $\hat{t}$  approximation) with  $\hat{s} = (q + p_2)^2 = -Q^2 + 2q \cdot p_2 = \frac{Q^2}{z}(1 - z)$  :

$$|\mathcal{M}|^2 = 32\pi^2 (e_q^2 \alpha \alpha_s) \frac{4}{3} \left[ \frac{-\hat{t}}{\hat{s}} - \frac{\hat{s}}{\hat{t}} + \frac{2\hat{u}Q^2}{\hat{s}\hat{t}} \right] \quad (3.63)$$

$$= 32\pi^2 (e_q^2 \alpha \alpha_s) \frac{4}{3} \frac{1}{\hat{t}} \left[ \hat{s} - \frac{2Q^2(-Q^2 - \hat{s})}{\hat{s}} - \frac{2Q^2(-\hat{t})}{\hat{s}} + \frac{\hat{t}^2}{\hat{s}} \right] \quad (3.64)$$

$$\rightsquigarrow \text{small } \hat{t} \text{ approximation} \quad (3.65)$$

$$\approx 32\pi^2 (e_q^2 \alpha \alpha_s) \frac{4}{3} \frac{1}{\hat{t}} \left[ \hat{s} + \frac{2Q^2(Q^2 + \hat{s})}{\hat{s}} + \dots \right] \quad (3.66)$$

$$= 32\pi^2 (e_q^2 \alpha \alpha_s) \frac{4}{3} \frac{1}{\hat{t}} \left[ \hat{s} + \frac{2Q^2}{1 - z} + \dots \right] \quad (3.67)$$

$$= 32\pi^2 (e_q^2 \alpha \alpha_s) \frac{4}{3} \frac{1}{t} \left[ \frac{Q^2(1 + z^2)}{z(1 - z)} + \dots \right] \quad (3.68)$$

$$= 32\pi^2 (e_q^2 \alpha \alpha_s) \frac{(1 - z)}{k_T^2} \frac{Q^2}{z} P_{qq}(z) \quad (3.69)$$

where we have introduced the splitting function  $P_{qq}(z)$  with  $z = \frac{Q^2}{2q \cdot p_2}$ :

$$P_{qq} = \frac{4}{3} \frac{1 + z^2}{1 - z} \quad (3.70)$$

Inserting eq.(3.69) into eq.(3.62) we obtain:

$$\frac{d\sigma}{dk_T^2} = \frac{1}{16\pi} \frac{1}{\hat{s} + Q^2} \frac{1}{\hat{s}} \frac{1}{1 - z} |\mathcal{M}|^2 \quad (3.71)$$

$$= \frac{1}{16\pi} \frac{1}{\hat{s} + Q^2} \frac{1}{\hat{s}} \frac{1}{1 - z} 32\pi^2 (e_q^2 \alpha \alpha_s) \frac{(1 - z)}{k_T^2} \frac{Q^2}{z} P_{qq}(z) \quad (3.72)$$

$$= \frac{4\pi^2 \alpha}{\hat{s}} e_q^2 \frac{\alpha_s}{2\pi} \frac{1}{k_T^2} P_{qq}(z) \quad (3.73)$$

$$= \sigma_0 e_q^2 \frac{\alpha_s}{2\pi} \frac{1}{k_T^2} P_{qq}(z) \quad (3.74)$$

In order to obtain the contribution to the total cross section, we must integrate over  $k_T$ :

$$\sigma^{QCD} = \int_{k_{t \min}}^{k_{t \max}} dk_T^2 \frac{d\sigma}{dk_T^2} \quad (3.75)$$

$$= \sigma_0 e_q^2 \frac{\alpha_s}{2\pi} P_{qq}(z) \log \frac{k_{t \max}^2}{k_{t \min}^2} \quad (3.76)$$

where  $k_{t \max}$  is the maximal  $p_t$  that can be reached:

$$k_{t \max}^2 = \frac{\hat{s}}{4} = \frac{Q^2(1 - z)}{4z} \quad (3.77)$$

The integral in Eq.(3.76) is divergent for  $k_{t\min} \rightarrow 0$ , therefore we need to introduce a lower (artificial) cut,  $k_{t\min} = \kappa$ . We then obtain:

$$\begin{aligned}\sigma^{QCDC} &= \sigma_0 e_q^2 \frac{\alpha_s}{2\pi} P_{qq}(z) \log \frac{Q^2(1-z)}{4z\kappa^2} + \dots \\ &= \sigma_0 e_q^2 \frac{\alpha_s}{2\pi} P_{qq}(z) \left[ \log \frac{Q^2}{\kappa^2} + \log \frac{1-z}{4z} + \dots \right]\end{aligned}$$

In order to obtain a measurable cross section, we must include the parton density functions. We recall also the QPM result:

$$\sigma^{QPM} = \sigma_0 e_q^2 \int_x^1 \delta(1-z) f_q(\xi) \delta(x-z\xi) dz d\xi \quad (3.78)$$

$$\sigma^{QPM} = \sigma_0 e_q^2 \int_x^1 \frac{d\xi}{\xi} f_q(\xi) \delta\left(\frac{x}{\xi} - 1\right) \quad (3.79)$$

and for QCDC:

$$\sigma^{QCDC} = \sigma_0 e_q^2 \frac{\alpha_s}{2\pi} \int_x^1 f_q(\xi) \delta(x-z\xi) dz d\xi P_{qq}(z) \left( \log \frac{Q^2}{\kappa^2} + \log \frac{1-z}{4z} + \dots \right) \quad (3.80)$$

$$\sigma^{QCDC} = \sigma_0 e_q^2 \frac{\alpha_s}{2\pi} \int_x^1 \frac{d\xi}{\xi} f_q(\xi) P_{qq}\left(\frac{x}{\xi}\right) \left( \log \frac{Q^2}{\kappa^2} + \log \frac{1-z}{4z} + \dots \right) \quad (3.81)$$

We can relate this with the expression for the structure function  $F_2(x, Q^2)$  (see eq.(3.10):

$$\sigma^{\gamma p} = \frac{4\pi\alpha}{Q^2} F_2(x, Q^2) = \frac{F_2(x, Q^2)}{x} \sigma_0 \quad (3.82)$$

$$\frac{F_2}{x} = \frac{\sigma^{\gamma p}}{\sigma_0} = \sum e_q^2 \int_x^1 \frac{d\xi}{\xi} f_q(\xi) \left[ \delta\left(1 - \frac{x}{\xi}\right) + \right. \quad (3.83)$$

$$\left. \frac{\alpha_s}{2\pi} P_{qq}\left(\frac{x}{\xi}\right) \left[ \log\left(\frac{Q^2}{\kappa^2}\right) + \log\left(\frac{1-z}{4z}\right) + \dots \right] + C_q(z, \dots) \right] \quad (3.84)$$

### 3.4.2 BGF process

The matrix element for the boson gluon fusion process  $\gamma^* g \rightarrow q\bar{q}$  is given in :

$$|\mathcal{M}|^2 = 32\pi^2 (e_q^2 \alpha \alpha_s) \frac{1}{2} \left[ \frac{\hat{u}}{\hat{t}} + \frac{\hat{t}}{\hat{u}} - \frac{2\hat{s}Q^2}{\hat{t}\hat{u}} \right] \quad (3.85)$$

$$\rightsquigarrow \text{small } \hat{t} \text{ approximation} \quad (3.86)$$

$$= 32\pi^2 (e_q^2 \alpha \alpha_s) \frac{1}{2} \frac{1}{\hat{t}} \left[ \hat{u} - \frac{2\hat{s}Q^2}{\hat{u}} \right] \quad (3.87)$$

$$= 32\pi^2 (e_q^2 \alpha \alpha_s) \frac{1}{2} \frac{1}{\hat{t}} \left[ -(Q^2 + \hat{s}) + \frac{2\hat{s}Q^2}{Q^2 + \hat{s}} \right] \quad (3.88)$$

$$= 32\pi^2 (e_q^2 \alpha \alpha_s) \frac{1}{2} \frac{-1}{\hat{t}} \left[ \frac{(Q^2 + \hat{s})^2 - 2\hat{s}Q^2}{Q^2 + \hat{s}} \right] \quad (3.89)$$

$$= 32\pi^2 (e_q^2 \alpha \alpha_s) \frac{1}{2} \frac{-1}{\hat{t}} \left[ \frac{Q^4 + \hat{s}^2}{Q^2 + \hat{s}} \right] \quad (3.90)$$

$$= 32\pi^2 (e_q^2 \alpha \alpha_s) \frac{1}{2} \frac{-1}{\hat{t}} \frac{Q^2}{z} [z^2 + (1-z)^2] \quad (3.91)$$

Inserting eq.(3.91) into eq.(3.62) we obtain:

$$\frac{d\sigma}{dk_T^2} = \frac{1}{16\pi} \frac{1}{\hat{s} + Q^2} \frac{1}{\hat{s}} \frac{1}{1-z} |\mathcal{M}|^2 \quad (3.92)$$

$$= \frac{1}{16\pi} \frac{1}{\hat{s} + Q^2} \frac{1}{\hat{s}} 32\pi^2 (e_q^2 \alpha \alpha_s) \frac{1}{2} \frac{Q^2}{z} \frac{1}{k_T^2} [z^2 + (1-z)^2] \quad (3.93)$$

$$= \pi \alpha \alpha_s e_q^2 \frac{1}{\hat{s}} \frac{1}{k_T^2} [z^2 + (1-z)^2] \quad (3.94)$$

$$= \sigma_0 e_q^2 \frac{\alpha_s}{2\pi} \frac{1}{k_T^2} \left[ \frac{1}{2} (z^2 + (1-z)^2) \right] \quad (3.95)$$

$$= \hat{\sigma}_0 e_q^2 \frac{\alpha_s}{2\pi} \frac{1}{k_\perp^2} P_{qg}(z) \quad (3.96)$$

where we have introduced the splitting function  $P_{qg}$ :

$$P_{qg} = \frac{1}{2} (z^2 + (1-z)^2) \quad (3.97)$$

Integrating the cross section eq(3.96) over  $k_T$  we obtain (in analogy to the QCDC process):

$$\sigma^{BGF} = \sigma_0 e_q^2 \frac{\alpha_s}{2\pi} P_{qg}(z) \log \frac{Q^2(1-z)}{4z\kappa^2} \quad (3.98)$$

$$= \sigma_0 e_q^2 \frac{\alpha_s}{2\pi} P_{qg}(z) \log \frac{Q^2}{\kappa^2} + \dots \quad (3.99)$$

In the BGF case the parton density is the gluon density (in contrast to the QCDC process). We rewrite the cross section in terms of  $F_2(x, Q^2)$  and obtain:

$$\sigma^{BGF} = \sigma_0 e_q^2 \frac{\alpha_s}{2\pi} \int_x^1 g(\xi) \delta(x - z\xi) dz d\xi P_{qg}(z) \log \frac{Q^2}{\kappa^2} \quad (3.100)$$

$$\sigma^{BGF} = \sigma_0 e_q^2 \frac{\alpha_s}{2\pi} \int_x^1 \frac{d\xi}{\xi} g(\xi) P_{qg}\left(\frac{x}{\xi}\right) \log \frac{Q^2}{\kappa^2} \quad (3.101)$$

Putting everything together we obtain for  $F_2/x$ :

$$\frac{F_2}{x} = \frac{\sigma^{\gamma p}}{\sigma_0} = \sum e_q^2 \int_x^1 \frac{d\xi}{\xi} \left( f_q(\xi) \left[ \delta \left( 1 - \frac{x}{\xi} \right) + \frac{\alpha_s}{2\pi} P_{qq} \left( \frac{x}{\xi} \right) \log \left( \frac{Q^2}{\kappa^2} \right) \right] \right. \quad (3.102)$$

$$\left. + g(\xi) \left[ \frac{\alpha_s}{2\pi} P_{qg} \left( \frac{x}{\xi} \right) \log \left( \frac{Q^2}{\kappa^2} \right) \right] \right) \quad (3.103)$$

We are still left with the arbitrary cutoff  $\kappa$ . Now we use a trick to remove it: we define scale dependent parton densities:

$$\begin{aligned} q_i(x, \mu^2) &= q_i^0(x) + \frac{\alpha_s}{2\pi} \int_x^1 \frac{d\xi}{\xi} \left[ q_i^0(\xi) P_{qq} \left( \frac{x}{\xi} \right) \log \left( \frac{\mu^2}{\kappa^2} \right) + C_q \left( \frac{x}{\xi} \right) \right] + \dots \\ g(x, \mu^2) &= g^0(x) + \frac{\alpha_s}{2\pi} \int_x^1 \frac{d\xi}{\xi} \left[ g^0(\xi) P_{qg} \left( \frac{x}{\xi} \right) \log \left( \frac{\mu^2}{\kappa^2} \right) + C_g \left( \frac{x}{\xi} \right) \right] + \dots \end{aligned} \quad (3.104)$$

where we have now put the divergent part ( $\kappa \rightarrow 0$ ) into a redefinition of the parton density with the price that the parton density is now scale dependent with scale  $\mu^2$ . Inserting this into the equation eq.(3.103), we obtain:

$$\begin{aligned} \frac{F_2}{x} &= \sum e_q^2 \int_x^1 \frac{d\xi}{\xi} \left( q(\xi, \mu^2) \left[ \delta \left( 1 - \frac{x}{\xi} \right) + \frac{\alpha_s}{2\pi} P_{qq} \left( \frac{x}{\xi} \right) \log \left( \frac{Q^2}{\mu^2} \right) \right] \right. \\ &\quad \left. + g(\xi, \mu^2) \left[ \frac{\alpha_s}{2\pi} P_{qg} \left( \frac{x}{\xi} \right) \log \left( \frac{Q^2}{\mu^2} \right) \right] \right) \end{aligned} \quad (3.105)$$

## Chapter 4

# Parton evolution equation

Here we will derive the evolution equation for the parton densities in the collinear (small  $t$ ) limit, the so called DGLAP evolution equations (named after the authors Dokshitzer, Gribov, Lipatov, Altarelli, Parisi [28–31]).

The expression for the deep inelastic scattering cross section (or the structure function  $F_2$ ) including  $\mathcal{O}(\alpha_s)$  corrections is given by:

$$\begin{aligned} \frac{\sigma^{\gamma^*p}}{\sigma_0} = \frac{F_2}{x} = & \sum e_q^2 \int \frac{d\xi}{\xi} \left( q(\xi, \mu^2) \left[ \delta \left( 1 - \frac{x}{\xi} \right) + \frac{\alpha_s}{2\pi} P_{qq} \left( \frac{x}{\xi} \right) \log \left( \frac{Q^2}{\mu^2} \right) \right] \right. \\ & \left. + g(\xi, \mu^2) \left[ \frac{\alpha_s}{2\pi} P_{qg} \left( \frac{x}{\xi} \right) \log \left( \frac{Q^2}{\mu^2} \right) \right] \right) \end{aligned} \quad (4.1)$$

The cross section for small transverse momenta (or at small  $t$ ) is divergent, and therefore gives a dominant contribution to the total cross section. For the price of a scale dependent parton density we have moved the divergent behavior into the bare (and not observable) parton densities, with the result that the expression became finite (a procedure called renormalization).

Since the  $\gamma p$  cross section  $\sigma^{\gamma^*p}$  (or equivalently the structure function  $F_2$ ) as an observable cannot depend on the arbitrary scale  $\mu^2$ , we must require, that it is  $\mu^2$ -scale independent. This is satisfied by the requirement

$$\frac{\partial F_2}{\partial \mu^2} = 0$$

Using eq.(4.1) (for simplicity we treat here only the quark part, the gluon part is treated similarly) we obtain:

$$\frac{\delta F_2}{\delta \mu^2} = \int \frac{d\xi}{\xi} \left( \frac{\partial q(\xi, \mu^2)}{\partial \mu^2} \left[ \delta \left( 1 - \frac{x}{\xi} \right) + \frac{\alpha_s}{2\pi} P_{qq} \left( \frac{x}{\xi} \right) \log \left( \frac{Q^2}{\mu^2} \right) \right] \right) \quad (4.2)$$

$$\begin{aligned} & + q(\xi, \mu^2) \frac{\alpha_s}{2\pi} P_{qq} \left( \frac{x}{\xi} \right) \frac{\partial}{\partial \mu^2} [\log Q^2 - \log \mu^2] \\ = & \frac{\partial q(x, \mu^2)}{\partial \mu^2} + \int \frac{d\xi}{\xi} \frac{\alpha_s}{2\pi} P_{qq} \left( \frac{x}{\xi} \right) \log \frac{Q^2}{\mu^2} \frac{\partial q(\xi, \mu^2)}{\partial \mu^2} \\ & + \int \frac{d\xi}{\xi} q(\xi, \mu^2) \frac{\alpha_s}{2\pi} P_{qq} \left( \frac{x}{\xi} \right) \left( -\frac{1}{\mu^2} \right) \end{aligned} \quad (4.3)$$

Now we collect all terms of  $\mathcal{O}(\alpha_s)$  (note the second term in eq.(4.3) is of  $\mathcal{O}(\alpha_s^2)$  since  $\frac{dq}{d \log \mu^2} \sim \mathcal{O}(\alpha_s)$  and therefore does not contribute) and we obtain:

$$\frac{dq_i(x, \mu^2)}{d \log \mu^2} = \frac{\alpha_s}{2\pi} \int_x^1 \frac{d\xi}{\xi} \left[ q_i(\xi, \mu^2) P_{qq} \left( \frac{x}{\xi} \right) \right] \quad (4.4)$$

Including also the gluon part we obtain:

$$\frac{dq_i(x, \mu^2)}{d \log \mu^2} = \frac{\alpha_s}{2\pi} \int_x^1 \frac{d\xi}{\xi} \left[ q_i(\xi, \mu^2) P_{qq} \left( \frac{x}{\xi} \right) + g(\xi, \mu^2) P_{qg} \left( \frac{x}{\xi} \right) \right] \quad (4.5)$$

and similarly for the gluons

$$\frac{dg(x, \mu^2)}{d \log \mu^2} = \frac{\alpha_s}{2\pi} \int_x^1 \frac{d\xi}{\xi} \left[ \sum_i q_i(\xi, \mu^2) P_{gq} \left( \frac{x}{\xi} \right) + g(\xi, \mu^2) P_{gg} \left( \frac{x}{\xi} \right) \right] \quad (4.6)$$

The splitting functions are given by:

$$P_{qq}(z) = \frac{4}{3} \left( \frac{1+z^2}{1-z} \right) \quad (4.7)$$

$$P_{gq}(z) = \frac{4}{3} \left( \frac{1+(1-z)^2}{z} \right) \quad (4.8)$$

$$P_{qg}(z) = \frac{1}{2} (z^2 + (1-z)^2) \quad (4.9)$$

$$P_{gg}(z) = 6 \left( \frac{1-z}{z} + \frac{z}{1-z} + z(1-z) \right) \quad (4.10)$$

Eq.4.5 and 4.6 are the DGLAP evolution equations in leading order of  $\alpha_s$ . They describe the evolution of the parton density with the scale  $\mu^2$ . By knowing the parton density at any scale  $\mu^2$ , these equations predict the parton density at any other scale. Although we cannot calculate the parton densities from first principles, these equations allow us to predict the parton densities at any scale, once they are determined at another scale. In Fig. 4.1 is shown the comparison of the measurement of the structure function  $\sigma^{red}(x, Q^2)$  with the prediction from a DGLAP evolution (for  $\sigma^{red}(x, Q^2)$  as a function of  $Q^2$  see Fig. 3.3). The Reduced cross section  $\sigma^{red}(x, Q^2)$  is related to  $F_2(x, Q^2)$  by:

$$\sigma^{red} = \frac{d^2\sigma}{dx dQ^2} \frac{Q^4 x}{2\pi\alpha^2(1+(1-y)^2)} = F_2 - \frac{y^2}{1+(1-y)^2} F_L \quad (4.11)$$

with  $F_L$  being the longitudinal structure function. The prediction agrees with the measurement remarkably well over several orders of magnitude in  $x$  and  $Q^2$ . This is a real triumph of the theory.

## 4.1 Conservation and Sum Rules

In the following we investigate further the evolution equations.

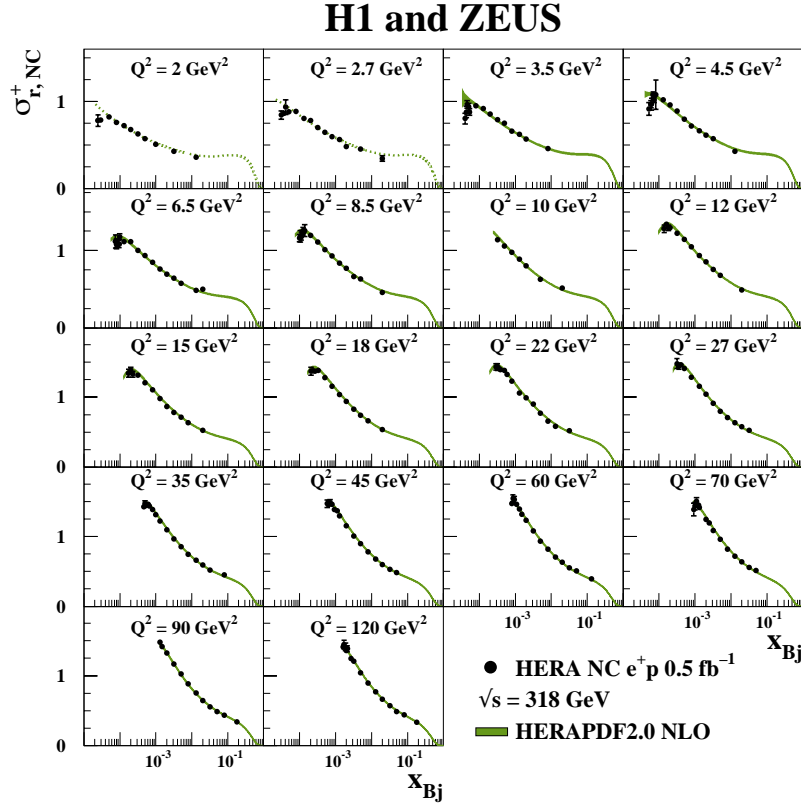


Figure 4.1: The reduced cross section  $\sigma_r^{red}(x, Q^2)$  as a function of  $x$  for different regions in  $Q^2$  as measured in DIS scattering  $e + p \rightarrow e' + X$  at HERA [27].

#### 4.1.1 Flavor Conservation

The scale dependent quark density as a function of the bare parton density  $q_0$  and the scale dependent divergent part ( $\kappa \rightarrow 0$ ) can be written as:

$$q(x, \mu^2) = \int_x^1 \frac{d\xi}{\xi} q_0(\xi) \left[ \delta\left(1 - \frac{x}{\xi}\right) + \frac{\alpha_s}{2\pi} P_{qq} \left( \frac{x}{\xi} \right) \log \frac{\mu^2}{\kappa^2} + \dots \right] \quad (4.12)$$

$$= \int_x^1 \frac{d\xi}{\xi} q_0(\xi) \hat{q}(z, \mu^2) + \dots \quad (4.13)$$

$$= \int_x^1 d\xi \int_0^1 dz \delta(x - z\xi) q_0(\xi) \hat{q}(z, \mu^2) + \dots \quad (4.14)$$

with

$$\hat{q}(z, \mu^2) = \delta(1 - z) + \frac{\alpha_s}{2\pi} P_{qq}(z) \log \frac{\mu^2}{\kappa^2} \quad (4.15)$$

where we have used  $z = \frac{x}{\xi}$  and  $\delta(1 - z)dz = \delta(1 - \frac{x}{\xi})dz = \xi \delta(\xi - x)dz$ .

However, this is not the full expression in  $\mathcal{O}(\alpha_s)$ , since we have not yet included virtual gluon radiation, self-energy insertions on the quark leg and vertex corrections. One can calculate the virtual corrections explicitly, but here we use the argument of conservation of quark (and baryon)

number: the integral over  $z$  of the quark distribution cannot vary with  $\mu^2$ :

$$\int_0^1 dz \hat{q}(z, \mu^2) = 1 \quad (4.16)$$

For this we redefine the splitting function as:

$$P_{qq}(z) = \hat{P}_{qq}(z) + k \cdot \delta(1 - z) \quad (4.17)$$

With this we get:

$$\int dz \left[ \delta(1 - z) + \frac{\alpha_s}{2\pi} \left( \hat{P}_{qq}(z) + k \cdot \delta(1 - z) \right) \log \frac{\mu^2}{\kappa^2} \right] = 1$$

With  $\log \frac{\mu^2}{\kappa^2} \neq 0$  we obtain

$$\int_0^1 dz \frac{\alpha_s}{2\pi} \left( \hat{P}(z) + k \cdot \delta(1 - z) \right) = 0$$

Some of the splitting functions are divergent for  $z \rightarrow 1$  and we cannot perform the integral easily. However we note, that the region  $z \rightarrow 1$  leads to no real emission and this has a final state similar to a virtual contribution to the no-emission diagram. To treat this singularity formally we introduce a " + " distribution (similar to the  $\delta$ -distribution which is only defined inside an integral):

$$\int_0^1 dx \frac{f(x)}{(1-x)_+} = \int_0^1 dx \frac{f(x) - f(1)}{(1-x)} \quad (4.18)$$

or in general [32]:

$$\begin{aligned} \int_0^1 dx f(x) [F(x)]_+ &= \int_0^1 dx (f(x) - f(1)) F(x) \\ \text{with } \int_0^1 dx [F(x)]_+ &= 0 \end{aligned}$$

We now use the expression for the quark splitting  $\hat{P}_{qq}(z) = \frac{1+z^2}{(1-z)_+}$ :

$$\int_0^1 dz P_{qq}(z) = \int_0^1 dz \left[ \frac{1+z^2}{(1-z)_+} + k \cdot \delta(1-z) \right] \quad (4.19)$$

$$= \int_0^1 dz \frac{1+z^2-2}{1-z} + k \quad (4.20)$$

$$= k + \int_0^1 dz \frac{-(1-z^2)}{1-z} \quad (4.21)$$

$$= k - \int_0^1 dz \frac{(1+z)(1-z)}{1-z} \quad (4.22)$$

$$= k - \int_0^1 dz (1+z) = k - \frac{3}{2} \quad (4.23)$$

where in eq.(4.20) the expression  $f(z) - f(1) = 1 - z^2 - 2$  has been used. Thus we obtain:

$$P_{qq}(z) = \frac{1+z^2}{(1-z)_+} + \frac{3}{2} \delta(1-z) \quad (4.24)$$



With this expression for  $P_{qq}$  we ensure that soft singularities are properly cancelled. This expression is essential to ensure that the sum rules are fulfilled (here for the proton case) independently of  $\mu^2$ :

$$\begin{aligned} \int_0^1 dx u_v(x, \mu^2) &= 2 \\ \int_0^1 dx d_v(x, \mu^2) &= 1 \end{aligned}$$

In Fig. 4.2 the different diagrams which contribute to  $F_2(x, Q^2)$  at  $\mathcal{O}(\alpha_s)$  are shown.

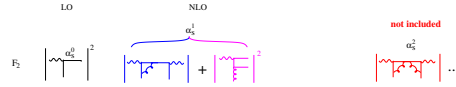


Figure 4.2: The different diagrams which contribute to  $F_2(x, Q^2)$  at  $\mathcal{O}(\alpha_s)$ . Note that at  $\mathcal{O}(\alpha_s)$  only the interference diagram of  $\mathcal{O}(\alpha_s^0)$  and the virtual contribution together with the real  $\mathcal{O}(\alpha_s)$  diagram contribute, while the virtual diagram squared would give  $\mathcal{O}(\alpha_s^2)$ .

#### 4.1.2 Conservation Rules of Splitting Functions

In this section we will check explicitly the conservation of momentum fractions using the momentum sum rule:

$$\int_0^1 dx x \left( \sum_i q_i(x, Q^2) + g(x, Q^2) \right) = 1 \quad (4.25)$$

to obtain constraints on the splitting functions.

We apply the momentum sum rule and make use of the DGLAP evolution equation for the quark and gluons:

$$\begin{aligned} \frac{dq_i(x, \mu^2)}{d \log \mu^2} &= \frac{\alpha_s}{2\pi} \int_x^1 \frac{d\xi}{\xi} \left[ q_i(\xi, \mu^2) P_{qq} \left( \frac{x}{\xi} \right) + g(\xi, \mu^2) P_{qg} \left( \frac{x}{\xi} \right) \right] \\ \frac{dg(x, \mu^2)}{d \log \mu^2} &= \frac{\alpha_s}{2\pi} \int_x^1 \frac{d\xi}{\xi} \left[ \sum_i q_i(\xi, \mu^2) P_{gq} \left( \frac{x}{\xi} \right) + g(\xi, \mu^2) P_{gg} \left( \frac{x}{\xi} \right) \right] \end{aligned}$$

Summing over all quark flavors and integrating over  $\log \mu^2$  gives:

$$\begin{aligned} \int_0^1 dx x \left( \sum_i q_i(x, Q^2) + g(x, Q^2) \right) &= \int d \log \mu^2 \int_0^1 dx \left[ \sum_i x q_i(x, \mu_0^2) \right. \\ &\quad + \frac{\alpha_s}{2\pi} \int \frac{d\xi}{\xi} \left( \sum_i x q_i(\xi, \mu^2) P_{qq} + 2n_f x g(\xi, \mu^2) P_{qg} \right) \\ &\quad \left. + x g(x, \mu_0^2) + \frac{\alpha_s}{2\pi} \int \frac{d\xi}{\xi} (x g(x, \mu^2) P_{gg} + x q(\xi, \mu^2) P_{gq}) \right] \end{aligned}$$

with  $n_f$  being the number of flavors. With a change of the order of the integration from  $\int dx \int d\xi$  to  $\int d\xi \int dx$  and using  $z = x/\xi$  we obtain:

$$\begin{aligned}
\int_0^1 dx \, x \left( \sum_i q_i(x, Q^2) + g(x, Q^2) \right) &= \int_0^1 dx \sum_i x q_i(x, \mu_0^2) + x g(x, \mu_0^2) \\
&\quad + \frac{\alpha_s}{2\pi} \int d \log \mu^2 \int_0^1 dz \int_x^1 d\xi \left[ \sum_i z \xi q_i(\xi, \mu^2) P_{qq} \right. \\
&\quad \left. + 2n_f z \xi g(\xi, \mu^2) P_{qg} + z \xi g(\xi, \mu^2) P_{gg} + z \xi q(\xi, \mu^2) P_{gq} \right] \\
&= \int_0^1 dx \sum_i x q_i(x, \mu_0^2) + x g(x, \mu_0^2) \\
&\quad + \frac{\alpha_s}{2\pi} \int d \log \mu^2 \int_0^1 dz \int_x^1 d\xi \left[ \sum_i \xi q_i(\xi, \mu^2) (z (P_{qq} + P_{gq})) \right. \\
&\quad \left. + \xi g(\xi, \mu^2) (z (P_{gg} + 2n_f P_{qg})) \right]
\end{aligned}$$

Since the momentum sum rule has to be satisfied for all  $\mu^2$ , we obtain:

$$\int_0^1 dz \, z (P_{qq} + P_{gq}) = 0 \quad (4.26)$$

$$\int_0^1 dz \, z (P_{gg} + 2n_f P_{qg}) = 0 \quad (4.27)$$

## 4.2 Collinear factorization

Collinear factorization means that the collinear singularities are factorized into process independent parton distributions and perturbatively calculable process dependent hard scattering cross sections (or coefficient functions). A detailed discussion on factorization can be found in [33, 34].

The cross section of scattering process of vector boson  $V$  on a hadron  $h$  can be written as:

$$\sigma(V + h) = f_h(\mu_f) \otimes C_a^V(\mu_f, \mu_r), \quad (4.28)$$

where  $f$  is the parton distribution function and  $C_a^V$  is the hard scattering cross section which is infrared safe and calculable in pQCD. The index  $a$  indicates, that this cross section depends on the type of the incoming partons. In addition,  $C_a^V$  depends on the factorization ( $\mu_f$ ) and renormalization ( $\mu_r$ ) scales, but is independent from long distance effects, especially independent on the hadron  $h$ . For example, in deep inelastic scattering the  $C_a^V$  are the same for scattering on a pion, proton, neutron etc. The parton distribution function  $f$  contains all the infrared sensitivity and is specific for the hadron  $h$  and also depends on the factorization scale  $\mu_f$ . The parton distribution function  $f$  are universal and independent on the hard scattering.

Please note, that the factorization theorems are only proven for a few processes [34]:

- deep inelastic scattering (DIS)
- diffractive deep inelastic scattering
- Drell Yan (DY) production in hadron hadron collisions
- single particle inclusive spectra (fragmentation functions)

For all other processes, factorization is assumed (and it is shown by comparing predictions with measurements, that this assumption is rather successful).

### 4.2.1 Factorization Schemes

Different schemes for separating the long from short distance parts are available (factorization schemes). The difference between them is, which pieces of the cross section are factorized into the parton density functions. Common schemes are:

- **DIS scheme**

$$F_2(x, Q^2) = x \sum_i e_i^2 q_i(x, Q^2)$$

where the index  $i$  runs over all parton flavors and  $q(x, Q^2)$  is the quark (or antiquark) density. Gluons enter only via the evolution of the quark densities. This formula is required to hold at all orders in  $\alpha_s$ . The DIS scheme is obtained from  $\mu^2 = Q^2$ .

- $\overline{\text{MS}}$  scheme (modified minimal subtraction)

Only the divergent pieces are absorbed into the quark and gluon densities. The structure function  $F_2(x, Q^2)$  is then:

$$F_2^{\overline{\text{MS}}}(x, Q^2) = x \sum_q e_q^2 \int \frac{dx_2}{x_2} \left[ q^{\overline{\text{MS}}}(x_2, Q^2) \left[ \delta \left( 1 - \frac{x}{x_2} \right) + \frac{\alpha_s}{2\pi} C_q^{\overline{\text{MS}}} \left( \frac{x}{x_2} \right) \right] + g^{\overline{\text{MS}}}(x_2, Q^2) \frac{\alpha_s}{2\pi} C_g^{\overline{\text{MS}}} \left( \frac{x}{x_2} \right) \right]$$

Once a specific scheme is chosen, it has to be used for both the parton density and the partonic cross section, otherwise inconsistent results are obtained.

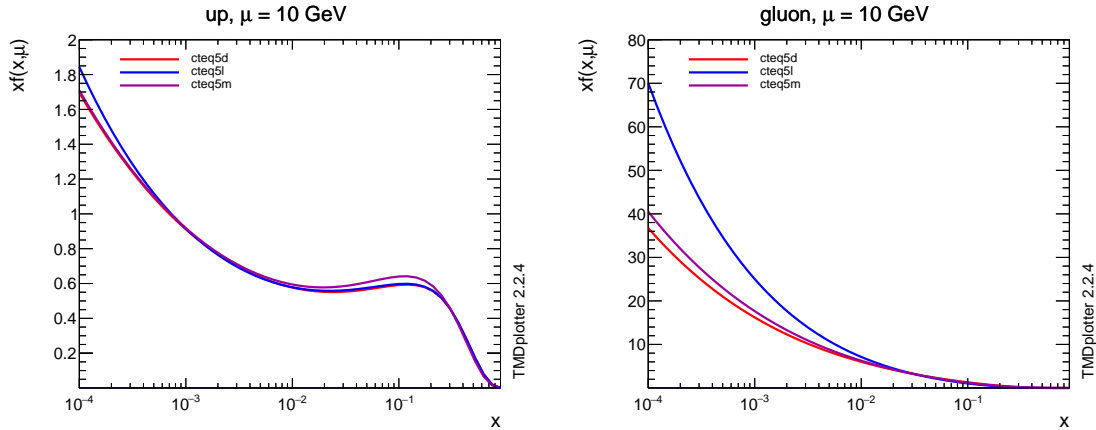


Figure 4.3: The up-quark (left) and gluon (right) densities as a function of  $x$  at  $\mu = 10$  GeV obtained in [35] in LO (CTEQ5L) and in NLO in the DIS (CTEQ5D) and  $\overline{\text{MS}}$  (CTEQ5M) scheme [36,37]

## 4.3 Solution of DGLAP equations

Several methods exist to solve the DGLAP equations, here we only consider a numerical solution of the integro-differential equations. We first consider a solution of the evolution equation at small

$x$  and then discuss the more general case.

### 4.3.1 Double Leading Log approximation for small $x$

In this section we consider only the limit of small  $x$ . In this limit, only the gluon density contributes with the splitting function  $P_{gg}(x) \rightarrow 6/x$ . All other contributions are small and can be neglected. With this the evolution equation eq.(4.6) becomes:

$$\frac{dg(x, \mu^2)}{d \log \mu^2} = \frac{\alpha_s}{2\pi} \int_x^1 \frac{d\xi}{\xi} \left[ g(\xi, \mu^2) P_{gg} \left( \frac{x}{\xi} \right) \right] \quad (4.29)$$

This equation can be integrated to give:

$$xg(x, \mu^2) = xg(x, \mu_0^2) + \frac{\alpha_s}{2\pi} \int_{\mu_0^2}^{\mu^2} \frac{d\mu'^2}{\mu'^2} \int_x^1 \frac{d\xi}{\xi} xg(\xi, \mu'^2) P\left(\frac{x}{\xi}\right) \quad (4.30)$$

$$= xg(x, \mu_0^2) + \frac{3\alpha_s}{\pi} \int_{\mu_0^2}^{\mu^2} \frac{d\mu'^2}{\mu'^2} \int_x^1 \frac{d\xi}{\xi} \xi g(\xi, \mu'^2) \quad (4.31)$$

This equation is an integral equation of Fredholm type

$$\phi(x) = f(x) + \lambda \int_a^b K(x, y) \phi(y) dy$$

and can be solved by iteration (Neumann series):

$$\begin{aligned} \phi_0(x) &= f(x) \\ \phi_1(x) &= f(x) + \lambda \int_a^b K(x, y) f(y) dy \\ \phi_2(x) &= f(x) + \lambda \int_a^b K(x, y_1) f(y_1) dy_1 + \lambda^2 \int_a^b \int_a^b K(x, y_1) K(y_1, y_2) f(y_2) dy_2 dy_1 \end{aligned}$$

This can be written in a compact form:

$$\phi_n(x) = \sum_{i=0}^n \lambda^i u_i(x) \quad (4.32)$$

with

$$\begin{aligned} u_0(x) &= f(x) \\ u_1(x) &= \int_a^b K(x, y) f(y) dy \\ u_n(x) &= \int_a^b \cdots \int_a^b K(x, y_1) K(y_1, y_2) \cdots K(y_{n-1}, y_n) f(y_n) dy_1 \cdots dy_n \end{aligned}$$

with the solution:

$$\phi(x) = \lim_{n \rightarrow \infty} q_n(x) = \lim_{n \rightarrow \infty} \sum_{i=0}^n \lambda^i u_i(x) \quad (4.33)$$

Applying this method to solve the evolution equation for the gluon density at small  $x$  eq.(4.31) with  $xg(x, \mu_0^2) = xg_0(x) = C$ , we obtain:

$$xg_1(x, t) = \frac{3\alpha_s}{\pi} C \int_{t_0}^t d\log t' \int_x^1 d\log \xi = \frac{3\alpha_s}{\pi} \log \frac{t}{t_0} \log \frac{1}{x} C \quad (4.34)$$

$$xg_2(x, t) = \frac{1}{2} \frac{1}{2} \left( \frac{3\alpha_s}{\pi} \log \frac{t}{t_0} \log \frac{1}{x} \right)^2 C \quad (4.35)$$

$\vdots$

$$xg_n(x, t) = \frac{1}{n!} \frac{1}{n!} \left( \frac{3\alpha_s}{\pi} \log \frac{t}{t_0} \log \frac{1}{x} \right)^n C \quad (4.36)$$

$$xg(x, t) = \lim_{n \rightarrow \infty} \sum_n \frac{1}{n!} \frac{1}{n!} \left( \frac{3\alpha_s}{\pi} \log \frac{t}{t_0} \log \frac{1}{x} \right)^n C \quad (4.37)$$

Using the modified Bessel function:

$$I_0(z) = \sum_{k=0}^{\infty} \frac{\left(\frac{1}{4}z^2\right)^k}{(k!)^2} = \frac{e^z}{\sqrt{2\pi z}} \quad (4.38)$$

We identify

$$z = 2\sqrt{\frac{3\alpha_s}{\pi} \log \frac{t}{t_0} \log \frac{1}{x}}$$

to obtain:

$$xg(x, t) \sim C \exp \left( 2\sqrt{\frac{3\alpha_s}{\pi} \log \frac{t}{t_0} \log \frac{1}{x}} \right) \quad (4.39)$$

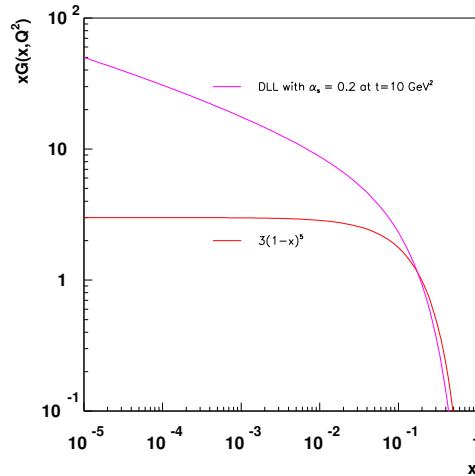


Figure 4.4: The gluon density from  $xG(x) = 3(1-x)^5$  and the DLL result with  $\alpha_s = 0.2$  and  $t = 10 \text{ GeV}^2$ .

Please note that this result has been obtained by taking the limit of large double leading logarithms:

- small  $x$  limit in the splitting function which leads to  $\log 1/x$
- small  $t$  limit to obtain evolution equation, which leads to  $\log 1/t$ .

The DLL solution of the evolution equations results in a rapid rise of the gluon density at small  $x$ , however only so-called contributions from strongly ordered (decreasing) values of  $x$  and strongly ordered (increasing) values of  $t$  are considered. Note, that the unlimited rise at small  $x$  is of course unphysical, and for a realistic description a sort of taming (or saturation) of the distribution is required.

### 4.3.2 From evolution equation to parton branching

In the previous section we have seen how to solve the evolution equation iteratively. By performing the small  $x$  limit, we avoided the difficulties with the soft divergencies at large  $x$ ; we did not need to use the plus-prescription of the splitting function.

In this section we now discuss how to solve the full evolution equation and how to treat the soft limit. The divergency of a soft real emission is cancelled by virtual contributions, that is, we can define so-called "resolvable" branchings, which are splittings of one into two (or more) partons, where at least in principle we can resolve the splitting. The "non-resolvable" branchings consist of a contribution without branching and the virtual contributions. A detailed discussion of the parton evolution can be found in [24]. The full application of this idea is described as the Parton Branching method in Refs. [38, 39].

We define a "Sudakov" form factor  $\Delta_s$ :

$$\Delta_s(t) = \exp \left( - \int dz \int_{t_0}^t \frac{\alpha_s}{2\pi} \frac{dt'}{t'} P(z) \right) \quad (4.40)$$

and use the evolution equation with the "+" prescription (using  $t = \mu^2$ ):

$$t \frac{\partial}{\partial t} f(x, t) = \int \frac{dz}{z} \frac{\alpha_s}{2\pi} P_+(z) f\left(\frac{x}{z}, t\right)$$

Inserting the explicit expression for  $P_+$  we obtain:

$$t \frac{\partial}{\partial t} f(x, t) = \int_0^1 \frac{dz}{z} \frac{\alpha_s}{2\pi} P(z) f\left(\frac{x}{z}, t\right) - \frac{\alpha_s}{2\pi} f(x, t) \int_0^1 dz P(z) \quad (4.41)$$

where we have used the definition in eq.(4.18):

$$\begin{aligned} \int_0^1 dz \frac{f(z)}{z} P_+(z) &= \int_0^1 dz \left( \frac{f(\frac{x}{z})}{z} - f(x) \right) P(z) \\ &= \int_0^1 dz \frac{f(\frac{x}{z})}{z} P(z) - f(x) \int_0^1 dz P(z) \end{aligned}$$

Using

$$\frac{\partial e^{-a(x)}}{\partial x} = -e^{-a(x)} \frac{\partial a(x)}{\partial x}$$

we obtain:

$$\frac{\partial \Delta_s}{\partial t} = -\Delta_s \left[ \frac{1}{t} \int dz \frac{\alpha_s}{2\pi} P(z) \right] \quad (4.42)$$

$$\rightsquigarrow \frac{t}{\Delta_s} \frac{\partial \Delta_s}{\partial t} = - \int dz \frac{\alpha_s}{2\pi} P(z) \quad (4.43)$$

Inserting this into eq.(4.41) we obtain:

$$t \frac{\partial}{\partial t} f(x, t) = \int \frac{dz}{z} \frac{\alpha_s}{2\pi} P(z) f\left(\frac{x}{z}, t\right) + f(x, t) \frac{t}{\Delta_s} \frac{\partial \Delta_s}{\partial t} \quad (4.44)$$

Multiplying eq.(4.44) with  $1/\Delta_s$  and using  $\frac{\partial}{\partial t} \frac{f}{\Delta_s} = \frac{1}{\Delta_s} \frac{\partial f}{\partial t} - \frac{f}{\Delta_s^2} \frac{\partial \Delta_s}{\partial t}$  we obtain:

$$\frac{t}{\Delta_s} \frac{\partial f(x, t)}{\partial t} - \frac{t}{\Delta_s^2} f(x, t) \frac{\partial \Delta_s}{\partial t} = \int \frac{dz}{z} \frac{1}{\Delta_s} \frac{\alpha_s}{2\pi} P(z) f\left(\frac{x}{z}, t\right) \quad (4.45)$$

$$t \frac{\partial}{\partial t} \frac{f(x, t)}{\Delta_s} = \int \frac{dz}{z} \frac{1}{\Delta_s} \frac{\alpha_s}{2\pi} P(z) f\left(\frac{x}{z}, t\right) \quad (4.46)$$

which is the DGLAP evolution equation in a form using the Sudakov form factor  $\Delta_s$  as defined in eq.(4.40).

We can now integrate eq.(4.46) to obtain:

$$f(x, t) = f(x, t_0) \Delta(t) + \int \frac{dt'}{t'} \frac{\Delta(t)}{\Delta(t')} \frac{\alpha_s(t')}{2\pi} \int \frac{dz}{z} P(z) f\left(\frac{x}{z}, t'\right) \quad (4.47)$$

where we have used

$$\int_{t_0}^t \frac{\partial}{\partial t'} \frac{f(x, t')}{\Delta_s} dt' = \int \frac{dt'}{t'} \frac{1}{\Delta_s} \frac{\alpha_s}{2\pi} \int \frac{dz}{z} P(z) f\left(\frac{x}{z}, t'\right) \quad (4.48)$$

From eq.(4.47) we can now interpret the Sudakov form factor as being the probability for evolution without any resolvable branching from  $t_0$  to  $t$ .

We have been sloppy in defining  $\Delta_s(t)$  in eq.(4.40), as we did not specify the integration limits for the  $z$  integration. In the following we show, that the evolution equation can be written with an upper limit  $z_M$  of the  $z$  integral. We start from eq.(4.41) with the expansion of the plus prescription:

$$\begin{aligned} t \frac{\partial}{\partial t} f(x, t) &= \int_0^{z_M} \frac{dz}{z} \frac{\alpha_s}{2\pi} P(z) f\left(\frac{x}{z}, t\right) + \int_{z_M}^1 \frac{dz}{z} \frac{\alpha_s}{2\pi} P(z) f\left(\frac{x}{z}, t\right) \\ &\quad - \frac{\alpha_s}{2\pi} f(x, t) \int_0^{z_M} dz P(z) - \frac{\alpha_s}{2\pi} f(x, t) \int_{z_M}^1 dz P(z) \end{aligned} \quad (4.49)$$

If  $z_M$  is large enough, then we can replace  $\frac{dz}{z} f\left(\frac{x}{z}, t\right)$  with  $dz f(x, t)$  and we obtain:

$$\begin{aligned} t \frac{\partial}{\partial t} f(x, t) &= \int_0^{z_M} \frac{dz}{z} \frac{\alpha_s}{2\pi} P(z) f\left(\frac{x}{z}, t\right) + f(x, t) \int_{z_M}^1 dz \frac{\alpha_s}{2\pi} P(z) \\ &\quad - \frac{\alpha_s}{2\pi} f(x, t) \int_0^{z_{cut}} dz P(z) - \frac{\alpha_s}{2\pi} f(x, t) \int_{z_{cut}}^1 dz P(z) \\ &= \int_0^{z_M} \frac{dz}{z} \frac{\alpha_s}{2\pi} P(z) f\left(\frac{x}{z}, t\right) - \frac{\alpha_s}{2\pi} f(x, t) \int_0^{z_M} dz P(z) \end{aligned} \quad (4.50)$$

What did we gain ? We needed to treat the singularity at  $z \rightarrow 1$ . For this, we now introduce a upper cut-off  $z_M = 1 - \epsilon$ . Branchings with  $z > z_M$  are now classified as unresolved: they involve the emission of undetectable partons [24]. The Sudakov form factor sums virtual and real corrections

to all orders; the virtual corrections affect the non-branching probability are included via unitarity: the resolvable branching probability gives via unitarity the sum of virtual and unresolvable contributions.

Eq.(4.47) can now be solved by iteration, in the same way as before. The starting function  $f_0$  is just the first term in eq.(4.47). The first iteration  $f_1$  involves one branching:

$$\begin{aligned} f_0(x, t) &= f(x, t_0)\Delta(t) \\ f_1(x, t) &= f(x, t_0)\Delta(t) + \frac{\alpha_s}{2\pi} \int_{t_0}^t \frac{dt'}{t'} \frac{\Delta(t)}{\Delta(t')} \int_x^1 \frac{dz}{z} \tilde{P}(z) f(x/z, t_0) \Delta(t') \end{aligned} \quad (4.51)$$

The iteration is illustrated in fig.4.5 The term  $f_0$  in eq.(4.51) is illustrated in the left part of Fig. 4.5:

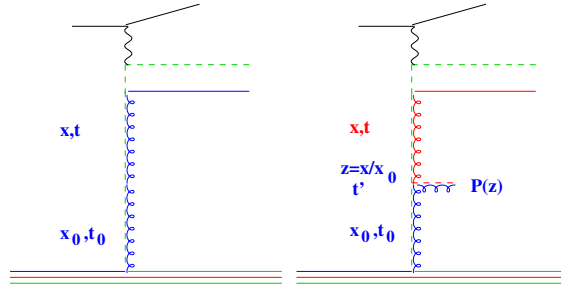


Figure 4.5: Schematic representation of the first branchings in an iterative procedure to solve the evolution equation

the evolution from  $t_0$  to  $t$  without any resolvable branching. The term  $f_1$  in eq.(4.51) is shown in the right part of Fig. 4.5: there is evolution from  $t_0$  to  $t'$  without any resolvable branching, then at  $t'$  the branching happens, where the splitting is given by the splitting function  $P(z)$ ; then the evolution continues without any resolvable branching from  $t'$  to  $t$ .

The full solution of the integral equation by iteration is then:

$$\begin{aligned} f_0(x, t) &= f(x, t_0)\Delta(t) \\ f_1(x, t) &= f(x, t_0)\Delta(t) + \frac{\alpha_s}{2\pi} \int_{t_0}^t \frac{dt'}{t'} \frac{\Delta(t)}{\Delta(t')} \int \frac{dz}{z} \tilde{P}(z) f(x/z, t_0) \Delta(t') \\ &= f(x, t_0)\Delta(t) + \log \frac{t}{t_0} A \otimes \Delta(t) f(x/z, t_0) \\ f_2(x, t) &= f(x, t_0)\Delta(t) + \log \frac{t}{t_0} A \otimes \Delta(t) f(x/z, t_0) + \\ &\quad \frac{1}{2} \log^2 \frac{t}{t_0} A \otimes A \otimes \Delta(t) f(x/z, t_0) \\ f(x, t) &= \lim_{n \rightarrow \infty} f_n(x, t) = \lim_{n \rightarrow \infty} \sum_n \frac{1}{n!} \log^n \left( \frac{t}{t_0} \right) A^n \otimes \Delta(t) f(x/z, t_0) \end{aligned} \quad (4.52)$$

where  $A = \int \frac{dz}{z} \tilde{P}(z)$  is a symbolic representation of the integral over  $z$  and  $\otimes$  indicates that a convolution has to be performed. The eq.(4.52) shows the solution of the DGLAP evolution equation is a resummation to all orders in  $\alpha_s \log t$ .<sup>1</sup>

<sup>1</sup>It is interesting to note, that only the  $1/(1-z)$  part of the splitting functions is needed in the Sudakov form factor. This simplifies the solution process.



The Sudakov form factor can be interpreted in terms of a probability: it is a poisson distribution with zero mean  $P(0, p) = e^{-p}$ . If the poisson distribution gives the probability to observe  $n$  emissions, then  $P(0, p)$  gives the probability for no emission and is the so-called "non-branching probability". The one-branching probability is given in terms of Poisson statistics by:  $P(1, p) = pe^{-p}$ , which is exactly the first iteration of the evolution equation:

$$f(x, t) = f(x, t_0) \Delta_s(t) + \int dz \int dx' \int \frac{dt'}{t'} \cdot \frac{\Delta_s(t)}{\Delta_s(t')} \frac{\alpha_s}{2\pi} \tilde{P}(z) \times f(x', t_0) \Delta_s(t') \delta(x - zx') \quad (4.53)$$

where delta function has been introduced to make the different integration steps visible.

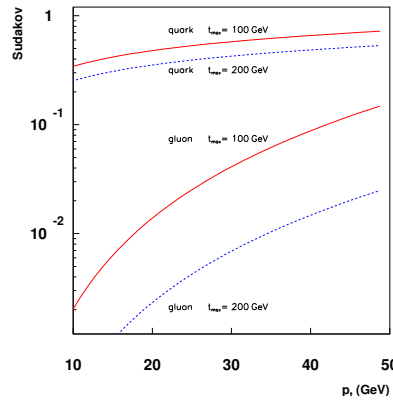


Figure 4.6: Sudakov form factor as a function of the lower scale  $p_t$  for gluon and quark splitting functions using  $\alpha_s = 0.2$ . The upper scale is set to  $t_{max} = 100(200)$  GeV.

### 4.3.3 Ordering conditions

The DGLAP equation describes successive parton emissions from small to large scales  $t$ . With the introduction of Sudakov form factors, we order those emissions, since the Sudakov form factor gives the probability of no emission between  $t_1$  and  $t_2$ . When simulating each individual emission, we can ask about a physical meaning of the evolution scale  $t$ . In the following we describe the so-called *angular ordering*, which means that emissions that do not follow an increasing angle of the emitted parton are highly suppressed. Angular ordering was already discussed in cosmic ray studies and known as the "Chudakov effect" (1955).

In a process  $b \rightarrow a + c$  (Fig. 4.7), applying light-cone kinematics, one can calculate  $q_{t,c}$  from conservation of the plus momentum for particle  $a$  moving along the  $z$ -axis, with  $p_b^+ = zp_a^+$  and  $p_c^+ = (1-z)p_b^+$ . We use  $p_a^2 = 2p_a^+p_a^- - k_{ta}^2$  and assume  $k_{tb} = 0$ ,  $k_{ta} = -k_{tc} = q_t$  and apply light-cone

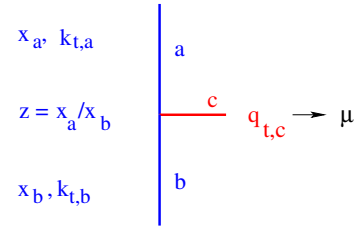


Figure 4.7: Illustration of a general splitting process:  $b \rightarrow a + c$

momentum conservation of  $p^+$  and  $p^-$  to obtain:

$$p_b^- = p_a^- + p_c^- \quad (4.54)$$

$$\frac{p_b^2}{2p_b^+} = \frac{p_a^2 + q_t^2}{2p_a^+} + \frac{p_c^2 + q_t^2}{2p_c^+} \quad (4.55)$$

$$\frac{p_b^2}{2p_b^+} = \frac{p_a^2 + q_t^2}{2p_b^+ z} + \frac{p_c^2 + q_t^2}{2p_b^+ (1-z)} \quad (4.56)$$

and obtain:

$$p_b^2 = \frac{p_a^2 + q_t^2}{z} + \frac{p_c^2 + q_t^2}{1-z} \quad (4.57)$$

### Virtuality Ordering

In virtuality ordering we associate the evolution scale  $t$  with the virtuality  $Q^2$  of the propagating parton, no details about the emissions are needed. However we can calculate kinematic relations between the propagating and emitted partons, and build relations to the transverse momentum of the parton.

For a space-like branching with  $\mu^2 = -p_a^2$  and taking  $p_b^2 = p_c^2 = 0$ , one obtains from eq.(4.57): [40–42]:

$$q_{t,c}^2 = (1-z)\mu^2 \quad (4.58)$$

### Transverse Momentum Ordering

In transverse momentum ordering the evolution scale is simply associated with the transverse momentum of either the propagating parton  $k_T$  or the emitted parton  $q_T$ .

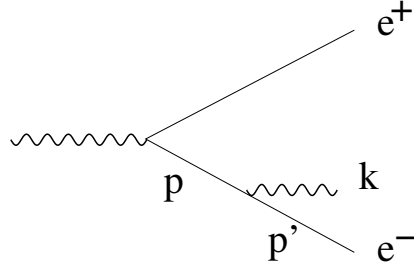
In the region of small  $x$  (taking  $z \rightarrow 0$ ) eq.(4.57) reduces to  $q_{t,c} = \mu$  (called  $q_T$ -ordering).

### Angular Ordering

The ordering condition of successive parton emission determines how many partons can be radiated in a certain region of phase space. Subsequent emissions can be suppressed because of destructive interference effects. The angular ordering condition takes these interference effect approximately into account.

We first describe the angular ordering condition [24, 25] for the case of photon radiation from a  $e^+e^-$  pair, then we discuss the more complicated QCD case. We consider a process  $\gamma \rightarrow e^+e^-\gamma$  as shown in Fig. 4.8 and we calculate the lifetime of the  $e^+e^-$  pair:  $\Delta t = \frac{1}{\Delta E}$ . We use lightcone vectors  $p'$  for the outgoing electron and  $p$  for the intermediate electron before photon radiation (we neglect the electron mass  $m_e$ ) and we take  $z$  as the longitudinal momentum fraction of the radiated photon  $k$ :

$$\begin{aligned} p &= \frac{1}{\sqrt{2}}(p^+, p^-, 0) = \frac{1}{\sqrt{2}}(p^+, 0, 0) \\ p' &= \frac{1}{\sqrt{2}}((1-z)p^+, p^-, -k_T) = \frac{1}{\sqrt{2}}\left((1-z)p^+, \frac{k_T^2}{(1-z)p^+}, -k_T\right) \\ k &= \frac{1}{\sqrt{2}}(zp^+, k^-, k_T) = \frac{1}{\sqrt{2}}(zp^+, \frac{k_T^2}{zp^+}, k_T) \end{aligned}$$

Figure 4.8: Schematic representation of the angular ordering constraint in  $e^+e^-$  scattering.

We calculate the energy imbalance  $\Delta E$  with:

$$\begin{aligned}
 \Delta E &= p' + k - p \\
 &= \frac{1}{2} ((p' + k)^+ + (p' + k)^-) - \frac{1}{2} (p^+ + p^-) \\
 &= \frac{1}{2} \left( p^+ + \frac{k_T^2}{z(1-z)p^+} - p^+ \right) = \frac{1}{2} \frac{k_T^2}{z(1-z)p^+} \\
 \rightsquigarrow \Delta E &= \frac{1}{2} \frac{k_T^2}{zp^+} \text{ for } z \rightarrow 0
 \end{aligned}$$

using:

$$\begin{aligned}
 p' + k &= \left( (1-z)p^+ + zp^+, \frac{k_T^2}{(1-z)p^+} + \frac{k_T^2}{zp^+}, 0 \right) \\
 &= \left( p^+, \frac{zk_T^2 + (1-z)k_T^2}{z(1-z)p^+}, 0 \right) = \left( p^+, \frac{k_T^2}{z(1-z)p^+}, 0 \right)
 \end{aligned}$$

For small angles we have  $k_T \sim zp^+ \Theta_{e\gamma}$

$$\Delta E \sim \frac{1}{2} \frac{z^2 p^{+2} \Theta_{e\gamma}^2}{zp^+} = \frac{1}{2} zp^+ \Theta_{e\gamma}^2 = \frac{1}{2} k \Theta_{e\gamma}^2$$

Introducing the transverse wavelength  $\lambda_\perp^{-1} = k_T = \Theta_{e\gamma} k$  we obtain for the lifetime  $\Delta t$ :

$$\Delta t = \frac{1}{\Delta E} = 2 \frac{\lambda_\perp}{\Theta_{e\gamma}} \quad (4.59)$$

During the time  $\Delta t$ , the  $e^+e^-$  pair travels a distance:

$$\rho_\perp^{e^+e^-} = \Delta x \Delta t \sim \Theta_{ee} \Delta t = \theta_{e^+e^-} \frac{\lambda_\perp}{\Theta_{e\gamma}}$$

For  $\Theta_{e\gamma} \gg \Theta_{e^+e^-}$  we obtain:

$$\rho_\perp < \lambda_\perp$$

which means that the radiated photon cannot resolve any structure of the  $e^+e^-$  pair, it probes only the total charge which is zero.

The electron can emit photons if:

$$\begin{aligned}
 \rho_\perp &> \lambda_\perp \\
 \rightsquigarrow \Theta_{e\gamma} &< \theta_{e^+e^-}
 \end{aligned}$$

which is the angular ordering condition for QED. Outside this region, the cross section for radiation is suppressed.

In QCD a similar picture emerges, but the radiation of soft gluons from a pair of quarks is no longer zero (since the color charge is non-zero, and gluons can radiate from gluons), but the radiation is, as if it were emitted from the parent gluon (see Fig. 4.9). In QCD gluon emission is allowed:

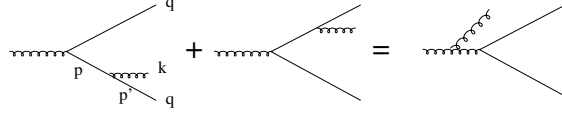


Figure 4.9: Schematic representation of radiation from a pair of quarks whose color charge is non-zero.

$$\begin{aligned} & \text{off } \bar{q} \text{ for } \Theta_{k\bar{q}} < \Theta_{q\bar{q}} \\ & \text{off } q \text{ for } \Theta_{kq} < \Theta_{q\bar{q}} \\ & \text{off parent } g \text{ for } \Theta_{kg} > \Theta_{q\bar{q}} \end{aligned}$$

such that soft gluon emission at large angles is suppressed (an explicit calculation can be found in [24]).

In the following we describe how the angular ordering condition is applied to the parton evolution. The vector of the radiated parton is denoted with  $q$ , and the energy component of this vector

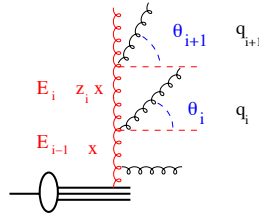


Figure 4.10: Schematic representation of radiation in an angular ordered region of phase space.

is given by  $q_0$ . The energy of the propagating parton is given by  $E$ . We define the transverse momenta as  $q_{ti} = |q_i^0| \sin \Theta_i$  (taking partons to be massless) where we define the splitting variable  $z = \frac{E_i}{E_{i-1}}$  for the  $i$  and  $(i-1)$  parton. Defining  $q_i = \frac{q_{ti}}{1-z_i}$  and the angles

$$\begin{aligned} \Theta_i &= \frac{q_i}{E_{i-1}} \\ \Theta_{i+1} &= \frac{q_{i+1}}{E_i} \end{aligned}$$

we obtain:

$$\begin{aligned} \Theta_i &> \Theta_{i-1} \\ \rightsquigarrow \frac{q_i}{E_{i-1}} &> \frac{q_{i-1}}{E_{i-2}} \\ \rightsquigarrow q_i &> \frac{E_{i-1}}{E_{i-2}} q_{i-1} = z_{i-1} q_{i-1} \end{aligned} \tag{4.60}$$

We finally obtain for the angular ordering:

$$q_{max} > z_n q_n, q_n > z_{n-1} q_{n-1}, \dots, q_1 > Q_0 \quad (4.61)$$

and referring to eq.(4.57):

$$q_{t,c}^2 = (1 - z)^2 \mu^2 \quad (4.62)$$

The angular ordering condition in Eq.(4.60) gives for  $z \rightarrow 0$  essentially no constraint on the values of  $q_i$  and therefore on  $q_T$ , allowing for a *random walk* in  $k_T$  space, as requested from the BFKL equation. On the other hand, at large  $z$  the angular ordering condition reduces to ordering in  $q_i$ , as requested from the DGLAP evolution equations.

## 4.4 Solution of evolution equation with Monte Carlo method

As described above, the evolution equations Eqs.(4.47) are integral equations of the Fredholm type

$$f(x) = f_0(x) + \lambda \int_a^b K(x, y) f(y) dy$$

and can be solved by iteration as a Neumann series

$$\begin{aligned} f_1(x) &= f_0(x) + \lambda \int_a^b K(x, y) f_0(y) dy \\ f_2(x) &= f_0(x) + \lambda \int_a^b K(x, y_1) f_0(y_1) dy_1 + \lambda^2 \int_a^b \int_a^b K(x, y_1) K(y_1, y_2) f_0(y_2) dy_2 dy_1 \\ &\dots \end{aligned} \quad (4.63)$$

using the kernel  $K(x, y)$ , with the solution

$$f(x) = \lim_{n \rightarrow \infty} \sum_{i=0}^n f_i(x). \quad (4.64)$$

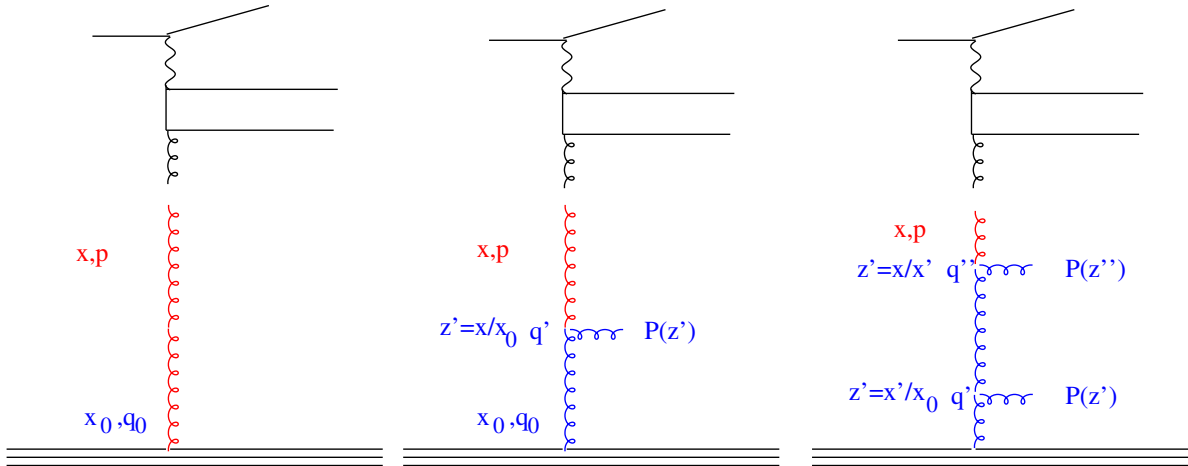


Figure 4.11: Evolution by iteration

In a Monte Carlo (MC) solution [38, 39, 43–45] we evolve from  $t_0$  to a value  $t'$  obtained from the Sudakov factor  $\Delta_s(t')$  (for a schematic visualisation of the evolution see fig. 4.11). Note that the Sudakov factor  $\Delta_s(t')$  gives the probability for evolving from  $t_0$  to  $t'$  without resolvable branching. The value  $t'$  is obtained from solving for  $t'$ :

$$R = \Delta_s(t'), \quad (4.65)$$

for a random number  $R$  in  $[0, 1]$ .

If  $t' > t$  then the scale  $t$  is reached and the evolution is stopped, and we are left with just the first term without any resolvable branching. If  $t' < t$  then we generate a branching at  $t'$  according to the splitting function  $\tilde{P}(z')$ , as described below, and continue the evolution using the Sudakov factor  $\Delta_s(t'', t')$ . If  $t'' > t$  the evolution is stopped and we are left with just one resolvable branching at  $t'$ . If  $t'' < t$  we continue the evolution as described above. This procedure is repeated until we generate  $t'$ 's which are larger than  $t$ . By this procedure we sum all kinematically allowed contributions in the series  $\sum f_i(x, p)$  and obtain an MC estimate of the parton distribution function.

With the Sudakov factor  $\Delta_s$  and using

$$\frac{\partial}{\partial t'} \Delta_s(t') = -\Delta_s(t') \left[ \frac{1}{t'} \right] \int^{z_M} dz P(z),$$

we can write the first iteration of the evolution equation as

$$\begin{aligned} f_1(x, t) &= f_0(x, t) \\ &+ \int_x^1 \frac{dz'}{z'} \int_{t_0}^t (-d\Delta_s(t')) P(z') f_0(x/z', t') \left[ \int^{z_M} dz P(z) \right]^{-1}. \end{aligned} \quad (4.66)$$

The integrals can be solved by a Monte Carlo method [21]:  $z$  is generated from

$$\int_{z_{min}}^z dz' P(z') = R_1 \int_{z_{min}}^{z_M} dz' P(z'), \quad (4.67)$$

with  $R_1$  being a random number in  $[0, 1]$ , and  $t'$  is generated from

$$\begin{aligned} R_2 &= \int_{-\infty}^x f(x') dx' = F(x) \\ &= \int_{t'}^{t''} \frac{\partial \Delta_s(t'')}{\partial t''} dt'' \\ &= \Delta_s(t') \end{aligned} \quad (4.68)$$

solving for  $t'$ , using  $z$  from above and another random number  $R_2$  in  $[0, 1]$ .

This completes the calculation on the first splitting. This procedure is repeated until  $t' > t$  and the evolution is stopped.

With  $z'$  and  $t'$  selected according to the above the first iteration of the evolution equation yields

$$\begin{aligned} x f_1(x, t) &= x f_0(x) \Delta_s(t) \\ &+ \sum_i \tilde{P}(z'_i) x'_i f_0(x'_i, t'_i) \left[ \int^{z_M} dz \tilde{P}(z) \right]^{-1}, \end{aligned} \quad (4.69)$$

with  $x'_i = x/z_i$ .

## 4.5 Exercises: Parton Evolution

6. Calculate the Sudakov form factor for the scales  $t_2 = 10, 100, 500 \text{ GeV}^2$  as a function of  $t_1$  and plot it as a function of  $t_1$ . Use  $q$  as the argument for  $\alpha_s$ , and check the differences. For the  $z$  integral use  $z_{min} = 0.01$  and  $z_{max} = 0.99$ .

$$\log \Delta_S = - \int_{t_1}^{t_2} \frac{dt}{t} \int_{z_{min}}^{z_{max}} dz \frac{\alpha_s}{2\pi} P(z)$$

Use the gluon and also the quark splitting functions :

$$P_{gg} = 6 \left( \frac{1-z}{z} + \frac{z}{1-z} + z(1-z) \right)$$

and

$$P_{qq} = \frac{4}{3} \frac{1+z^2}{1-z}$$

7. write a program to evolve a parton density  $g(x) = 3(1-x)^5/x$  from a starting scale  $t_0 = 1 \text{ GeV}^2$  to and higher scale  $t = 100 \text{ GeV}^2$ . Do the evolution only with fixed  $\alpha_s = 0.1$  and an approximate gluon splitting function  $P_{gg} = 6(\frac{1}{z} + \frac{1}{1-z})$ . To avoid the divergent regions use  $z_{min} = \epsilon$  and  $z_{max} = 1 - \epsilon$  with  $\epsilon = 0.1$ . Calculate the Sudakov form factor for evolving from  $t_1$  to  $t_2$  using only the  $\frac{1}{(1-z)}$  part of the splitting function. Generate  $z$  according to  $P_{gg}$ . Repeat the branching until you reach the scale  $t$ . Plot the  $xg(x)$  as a function of  $x$  for the starting distribution and for the evolved distribution. Repeat the same exercise but with  $P_{qq} = \frac{4}{3} \frac{1+z^2}{1-z}$ .

Calculate and plot the transverse momentum of the parton after the evolution. At the starting scale the partons can have a intrinsic  $k_T$ , which is generated by a gauss distribution with  $\mu = 0$  and  $\sigma = 0.7$  (use generating a gauss distribution from Exercise 1).

Compare the  $k_t$  distribution using  $P_{gg}$  and  $P_{qq}$ . What is different ?

## 4.6 Exercise: Parton Evolution

### 4.6.1 Sudakov form factor and Monte Carlo integration.

## 4.7 Sudakov form factor and Monte Carlo integration.

We calculate the Sudakov form factor and plot it for different upper scales as function of  $p_t$

**Authors: H. Jung, S. Taheri Monfared, P. L.S. Connor, R. Zlebcik**

```
[1]: import numpy as np
import matplotlib.pyplot as plt
from math import sqrt, log, pi, exp
```

The strong coupling  $\alpha_s$ , input  $q$  is in GeV

```
[2]: def alphaS(q):
    QCDlam = 0.2 #Lambda QCD for 3 flavours
    Qlam0 = 1 #scale freezing
    nf = 3 #number of flavours
    beta0 = (33 - 2*nf) / 6
    Qval = max(Qlam0, q)
    return pi / (beta0*log(Qval/QCDlam))
```

The splitting function at the LO without  $\alpha_s$  gluon  $\rightarrow$  gluon or quark  $\rightarrow$  quark splitting

```
[3]: def Splitting(z):
    # return 6*(1/z -2 +z*(1-z) + 1/(1-z)) # g -> g
    return 4/3*((1+z*z)/(1-z)) # q -> q
```

Integrand inside of the Sudakov, note this is a bit different from C++ example

```
[4]: def suda(t1, t2):
    # Generate randomly q2
    q2 = t1*pow(t2/t1, rng.random())
    # we generate here z1 = 1-z,
    # because we have a pole in the splitting functions \sim 1/(1-z)
    # Generate randomly z1
    z1min, z1max = 0.01, 0.99
    z1 = z1min*pow(z1max/z1min, rng.random())

    z = 1. - z1
    q = sqrt(q2)
    integrand = alphaS(q)/2/pi * Splitting(z) /q2
    weight = q2*log(t2/t1) * z1*log(z1max/z1min)
    return integrand*weight
```

Book a histogram

```
[5]: npoints = 100000
ntmax = 20
tmin, tmax = 1., 500.
xceters=[]
# define histo to get easily bin edges and bin centers
histogram, bin_edge = np.histogram([], bins=ntmax, range=[tmin, tmax])
xceters = (bin_edge[:-1] + bin_edge[1:]) / 2
```

```
[6]: rng = np.random.default_rng(1234) # initialise random number generator PCG-64
print(rng)
```

Generator (PCG64)

```
[7]: # Loop over data points in the histogram
sum0 = sum00 = 0
sudakov=[]
sudError=[]
# Intergrate Sudakov between qt^2=tmin and tmax
for nt in range(0, ntmax):
    t1 = xceters[nt]
    t2 = tmax
    for i in range(npoints):
        ff = suda(t1, t2)
        sum0 += ff
        sum00 += ff**2

    sum0 /= npoints
    sum00 /= npoints
    sigma2 = sum00 - sum0*sum0
```



```

error = sqrt(sigma2/npoints)
sud = exp(-sum0)
sude = sud * error #Error of the sudakov
sudakov.append(sud)
sudError.append(sude)

print (" t2 = ", tmax , " qt2 = ", t1 , " Delta_S = " , sud , " +-" , sude)

#print (" sudakov ", sudakov)
plt.plot(xcenters, sudakov, label='Suda')
plt.errorbar(xcenters, sudakov, yerr=sudError)

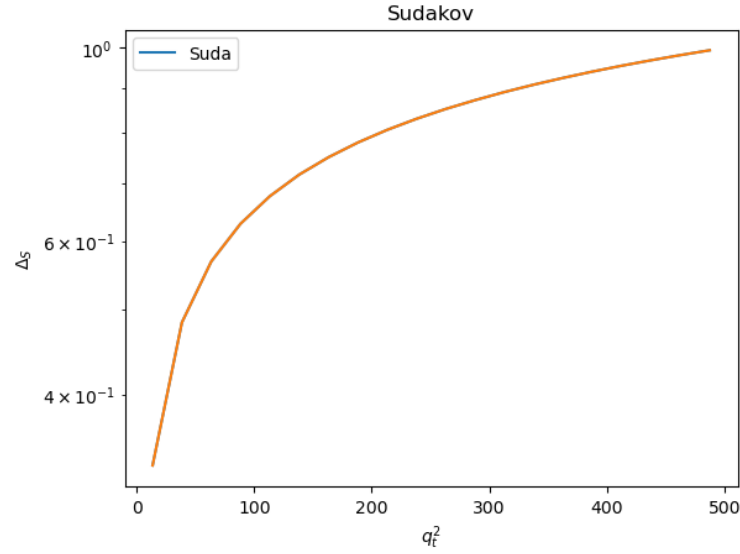
# Naming the x-axis, y-axis and the whole graph
plt.xlabel(r'$q_t^2$')
plt.ylabel(r'$\Delta_S$')
plt.title("Sudakov")
plt.yscale('log')

# Adding legend, which helps us recognize the curve according to it's color
plt.legend()

# To load the display window
plt.show()

t2 = 500.0 qt2 = 13.475 Delta_S = 0.33153538792494747 +-
0.00026899938647328894
t2 = 500.0 qt2 = 38.425 Delta_S = 0.483904096659392 +-
0.00022894398647500195
t2 = 500.0 qt2 = 63.375 Delta_S = 0.5684360893333312 +-
0.00020071633849311115
t2 = 500.0 qt2 = 88.32499999999999 Delta_S = 0.6282537525726155 +-
0.00017740211371734254
t2 = 500.0 qt2 = 113.275 Delta_S = 0.6757370962012309 +-
0.00015920193938944653
t2 = 500.0 qt2 = 138.225 Delta_S = 0.7153500714069108 +-
0.00014293188256717015
t2 = 500.0 qt2 = 163.175 Delta_S = 0.7490102253097977 +-
0.0001283391559547971
t2 = 500.0 qt2 = 188.125 Delta_S = 0.7787042203414885 +-
0.00011482836100188605
t2 = 500.0 qt2 = 213.075 Delta_S = 0.8052156521559881 +-
0.00010270871994182428
t2 = 500.0 qt2 = 238.02499999999998 Delta_S = 0.8291269773934135 +-
9.105976344443842e-05
t2 = 500.0 qt2 = 262.975 Delta_S = 0.8510533326106029 +-
8.016989306467372e-05
t2 = 500.0 qt2 = 287.92499999999995 Delta_S = 0.8710869324161294 +-
6.993887214079194e-05
t2 = 500.0 qt2 = 312.875 Delta_S = 0.8899580816377016 +-
6.033933601640325e-05
t2 = 500.0 qt2 = 337.825 Delta_S = 0.9074921424955467 +-
5.146045237245406e-05
t2 = 500.0 qt2 = 362.775 Delta_S = 0.9238652842376135 +-
4.234195011242482e-05
t2 = 500.0 qt2 = 387.725 Delta_S = 0.9393805435380566 +-
3.4072796478875666e-05
t2 = 500.0 qt2 = 412.67499999999995 Delta_S = 0.9540999414053157 +-
2.6069211135343195e-05
t2 = 500.0 qt2 = 437.625 Delta_S = 0.9679522151752206 +-
1.821831697548885e-05
t2 = 500.0 qt2 = 462.575 Delta_S = 0.9812466426762932 +-
1.079581441738966e-05
t2 = 500.0 qt2 = 487.525 Delta_S = 0.9938844785526225 +-
3.5401886597359683e-06

```



[ ]:

#### 4.7.1 Demonstration of the parton evolution using MC method

1. generate starting distribution in  $x$  and add intrinsic transverse momentum  $k_T$ .
2. evolve starting distribution to large values of  $t$

Plot starting distribution and intrinsic  $k_T$  and plot evolved distribution as function of  $x$  and  $k_T$

```
[1]: # First lets load the libraries which will be needed
import numpy as np
import matplotlib.pyplot as plt
from math import sqrt, log, log10, pi, exp, sin, cos

[2]: # Define 4-vector operations
# px, py, pz, E
# dot product of 4-vectors
def pdot(a, b):
    return a[3]*b[3] - a[0]*b[0] - a[1]*b[1] - a[2]*b[2]
# Define addition of 4-vectors
def padd(a, b):
    return a[0]+b[0], a[1]+b[1], a[2]+b[2], a[3]+b[3]
# Define mass**2 of 4-vector
def pmass2(a):
    return a[3]*a[3] - a[0]*a[0] - a[1]*a[1] - a[2]*a[2]
# Define mass of 4-vector
def pmass(a):
    return sqrt(max(0., a[3]*a[3] - a[0]*a[0] - a[1]*a[1] - a[2]*a[2]))
# Define pT
def ppT(a):
    return sqrt(max(0., a[0]*a[0] + a[1]*a[1]))
# Define Rapidity
def pRapidity(a):
    arg = a[3]-a[2]
    if arg == 0:
        rap = -99999.
    else:
        rap = 0.5*log((a[3]+a[2])/(a[3]-a[2]))
    return rap
```

Define function which returns 2D point according to the Gaussian distribution

```
[3]: def gauss2D(sigma):
    kT = sigma * sqrt(-2.*log(rng.random()));
    phi = 2.*pi * rng.random()
    kx, ky = kT*cos(phi), kT*sin(phi)
    return (kx, ky)
```

Get starting PDF at the starting scale  $q^2$  ( $q^2=1$ )

```
[4]: Eb = 3500. # Beam energy
def get_starting_pdf(q2):
    xmin = 0.00001
    xmax = 0.999
    # get x value according to g(x)\sim 1/x
    x = xmin * (xmax/xmin)**rng.random()
    weightx = x*log(xmax/xmin)
    # use: xg(x) = 3 (1-x)**5
    pdf = 3.*pow((1-x),5.)/x

    # now generate intrinsic kt according to a gauss distribution
    kx, ky = gauss2D(0.7)
    En = sqrt(kx**2 + ky**2 + (x*Eb)**2)
    pvec=kx, ky, x*Eb, En
    return pvec, weightx * pdf
```

Calculate Sudakov form factor

```
[5]: def sudakov(t0):
    # here we calculate from the sudakov form factor the next t > t0
    epsilon = 0.1
    as2pi = 0.1/(2.*pi)
    Ca = 3.
    # for Pgg use fact = 2*Ca
    fac = 2.*Ca
    # use fixed alphas and only the 1/(1-z) term of the splitting fct

    r1 = rng.random()
    Pint=log((1.-epsilon)/epsilon) # for 1/(1-z) splitting fct
    t2 = -log(r1)/fac/as2pi/Pint
    t2 = t0 * exp(t2)
    assert(t2 >= t0)
    return t2
```

Splitting function which is needed to get the z on the branching point

```
[6]: def splitting():
    epsilon = 0.1

    as2pi = 0.1/2./pi

    # here we calculate the splitting variable z for 1/z and 1/(1-z)
    # use Pgg=6(1/z + 1/(1-z)) // for large z we use z -> 1-z

    g0 = 6.*as2pi * log((1.-epsilon)/epsilon)
    g1 = 6.*as2pi * log((1.-epsilon)/epsilon)
    gtot = g0 + g1

    zmin = epsilon
    zmax = 1.-epsilon

    r1 = rng.random()
    r2 = rng.random()

    z = zmin * (zmax/zmin)**r2
    if r1 > g0/gtot:
        z = 1. - z
    weightz = 1.
    return z
```

Evolve the PDF between scales  $q_0^2$  and  $q^2$ , calculate the kinematics of the parton

```
[7]: def evolve_pdf(q20, q2, p0):
    x = p0[2]/Eb
    kx = p0[0]
    ky = p0[1]
    weightx = 1.
    t1 = q20
    tcut = q2
    while t1 < tcut:
        # here we do now the evolution
        # first we generate t
        t0 = t1
        t1 = sudakov(t0)

        # now we generate z
        z = splitting()
        # since the sudakov involves only the 1/(1-z) part
        # of the splitting fct, we need to weight each branching
        # by the ratio of the integral of the full and
```

```

# approximate splitting fct

ratio_splitting = 2 # for using Pgg

if t1 < tcut:
    x = x*z
    weightx = weightx *ratio_splitting
    #
    # use here the angular ordering condition: sqrt(t1) = qt/(1-z)
    # and apply this also to the propagator gluons
    #
    phi = 2.*pi*rng.random()
    kx += sqrt(t1)*cos(phi)*(1.-z)
    ky += sqrt(t1)*sin(phi)*(1.-z)
    # kx += sqrt(t1)*cos(phi)
    # ky += sqrt(t1)*sin(phi)
    k=kx, ky, x*Eb, 0.
    return k, weightx

```

```

[8]: # initialise random number generator:
rng = np.random.default_rng(1234) # initialise random number generator PCG-64
print(rng)

```

Generator(PCG64)

Do the evolution between scales q20 and q21 npoints times

```

[9]: q20 = 1.
q21 = 100.**2
npoints = 100000
weightx = 1
Weight_x=[]
Weight_x0=[]
Weight_xlog10=[]
Weight_x0log10=[]

x0_log10=[]
x_log10=[]
k0_Pt= []
k_Pt = []
for n1 in range(npoints):
    # generate starting distribution in x and kt
    k0, weightx0 = get_starting_pdf(q20)
    # now do the evolution
    k, weightx = evolve_pdf(q20, q21, k0)
    weightx = weightx0 * weightx

    # weighting with 1/x0:
    # plot dxg(x)/dlogx *Jacobian, Jacobian dlogx/dx = 1/x
    # log(x) = 2.3026 log10(x)
    x = abs(k[2])/Eb
    x0 = abs(k0[2])/Eb
    x0_log10.append(log10(x0))
    x_log10.append(log10(x))
    k0_Pt.append(sqrt(k0[0]**2+k0[1]**2))
    k_Pt.append(sqrt(k[0]**2+k[1]**2))
    Weight_x0.append(weightx0)
    Weight_x.append(weightx)
    Weight_x0log10.append(weightx0/npoints/log(10))
    Weight_xlog10.append(weightx/npoints/log(10))

```

Plot the x distribution in the starting scale and after the evolution

```

[10]: fig, axs = plt.subplots(figsize=(6, 6),nrows=2, ncols=2,sharey=False, tight_layout=False)
histo1,bin_edge = np.histogram(x0_log10, bins=100, range=[-5,0],weights=Weight_x0, density=False)
xcenters = (bin_edge[:-1] + bin_edge[1:]) / 2
bin_width= (bin_edge[1:] - bin_edge[:-1])
# normalize histo with log(10) and bin_width
histo1 = histo1/log(10)/bin_width/npoints
# use step (instead plot) to plot histogram style
axs[0,0].step(xcenters, histo1)
axs[0,0].set_xlabel(r'$x_0$')
histo2,bin_edge = np.histogram(x_log10, bins=100, range=[-5,0],weights=Weight_x, density=False)
xcenters = (bin_edge[:-1] + bin_edge[1:]) / 2.
bin_width= (bin_edge[1:] - bin_edge[:-1])
histo2 = histo2/log(10)/bin_width/npoints
axs[0,1].step(xcenters, histo2)
axs[0,1].set_xlabel(r'$x$')

histo3,bin_edge = np.histogram(k0_Pt, bins=100, range=[0,10],weights=Weight_x0, density=False)

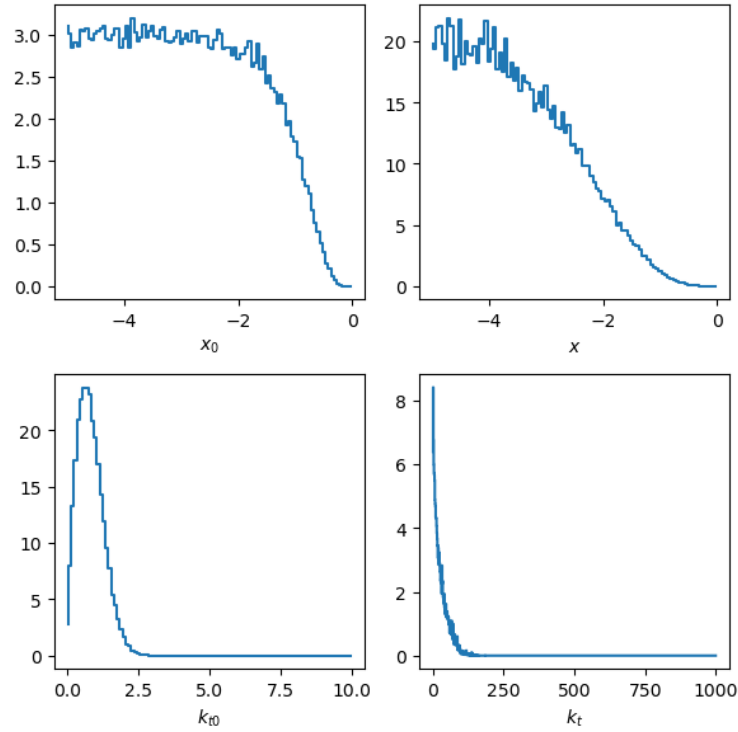
```

```

xcenters = (bin_edge[:-1] + bin_edge[1:]) / 2.
bin_width= (bin_edge[1:] - bin_edge[:-1])
histo3 = histo3/bin_width/npoints
axs[1,0].step(xcenters, histo3)
axs[1,0].set_xlabel(r'$k_{t0}$')
histo4,bin_edge = np.histogram(k_Pt, bins=1000, range=[0,1000],weights=Weight_x, density=False)
xcenters = (bin_edge[:-1] + bin_edge[1:]) / 2.
bin_width= (bin_edge[1:] - bin_edge[:-1])
histo4 = histo4/bin_width/npoints
axs[1,1].step(xcenters, histo4)
axs[1,1].set_xlabel(r'$k_t$')
#axs[1,1].set_xscale('log')

```

[10]: Text(0.5, 0, '\$k\_{t0}\$')





## Chapter 5

# The Parton Branching Method

The Parton Branching (PB) method is a method to solve evolution equations with Monte Carlo techniques by applying the concept of resolvable and non-resolvable branchings in terms of Sudakov form factors. Please note here, that resolvable branching does not necessarily mean experimentally resolvable, we use the wording just to distinguish it from a situation, where even in principle a branching could not be resolved. The separation of resolvable and non-resolvable branching is given in terms of  $z_M = 1 - \epsilon$ , with  $\epsilon \rightarrow 0$ , while numerically in the Monte Carlo calculation  $\epsilon \neq 0$ . In addition we divide the phase space into a perturbative and non-perturbative region: the perturbative region is defined by  $z \leq z_{\text{dyn}} = 1 - q/q_0$  and the nonperturbative region is then  $z_{\text{dyn}} < z < z_M$ , with  $q$  being the evolution scale and  $q_0$  some parameter of the order of a GeV.

### 5.1 The Parton Branching solution of the DGLAP equation

The method described in the previous section can now be applied to provide a Parton Branching solution of the DGLAP evolution equation. This method has been described in detail in Refs. [38,39].

We start by writing the DGLAP evolution equation for the momentum weighted parton density  $x f_a(x, \mu^2)$  of parton  $a$  with momentum fraction  $x$  at the scale  $\mu$  reads:

$$\mu^2 \frac{\partial x f_a(x, \mu^2)}{\partial \mu^2} = \sum_b \int_x^1 dz P_{ab}(\alpha_s(\mu^2), z) \frac{x}{z} f_b\left(\frac{x}{z}, \mu^2\right), \quad (5.1)$$

with the regularized DGLAP splitting functions  $P_{ab}$  describing the splitting of parton  $b$  into a parton  $a$ . The splitting functions  $P_{ab}$  can be decomposed as (in the notation of Ref. [38]):

$$P_{ab}(z, \alpha_s) = D_{ab}(\alpha_s) \delta(1 - z) + K_{ab}(\alpha_s) \frac{1}{(1 - z)_+} + R_{ab}(z, \alpha_s). \quad (5.2)$$

The coefficients  $D$  and  $K$  can be written as  $D_{ab}(\alpha_s) = \delta_{ab} d_a(\alpha_s)$ ,  $K_{ab}(\alpha_s) = \delta_{ab} k_a(\alpha_s)$  and the coefficients  $R_{ab}$  contain only terms which are not singular for  $z \rightarrow 1$ . Each of those three coefficients can be expanded in powers of  $\alpha_s$ :

$$d_a(\alpha_s) = \sum_{n=1}^{\infty} \left(\frac{\alpha_s}{2\pi}\right)^n d_a^{(n-1)}, \quad k_a(\alpha_s) = \sum_{n=1}^{\infty} \left(\frac{\alpha_s}{2\pi}\right)^n k_a^{(n-1)}, \quad R_{ab}(z, \alpha_s) = \sum_{n=1}^{\infty} \left(\frac{\alpha_s}{2\pi}\right)^n R_{ab}^{(n-1)}(z). \quad (5.3)$$

We introduce the real-emission branching probabilities  $P_{ab}^{(R)}(\alpha_s(\mu^2), z)$ ,

$$P_{ab}^{(R)}(\alpha_s(\mu^2), z) = K_{ab}(\alpha_s(\mu^2)) \frac{1}{1-z} + R_{ab}(\alpha_s(\mu^2), z) . \quad (5.4)$$

The evolution equation for the momentum weighted parton density  $xf_a(x, \mu^2)$  at scale  $\mu$  is then given by (as a solution of eq.(5.1), see also [24]) (we put  $\alpha_s/2\pi$  outside of the splitting functions  $P_{ab}(z)$ ):

$$xf_a(x, \mu^2) = \Delta_a^S(\mu^2) xf_a(x, \mu_0^2) + \sum_b \int_{\mu_0^2}^{\mu^2} \frac{d\mu'^2}{\mu'^2} \frac{\Delta_a^S(\mu^2)}{\Delta_a^S(\mu'^2)} \int_x^{z_M} dz \frac{\alpha_s}{2\pi} P_{ab}^{(R)}(z) \frac{x}{z} f_b\left(\frac{x}{z}, \mu'^2\right) \quad (5.5)$$

with the unregularized splitting functions  $\hat{P}_{ab}(z)$  (without the  $D_{ab}$  piece, replacing  $1/(1-z)_+$  by  $1/(1-z)$ ) and  $\mu_0$  being the starting scale.

We discuss the introduction of the Sudakov form factor as well as the integration limit  $z_M$  in the next subsections below.

### 5.1.1 The Momentum Sum Rule and the Sudakov form factor

Some of the splitting functions in eq.(5.2) contain singular parts for  $z \rightarrow 1$ , which are regulated via the plus-prescription  $\int_0^1 dz f(z) [g(z)]_+ = \int_0^1 [f(z) - f(1)] g(z)$  which yields:

$$\int_0^1 dz z [P(z)]_+ = \int_0^1 dz [zP^{(R)}(z) - P^{(R)}(z)] \quad (5.6)$$

In order to write the evolution equation for momentum weighted parton densities in terms of Sudakov form factors we apply the momentum sum rule  $\int_0^1 dz (zP_{qq}(z) + zP_{qg}(z)) = 0$ , eq.(4.26), and obtain for the quark density (written explicitly for quark and gluon densities):

$$\begin{aligned} \mu^2 \frac{\partial xq(x, \mu^2)}{\partial \mu^2} &= \frac{\alpha_s}{2\pi} \left[ \int_x^1 \frac{dz}{z} zP_{qq}^{(R)}(z) \frac{x}{z} q\left(\frac{x}{z}, \mu^2\right) + zP_{qg}^{(R)}(z) \frac{x}{z} g\left(\frac{x}{z}, \mu^2\right) \right] \\ &\quad - \frac{\alpha_s}{2\pi} xq(x, \mu^2) \int_0^1 dz P_{qq}^{(R)}(z) \\ &\quad - \frac{\alpha_s}{2\pi} xq(x, \mu^2) \left[ \int_0^1 dz zP_{qq}^{(R)}(z) + zP_{qg}^{(R)}(z) \right] \\ &= \frac{\alpha_s}{2\pi} \left[ \int_x^1 \frac{dz}{z} zP_{qq}^{(R)}(z) \frac{x}{z} q\left(\frac{x}{z}, \mu^2\right) + zP_{qg}^{(R)}(z) \frac{x}{z} g\left(\frac{x}{z}, \mu^2\right) \right] \\ &\quad - \cancel{\frac{\alpha_s}{2\pi} xq(x, \mu^2) \int_0^1 dz P_{qq}^{(R)}(z)} \\ &\quad - \frac{\alpha_s}{2\pi} xq(x, \mu^2) \left[ \int_0^1 dz zP_{qq}^{(R)}(z) - \cancel{\hat{P}_{qq}^{(R)}(z)} + zP_{qg}^{(R)}(z) \right] \\ &= \frac{\alpha_s}{2\pi} \left[ \int_x^1 \frac{dz}{z} zP_{qq}^{(R)}(z) \frac{x}{z} q\left(\frac{x}{z}, \mu^2\right) + zP_{qg}^{(R)}(z) \frac{x}{z} g\left(\frac{x}{z}, \mu^2\right) \right] \\ &\quad - \frac{\alpha_s}{2\pi} xq(x, \mu^2) \int_0^1 dz [zP_{qq}^{(R)}(z) + zP_{qg}^{(R)}(z)] , \end{aligned} \quad (5.7)$$



where we used in the second line the expansion of the plus-prescription in  $P_{qq}$ .

A similar structure can be obtained for the gluon density, applying the momentum sum rule  $\int_0^1 dz z (P_{gg} + 2n_f P_{qg}) = 0$ , as given in eq.(4.27):

$$\begin{aligned}
\mu^2 \frac{\partial xg(x, \mu^2)}{\partial \mu^2} &= \frac{\alpha_s}{2\pi} \left[ \int_x^1 \frac{dz}{z} z P_{gg}^{(R)}(z) \frac{x}{z} g\left(\frac{x}{z}, \mu^2\right) + 2n_f \int_x^1 \frac{dz}{z} z P_{gq}^{(R)}(z) \frac{x}{z} q\left(\frac{x}{z}, \mu^2\right) \right] \\
&\quad - \frac{\alpha_s}{2\pi} xg(x, \mu^2) \int_0^1 dz P_{gg}^{(R)}(z) \\
&\quad - \frac{\alpha_s}{2\pi} xg(x, \mu^2) \left[ \int_0^1 dz z P_{gg}^{(R)}(z) + 2n_f \int_0^1 dz z P_{gq}^{(R)}(z) \right] \\
&= \frac{\alpha_s}{2\pi} \left[ \int_x^1 \frac{dz}{z} z P_{gg}^{(R)}(z) \frac{x}{z} g\left(\frac{x}{z}, \mu^2\right) + z P_{gq}^{(R)}(z) \frac{x}{z} q\left(\frac{x}{z}, \mu^2\right) \right] \\
&\quad - \cancel{\frac{\alpha_s}{2\pi} xg(x, \mu^2) \int_0^1 dz P_{gg}^{(R)}(z)} \\
&\quad - \frac{\alpha_s}{2\pi} xg(x, \mu^2) \left[ \int_0^1 dz z P_{gg}^{(R)}(z) - \cancel{P_{gg}^{(R)}(z)} + 2n_f \int_0^1 dz z P_{gq}^{(R)}(z) \right] \\
&= \frac{\alpha_s}{2\pi} \left[ \int_x^1 \frac{dz}{z} z P_{gg}^{(R)}(z) \frac{x}{z} g\left(\frac{x}{z}, \mu^2\right) + 2n_f \int_x^1 \frac{dz}{z} z P_{gq}^{(R)}(z) \frac{x}{z} q\left(\frac{x}{z}, \mu^2\right) \right] \\
&\quad - \frac{\alpha_s}{2\pi} xg(x, \mu^2) \left[ \int_0^1 dz z P_{gg}^{(R)}(z) + 2n_f \int_0^1 dz z P_{gq}^{(R)}(z) \right] \tag{5.8}
\end{aligned}$$

The form of evolution equations in eqs.(5.7,5.8) have already the proper structure to identify the last term with a Sudakov form factor.

### 5.1.2 The limit $z_M$

We will show in the following that introducing an upper limit  $z_M$  in the integral of the evolution equations eqs.(5.7,5.8) will lead to consistent results, as long as  $z_M = 1 - \epsilon$  with  $\epsilon$  small, but not zero. We expand the parton density around  $z = 1$  (see [38]):

$$\frac{x}{z} f\left(\frac{x}{z}, \mu^2\right) = xf(x, \mu^2) + (1 - z) \frac{\partial xf(x, \mu^2)}{\partial \ln x} - \mathcal{O}(1 - z) \sim xf(x, \mu^2) \tag{5.9}$$

We write the evolution equation :

$$\begin{aligned}
\mu^2 \frac{\partial xq(x, \mu^2)}{\partial \mu^2} &= \frac{\alpha_s}{2\pi} \left[ \int_x^1 \frac{dz}{z} z P_{qq}^{(R)}(z) \frac{x}{z} q\left(\frac{x}{z}, \mu^2\right) + z P_{qg}^{(R)}(z) \frac{x}{z} g\left(\frac{x}{z}, \mu^2\right) \right] \\
&\quad - \frac{\alpha_s}{2\pi} xq(x, \mu^2) \int_0^1 dz \left[ z P_{qq}^{(R)}(z) + z P_{qg}^{(R)}(z) \right] \\
&= \frac{\alpha_s}{2\pi} \left[ \int_x^{z_M} \frac{dz}{z} z P_{qq}^{(R)}(z) \frac{x}{z} q\left(\frac{x}{z}, \mu^2\right) + z P_{qg}^{(R)}(z) \frac{x}{z} g\left(\frac{x}{z}, \mu^2\right) \right] \\
&\quad + \frac{\alpha_s}{2\pi} \left[ \int_{z_M}^1 dz \cancel{z P_{qq}^{(R)}(z) xq(x, \mu^2)} + P_{qg}^{(R)}(z) xg(x, \mu^2) \right] \\
&\quad - \frac{\alpha_s}{2\pi} xq(x, \mu^2) \int_0^{z_M} dz \left[ z P_{qq}^{(R)}(z) + z P_{qg}^{(R)}(z) \right] \\
&\quad - \frac{\alpha_s}{2\pi} xq(x, \mu^2) \int_{z_M}^1 dz \left[ \cancel{z P_{qq}^{(R)}(z)} + z P_{qg}^{(R)}(z) \right]
\end{aligned} \tag{5.10}$$

We use that  $R_{ab}$  has no power divergence for  $z \rightarrow 1$ , and the integration over  $R_{ab}$  for  $z_M < z < 1$  gives only  $\mathcal{O}(1 - z_M)$  which we finally can neglect (see discussion around eq.(2.20) in [38]). We obtain:

$$\begin{aligned}
\mu^2 \frac{\partial xq(x, \mu^2)}{\partial \mu^2} &= \frac{\alpha_s}{2\pi} \left[ \int_x^{z_M} \frac{dz}{z} z P_{qq}^{(R)}(z) \frac{x}{z} q\left(\frac{x}{z}, \mu^2\right) + z P_{qg}^{(R)}(z) \frac{x}{z} g\left(\frac{x}{z}, \mu^2\right) \right] \\
&\quad - \frac{\alpha_s}{2\pi} xq(x, \mu^2) \int_0^{z_M} dz \left[ z P_{qq}^{(R)}(z) + z P_{qg}^{(R)}(z) \right] + \mathcal{O}(1 - z_M),
\end{aligned} \tag{5.11}$$

The same arguments lead to the expression of the gluon density:

$$\begin{aligned}
\mu^2 \frac{\partial xg(x, \mu^2)}{\partial \mu^2} &= \frac{\alpha_s}{2\pi} \left[ \int_x^{z_M} \frac{dz}{z} z P_{gg}^{(R)}(z) \frac{x}{z} g\left(\frac{x}{z}, \mu^2\right) + 2n_f z P_{gq}^{(R)}(z) \frac{x}{z} q\left(\frac{x}{z}, \mu^2\right) \right] \\
&\quad - \frac{\alpha_s}{2\pi} xg(x, \mu^2) \left[ \int_0^{z_M} dz z P_{gg}^{(R)}(z) + 2n_f z P_{gq}^{(R)}(z) \right] + \mathcal{O}(1 - z_M),
\end{aligned} \tag{5.12}$$

We can now define a Sudakov form factor as:

$$\Delta_a^S(z_M, \mu^2) = \exp \left( - \sum_b \int_{\mu_0^2}^{\mu^2} \frac{d\mu'^2}{\mu'^2} \int_0^{z_M} dz \frac{\alpha_s}{2\pi} z P_{ba}^{(R)}(z) \right), \tag{5.13}$$

With

$$\frac{d \Delta_a^S(z_M, \mu^2, \mu_0^2)}{d \ln \mu^2} = - \Delta_a^S(z_M, \mu^2, \mu_0^2) \sum_b \int_0^{z_M} dz \frac{\alpha_s}{2\pi} z P_{ba}^{(R)}(z), \tag{5.14}$$

we obtain:

$$\begin{aligned}
\frac{d x f_a(x, \mu^2)}{d \ln \mu^2} &= \sum_b \int_x^{z_M} dz \frac{\alpha_s}{2\pi} P_{ab}^{(R)}(z) x f_b(x/z, \mu^2) \\
&\quad + \frac{1}{\Delta_a^S(\mu^2)} \frac{d \Delta_a^S(\mu^2)}{d \ln \mu^2} x f_a(x, \mu^2),
\end{aligned} \tag{5.15}$$

This evolution equation can be written in a similar form as eq.(5.1), but now in terms of real emission probabilities  $P_{ab}^{(R)}$  and Sudakov form factors:

$$\frac{d}{d \ln \mu^2} \left( \frac{x f_a(x, \mu^2)}{\Delta_a(\mu^2)} \right) = \sum_b \int_x^{z_M} dz \frac{\alpha_s}{2\pi} P_{ab}^{(R)}(z) \frac{x f_b(x/z, \mu^2)}{\Delta_a(\mu^2)}. \quad (5.16)$$

and write the evolution equation in terms of Sudakov form factors  $\Delta_a^S(z_M, \mu^2)$  (see eq.(5.5)):

$$x f_a(x, \mu^2) = \Delta_a^S(\mu^2) x f_a(x, \mu_0^2) + \sum_b \int_{\mu_0^2}^{\mu^2} \frac{d\mu'^2}{\mu'^2} \frac{\Delta_a^S(\mu'^2)}{\Delta_a^S(\mu^2)} \int_x^{z_M} dz \frac{\alpha_s}{2\pi} \hat{P}_{ab}(z) \frac{x}{z} f_b\left(\frac{x}{z}, \mu'^2\right) \quad (5.17)$$

This is the master equation for the evolution of parton densities applying the Parton Branching (PB) method.

Thus we observe that for  $z_M \rightarrow 1$  we have an expression of the DGLAP evolution equation in terms of Sudakov form factors. The advantage of using momentum weighted distributions is that, after application of momentum sum rule, a system of equations is obtained where in all terms the Sudakov form factor with the corresponding splitting function is present (not only for those terms with have a  $1/(1-z)$  term in the splitting function).

## 5.2 Determination of Parton Densities using the Parton-Branching Method

The method describes above has been used to determine collinear ( $k_T$ -integrated) parton densities.

In Fig. 5.1 the predictions of parton densities evolved to a large scale with the PB method [38] are shown and compared to calculations obtained with a conventional tool, QCDnum [46]. The predictions of the PB method are shown for different values of  $z_M$ . One can clearly see, that for values of  $z_M$  large enough, the predictions reproduce semi-analytical calculations exactly. Similar results have been obtained in Refs. [47–51].

This result is important in two aspects:

- the DGLAP evolution equation, solved with the concept of resolvable branchings, reproduces other solutions of DGLAP if the *soft resolution* scale  $z_M$  is large enough
- a iterative solution of the DGLAP equation using Monte Carlo techniques based on resolvable branchings as a Parton Branching method is equivalent to other solutions of DGLAP (i.e. QCDnum).

The PB-method has been used to determine collinear parton densities by a fit to inclusive DIS measurements [52], and two sets, depending which scale in  $\alpha_s$  is used, are obtained: PB-NLO-HERAI+II-set1 and PB-NLO-HERAI+II-set2: in set1 the evolution scale  $q$  is used, while in set2 the transverse momentum  $q(1-z)$  is used.

A remark on  $z_M$  is already important here:  $z_M$  must be close to one, otherwise a significant part of the parton evolution is left out. This will be further discussed in the section on Transverse Momentum Dependent (TMD) parton densities. Here we just illustrate the effect of  $z_M = z_{\text{dyn}} = 1 - q_0/q$ , with  $q_0$  being a free resolution parameter of the order of a GeV, on inclusive collinear distributions by performing the evolution, using the same parameters and starting distributions as in [52], but with a different cut on  $z_{\text{dyn}}$  (for details see [53]).

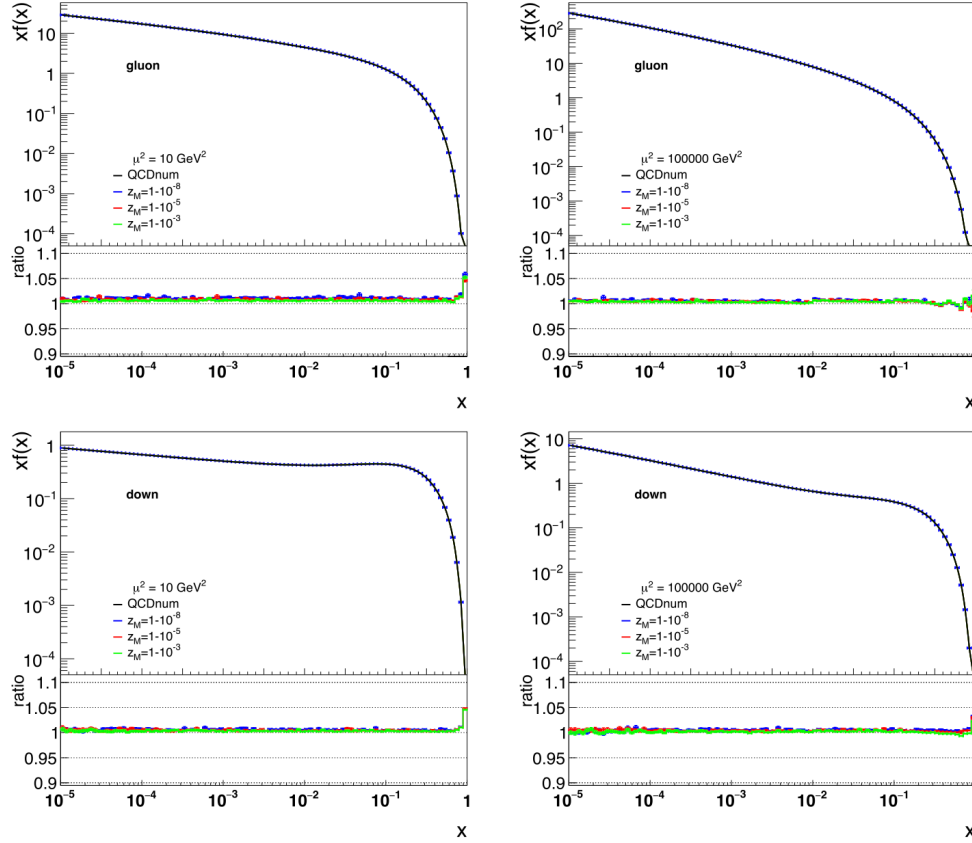


Figure 5.1: Integrated gluon and down-quark distributions at  $\mu^2 = 10 \text{ GeV}^2$  (left column) and  $\mu^2 = 10^5 \text{ GeV}^2$  (right column) obtained from the parton-branching solution for different values of  $z_M$ , compared with the result from QCDnum. The ratio plots show the ratio of the results obtained with the parton-branching method to the result from QCDnum. Figure taken from [38].

In Fig. 5.2 distributions for down-quarks are shown at different scales, illustrating the effect when  $z_M$  is smaller than one: soft gluons, with transverse momenta even below a resolution scale of  $q_0 = 1 \text{ GeV}$  play a very important role in collinear distributions, and cannot be neglected.

### 5.2.1 Connection of parton density with Cross Section

In this section we argue, that  $z_M \rightarrow 1$  on the basis of a connection to the cross section calculation. If  $z_M \ll 1$ , important pieces in the subtraction of collinear singularities from the hard cross section would be left uncanceled.

In section 3.79ff, where the splitting functions and the evolution equation were motivated, the integral over the momentum fraction was between  $x < \xi < 1$ . In calculations extending to next-to-leading order, it becomes even more obvious, that the integral over the splitting variable has to extend to one.

In the following we repeat the arguments from Ref. [53]: The calculation of deep inelastic scatter-

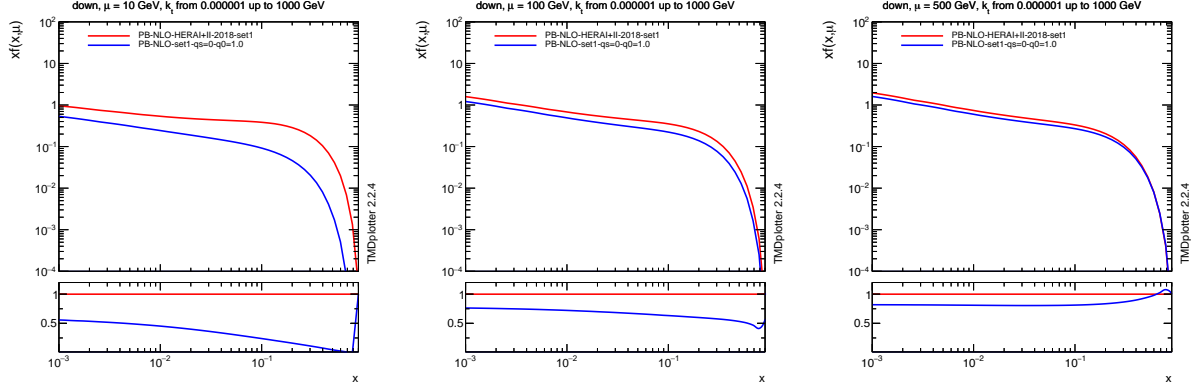


Figure 5.2: Integrated down-quark distributions at  $\mu = 10, 100$  GeV and  $\mu = 500$  GeV obtained from the PB approach for different values of  $z_M$ : PB-NLO-HERAI-II-set1 applies  $z_M \rightarrow 1$  and PB-NLO-set1 applies  $z_M = z_{\text{dyn}}$  with  $q_0 = 1$  GeV and without intrinsic  $-k_T$  distribution ( $q_s = 0$ ). The ratio plots show the ratios to the one for  $z_M \rightarrow 1$  (figures from [53]).

ing with NLO parton densities and coefficient functions, gives (see Ref. [24] eq. 4.80 ):

$$F_2(x, Q^2) = x \sum_{q, \bar{q}} e_q^2 \int_x^1 \frac{d\xi}{\xi} q(\xi, Q^2) \left[ \delta\left(1 - \frac{x}{\xi}\right) + \frac{\alpha_s}{2\pi} C_{\overline{\text{MS}}} \left(\frac{x}{\xi}\right) + \dots \right] \quad (5.18)$$

with the coefficient function  $C_{\overline{\text{MS}}}$  in  $\overline{\text{MS}}$ -scheme. The  $\overline{\text{MS}}$  coefficient function for massless quarks at  $\mathcal{O}(\alpha_s)$  read:

$$C_q^{\overline{\text{MS}}}(z) = C_F \left[ 2 \left( \frac{\log(1-z)}{1-z} \right)_+ - \frac{3}{2} \left( \frac{1}{1-z} \right)_+ - (1+z) \log(1-z) - \frac{1+z^2}{1-z} \log z + 3 + 2z - \left( \frac{\pi^2}{3} + \frac{9}{2} \right) \delta(1-z) \right] \quad (5.19)$$

For a consistent formulation, the integral over  $\xi$  in eq.(5.18) has to extend up to one, both in the expression for the cross section, as well as in the expression for the parton density, otherwise singular pieces remain uncanceled.



## Chapter 6

# Transverse Momentum Dependent parton distributions

In this chapter Transverse Momentum Dependent (TMD) parton distributions will be introduced. For a general overview on TMD parton densities see Ref. [54].

Instead of a formal introduction we start arguing why the transverse momenta, even if they are small, play a role in the parton evolution. This leads us to introduce an extension of the evolution equation including a transverse momentum dependence. Since we have to deal now also with partons emitted during the parton cascade, we need to reconsider the meaning of the evolution scale and give it a physical meaning.

### 6.1 Why are transverse momenta important for the evolution ?

Transverse momenta (or virtualities) in the initial state are coming from parton evolution: if a parton splits into two partons, the daughters must have transverse momenta. Therefore evolving a parton from a starting scale  $\mu_0^2$  up to a larger scale  $\mu^2$  involves automatically transverse momenta, up to the scale  $\mu^2$ . Such effects are visualized by using parton shower Monte Carlo event generators like PYTHIA [55,56], HERWIG [57–59], or RAPGAP [60,61]. The effect of transverse momenta to the parton evolution coming from parton shower event generators has been studied in [62]. A fit to the structure function  $F_2(x, Q^2)$  has been performed using the PYTHIA MC event generator. Without intrinsic transverse momenta and without parton showers the fit to the structure function gave the same result as the CTEQ6 (LO) PDFs [63]. However when parton showers were turned on, the parameters for the PDFs were very different. An example of this is shown in Fig. 6.1

The reason for the behaviour observed in Fig. 6.1 is the changed kinematics. Consider the process  $q + p_1 \rightarrow p_2$  with  $q^2 = -Q^2$ ,  $p_1^2 = -k^2$  and  $p_2^2 = m^2$ . This is the basic process for DIS scattering, except that now we do not neglect masses and transverse momenta. We use the definition of  $x_{Bj} = \frac{Q^2}{2q \cdot P}$ . Using energy momentum conservation we obtain:

$$\begin{aligned} (q + p_1)^2 &= p_2^2 \\ -Q^2 + 2q \cdot p_1 - k^2 &= m^2 \end{aligned}$$

Using the longitudinal momentum fraction  $\xi$  with  $p_1 = \xi P$ , with  $P$  being the proton momentum,

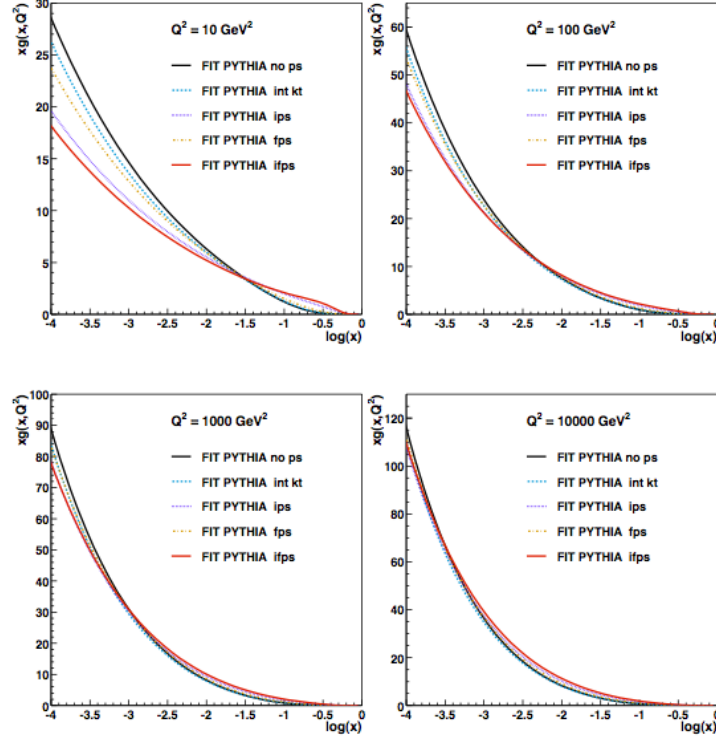


Figure 6.1: The gluon density as obtained from a DGLAP fit using the PYTHIA MC generator including parton showers (Plots from Ref. [62]).

we obtain:

$$\xi = \frac{Q^2 + m^2 + k^2 - 2\mathbf{q}\mathbf{p}_1}{2q \cdot P}$$

$$\xi \neq x_{Bj},$$

with  $\mathbf{q}$  and  $\mathbf{p}_1$  being the 2-dim transverse components of  $q$  and  $p_1$ . Depending on the values of  $m^2$  and  $k^2$ ,  $\xi$  can be very different from  $x_{Bj}$ .

For the correct treatment of the kinematics in a process with multigluon radiation, not only the transverse momentum is important, but also the mass  $m_{rem}$  [64], as illustrated in Fig. 6.2.

In the following we calculate the relation between the transverse momentum  $k_T$  and the virtuality  $k^2$ . Consider a photon with light-cone vector  $q = (0, q^-, q_t)$ , a gluon with vector  $k = (xP^+, k^-, k_T)$  and the incoming proton with  $P = (P^+, 0, 0)$ . From this we obtain:

$$\begin{aligned} q^2 &= -q_t^2 \\ k^2 &= 2xP^+k^- - k_T^2 \end{aligned} \tag{6.1}$$



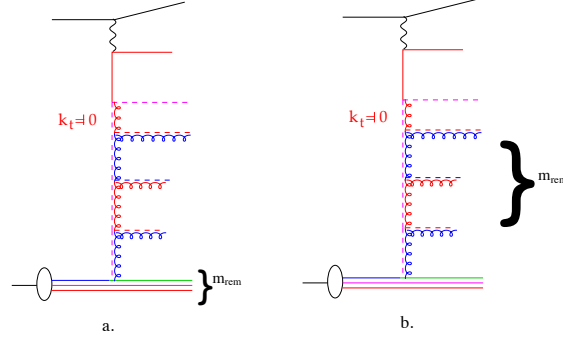


Figure 6.2: Illustration of the importance of the treatment of the mass  $m_{rem}$ : in the left only the proton remnants are included, in the right plot also the contribution of multiparton radiation is considered.

The mass of the remnant  $m_{rem}$  is (with  $P = k + r$  with  $r$  being the vector of the remnant system):

$$\begin{aligned}
 P &= k + r \quad \rightsquigarrow \quad r = P - k \\
 m_{rem}^2 &= (P - k)^2 = -2P^+k^- + k^2 = -2P^+k^- + 2xP^+k^- - k_T^2 \\
 &= -2P^+k^-(1 - x) - k_T^2 \\
 \rightsquigarrow 2P^+k^- &= -\frac{k_T^2 + m_{rem}^2}{1 - x} \\
 \rightsquigarrow k^2 &= -\frac{x(k_T^2 + m_{rem}^2) + k_T^2(1 - x)}{1 - x} \\
 &= -\frac{k_T^2 + xm_{rem}^2}{1 - x}
 \end{aligned}$$

Thus we see clearly, that with increasing  $m_{rem}$  the virtuality is no longer dominated by  $k_T$ , and the full history of multiparton radiation must be included in the calculation.

## 6.2 Transverse Momentum Dependent parton densities: Parton Branching TMD

In the following we describe an extension of the DGLAP evolution equation including the dependence on the transverse momenta  $k_T$  as described by the Parton Branching method [38]. Solving the evolution equation by an iterative method has also the advantage, that every single splitting is treated explicitly and kinematic relations can be applied in every branching, similarly to what is done in a parton shower process. Thus parton distributions can be obtained, not only depending on  $x$  and  $\mu$  (as in  $f(x, \mu^2)$ ), but also depending on the transverse momentum  $k_T$  of the propagating parton (as in TMD parton distributions  $\mathcal{A}(x, k_T, \mu)$ ).

### 6.2.1 The PB-TMD evolution equation

We can write down now the evolution equation for transverse momentum dependent parton densities  $\mathcal{A}(x, \mathbf{k}, \mu^2)$  by extending the expression of the DGLAP evolution equation eq.(4.47):

$$\begin{aligned} x\mathcal{A}_a(x, \mathbf{k}, \mu^2) &= \Delta_a(\mu^2) x\mathcal{A}_a(x, \mathbf{k}, \mu_0^2) + \sum_b \int \frac{d^2\mathbf{q}'}{\pi\mathbf{q}'^2} \frac{\Delta_a(\mu^2)}{\Delta_a(\mathbf{q}'^2)} \Theta(\mu^2 - \mathbf{q}'^2) \Theta(\mathbf{q}'^2 - \mu_0^2) \\ &\times \int_x^{z_M} dz \frac{\alpha_s}{2\pi} P_{ab}^{(R)}(z) \frac{x}{z} \mathcal{A}_b\left(\frac{x}{z}, \mathbf{k} + (1-z)\mathbf{q}', \mathbf{q}'^2\right), \end{aligned} \quad (6.2)$$

with the transverse momentum vectors (2-dim vectors)  $\mathbf{k}$  and  $\mathbf{q}$  to fully treat the transverse momentum dependence.

The final transverse momentum of the propagating parton is calculated as (see Fig. 4.7)

$$k_T = - \sum_c k_{tc}. \quad (6.3)$$

which enables one to determine the corresponding transverse momentum dependent (TMD) parton distribution  $\mathcal{A}(x, k_T, \mu)$ , in addition to the inclusive distribution  $f(x, \mu)$ , integrated over  $k_T$

$$\int \mathcal{A}(x, k_T, \mu) dk_T = f(x, \mu) \quad (6.4)$$

This evolution equation eq.(6.2) can be solved as before with iteration using a Monte Carlo method, the details are described in Ref. [38].

In the previous chapter we have described the solution of the DGLAP evolution equation using the Parton branching method, and found that the PB solution is equivalent to semi-analytical solutions if  $z_M$  is large enough. In Fig. 6.3 we show parton distributions as a function of the transverse momentum  $k_T$  for different values of  $z_M$ , for  $p_T$ -ordering and angular ordering conditions.

While for the integrated distributions a large enough  $z_M$  was enough to obtain stable and  $z_M$ -independent results, the transverse momentum distributions show a large  $z_M$  dependence for  $p_T$  ordering, while there is no dependence on  $z_M$  for angular ordering conditions. Please note, if virtuality ordering would be applied, with  $\mu = |k_{tc}|/(1-z)^2$ , also no dependence on  $z_M$  is observed. This result means, that soft gluons, even if they have very little energy, contribute significantly to the transverse momentum spectrum.

We have already seen the important role of soft gluons for inclusive distributions in Chapter 5.1, now for the transverse momentum distributions it becomes even more obvious. In Fig. 6.4 the effect of the  $z_M$  cut-off in the transverse momentum distribution is illustrated (see Ref [53]). Results obtained with the PB-approach for down quarks for PB-NLO-2018 Set1 with a default Gaussian width  $q_s = 0.5$  GeV for the intrinsic  $k_T$ -distribution are shown. To illustrate the effect of soft gluons in the evolution results are also shown when no intrinsic  $k_T$ -distribution is applied ( $q_s = 0$  GeV) and as well as neglecting applying  $z_{\text{dyn}} = 1 - q_0/q$ .

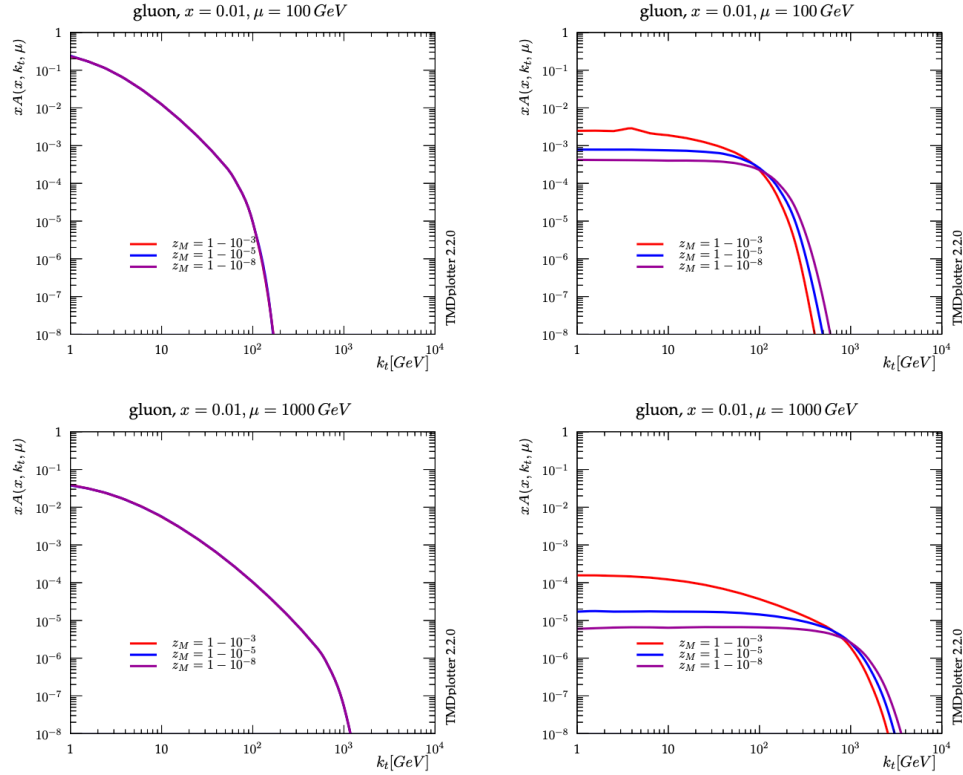


Figure 6.3: Transverse momentum gluon distribution versus  $k_T$  at  $x = 10^{-2}$  and  $\mu = 100$  GeV (upper row),  $\mu = 100$  GeV (lower row) for different values of the resolution scale parameter  $z_M = 1 - 10^{-3}, 1 - 10^{-5}, 1 - 10^{-8}$ : (left) angular ordering; (right) transverse momentum ordering. Figure taken from [38].

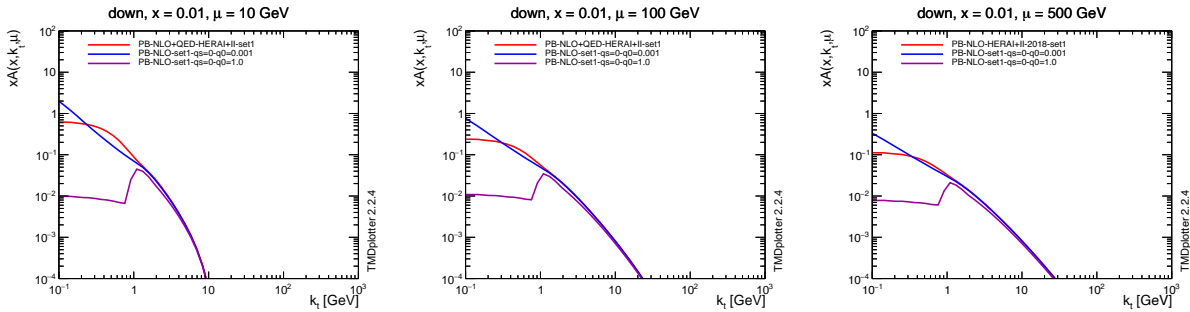


Figure 6.4: Transverse momentum distributions of down quarks at  $\mu = 10, 100$  GeV (left, middle column) and  $\mu = 500$  GeV (right column) obtained from the PB approach for  $z_M \rightarrow 1$  as well as  $z_M = z_{\text{dyn}} = 1 - q_0/q$ . The red curve shows PB-NLO-2018 Set1 (including intrinsic- $k_T$ ), the blue curve shows a prediction without including any intrinsic- $k_T$  distribution ( $q_s = 0$ ), and the magenta curve shows a prediction applying  $z_M = z_{\text{dyn}}$  with  $q_0 = 1.0$  GeV without including intrinsic- $k_T$  distributions.



## Chapter 7

# Drell-Yan production in Hadron-Hadron scattering

It is one of the striking features in particle physics that Feynman diagrams calculated for one process can be easily extended to other processes, where the incoming and final state particles are exchanged. This we can apply to use our knowledge obtained in  $ep$  scattering to the case of hadron hadron ( $pp$  or  $p\bar{p}$ ) scattering, as illustrated in Fig. 7.1

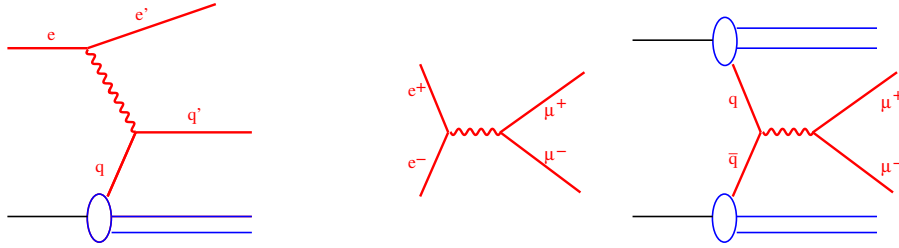


Figure 7.1: Schematic illustration of  $ep \rightarrow e'X$ ,  $e^+e^- \rightarrow \mu^+\mu^-$  and  $pp \rightarrow \mu^+\mu^-X$  diagrams

### 7.1 Inclusive Drell-Yan production in $pp$

From the matrix element  $ep_q \rightarrow e'p_{q'}$  in eq.(3.22) we obtain the matrix element for  $e^+e^- \rightarrow \mu^+\mu^-$ :

$$|\mathcal{M}|^2(e^+e^- \rightarrow \mu^+\mu^-) = 2(4\pi\alpha)^2 \frac{\hat{t}^2 + \hat{u}^2}{\hat{s}^2} \quad (7.1)$$

with

$$\begin{aligned} \hat{s} &= 4E_b^2 \\ \hat{t} &= -2E_b^2(1 - \cos\theta) \\ \hat{u} &= -2E_b^2(1 + \cos\theta) \end{aligned}$$

with  $\theta$  being the polar angle of the scattered  $\mu^+$  with respect to the incoming  $e^+$  and  $E_b$  being the energy of the incoming  $e^+$  in the center of mass frame of the  $e^+e^-$  pair.

The cross section is given by

$$\begin{aligned}
 \frac{d\sigma}{d\Omega} &= \frac{1}{64\pi^2\hat{s}} |\mathcal{M}|^2 \\
 &= \frac{1}{64\pi^2\hat{s}} (2\alpha^2(4\pi)^2) \frac{4E_b^4(1 - \cos\theta)^2 + 4E_b^4(1 + \cos\theta)^2}{16E_b^4} \\
 &= \frac{\alpha^2}{4\hat{s}} (1 + \cos^2\theta)
 \end{aligned}$$

This gives then the total cross section:

$$\sigma(e^+e^- \rightarrow \mu^+\mu^-) = \int_0^{2\pi} d\phi \int_{-1}^{+1} d\cos\theta \frac{\alpha^2}{4\hat{s}} (1 + \cos^2\theta) = \frac{4\pi\alpha^2}{3\hat{s}}$$

If we calculate the cross section for the crossed diagram  $q\bar{q} \rightarrow e^+e^-$  we must take into account the fractional charge of the quarks  $e_q^2$ , giving:

$$\sigma(q + \bar{q} \rightarrow \mu^+\mu^-) = \frac{4\pi\alpha^2}{3\hat{s}} e_q^2$$

and since quarks are not free but confined in hadrons we obtain:

$$\frac{d\sigma}{dM^2} = \sum_q \int dx_1 dx_2 f_q(x_1) f_{\bar{q}}(x_2) \frac{d\hat{\sigma}}{dM^2} \quad (7.2)$$

with  $f(x_1), f(x_2)$  being the parton distribution functions and  $x_1(x_2)$  being the fractional momenta of the protons carried by the partons and

$$\begin{aligned}
 \frac{d\hat{\sigma}}{dM^2} &= \frac{1}{3} \frac{1}{3} 3 \frac{4\pi\alpha^2}{3\hat{s}} e_q^2 \delta(\hat{s} - M^2) \\
 &= \frac{4\pi\alpha^2}{9\hat{s}} e_q^2 \delta(\hat{s} - M^2)
 \end{aligned} \quad (7.3)$$

with  $\hat{s} = x_1 x_2 s$  (neglecting masses of the incoming particles and partons),  $M$  being the mass of the  $q\bar{q}$  system and  $s$  being the proton-proton center-of-mass energy. The factors  $\frac{1}{3}$  in eq.(7.3) come from averaging over the initial 3 color states of  $q$  and  $\bar{q}$  while the factor 3 comes from the sum over the final state color singlet combinations. The process  $pp \rightarrow \mu^+\mu^- + X$  is called Drell-Yan process (DY), after the authors who calculated first the cross section [65].

Light-cone variables and the definition of rapidity is shown in Sec. A.2. The rapidity  $y$  is related to the ratio of the momentum fractions  $\frac{x_1}{x_2}$ , as shown in the following. Consider the process  $pp \rightarrow \mu^+\mu^- + X$  with the momenta of incoming partons

$$\begin{aligned}
 p_1 &= \frac{\sqrt{s}}{2} (x_1, 0, 0, x_1) \\
 p_2 &= \frac{\sqrt{s}}{2} (x_2, 0, 0, -x_2)
 \end{aligned}$$

then the rapidity  $y = \frac{1}{2} \log \frac{E+p_z}{E-p_z}$  of the  $\mu^+\mu^-$  is equal to the rapidity of the  $p_1 p_2$  pair with

$$\begin{aligned}
 E &= E_1 + E_2 = \frac{\sqrt{s}}{2} (x_1 + x_2) \\
 p_z &= p_{z1} + p_{z2} = \frac{\sqrt{s}}{2} (x_1 - x_2)
 \end{aligned}$$

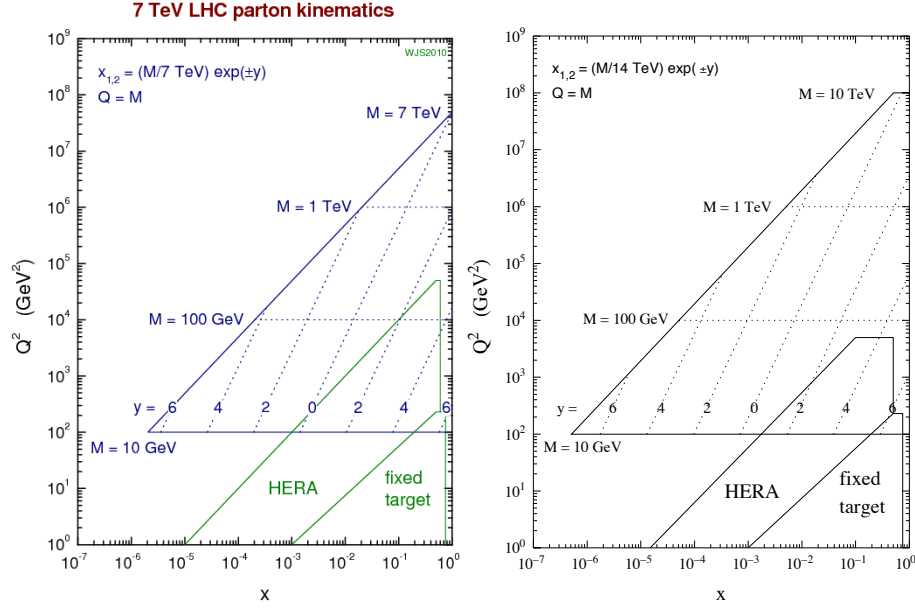


Figure 7.2: Kinematic relation of  $y$  with the momentum fraction  $x$  and the mass  $M$  for two different  $\sqrt{s}$  energies (taken from [66]).

The rapidity  $y$  of the incoming parton pair is then:

$$y = \frac{1}{2} \log \frac{E + p_z}{E - p_z} = \frac{1}{2} \log \frac{x_1}{x_2}$$

Defining  $\tau = \frac{M^2}{s} = x_1 x_2$  we obtain:

$$\begin{aligned} x_1 &= \sqrt{\tau} \exp(y) \\ x_2 &= \sqrt{\tau} \exp(-y) \end{aligned}$$

In Fig. 7.2 the relation between rapidity and the momentum fraction  $x$  is shown for different masses of the DY pair  $M^2$ .

The lowest order cross section of DY production is then:

$$\frac{d\sigma}{dM^2} = \frac{4\pi\alpha^2}{9M^2} \sum_q \int dx_1 dx_2 f_q(x_1) f_{\bar{q}}(x_2) e_q^2 \delta(\hat{s} - M^2) \quad (7.4)$$

$$= \frac{4\pi\alpha^2}{9M^2} \frac{1}{s} \sum_q e_q^2 \int dx_1 dx_2 f_q(x_1) f_{\bar{q}}(x_2) \delta\left(x_1 x_2 - \frac{M^2}{s}\right) \quad (7.5)$$

$$= \frac{4\pi\alpha^2}{9M^2} \frac{1}{s} \sum_q e_q^2 \int dx_1 dx_2 f_q(x_1) f_{\bar{q}}(x_2) \frac{1}{x_1} \delta\left(x_2 - \frac{\tau}{x_1}\right) \quad (7.6)$$

$$= \frac{4\pi\alpha^2}{9M^2} \frac{1}{s} \sum_q e_q^2 \int \frac{dx_1}{x_1} f_q(x_1) f_{\bar{q}}\left(x_2 = \frac{\tau}{x_1}\right) \quad (7.7)$$

$$\left(\frac{d\sigma}{dM^2 dy}\right)_{Born} = \frac{4\pi\alpha^2}{9M^2} \frac{1}{s} \sum_q e_q^2 f_q(x_1) f_{\bar{q}}\left(x_2 = \frac{\tau}{x_1}\right) \quad (7.8)$$

with  $dy = \frac{dx_1}{x_1}$ , where the terminology *Born* means lowest order.

### 7.1.1 Factorization of production and decay in Drell Yan processes

Calculating  $\mathcal{O}(\alpha_s)$  corrections to DY production involves  $2 \rightarrow 3$  processes. However, we can simplify the calculation if we apply the same methods as in DIS: we try to separate the production process from the decay, as illustrated in Fig. 7.3. By doing so, we can reduce the problem to a

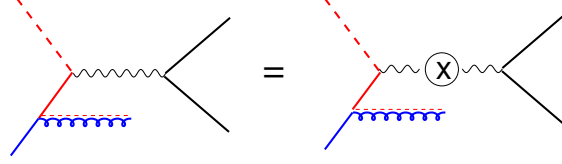


Figure 7.3: Schematic diagram to separate the production from the decay in a Drell Yan process.

simple calculation of a  $2 \rightarrow 2$  process. The cross section is then written in a factorized form:

$$d\sigma(q + \bar{q} \rightarrow l^+ + l^-) = d\sigma(q + \bar{q} \rightarrow \gamma^*) \otimes \frac{1}{Q^4} \otimes d\sigma(\gamma^* \rightarrow l^+ + l^-)$$

where the first term corresponds to the production, the second term is the photon propagator and the third term describes the decay.

The matrix element for  $\gamma^*(q) \rightarrow l^-(k_1) + l^+(k_2)$  is given by [22][see exercise 10.2]:

$$\begin{aligned} \mathcal{M}(\gamma^* \rightarrow l^+ l^-) &= e \bar{u}(k_1) \gamma_\mu \nu(k_2) \\ |\mathcal{M}(\gamma^* \rightarrow l^+ l^-)|^2 &= \frac{16\pi\alpha}{3} Q^2 \end{aligned}$$

with  $q^2 = Q^2$  being the timelike mass of  $\gamma^*$ .

The matrix element for  $q\bar{q} \rightarrow \gamma^*$  is given by:

$$|\mathcal{M}(q\bar{q} \rightarrow \gamma^*)|^2 = \frac{4\pi\alpha}{3} M^2 e_q^2 \quad (7.9)$$

with  $M^2 = Q^2$  being the mass of the  $q\bar{q}$  system (note: do not confuse this with the notation for the matrix element).

We write the cross section for  $q + \bar{q} \rightarrow l^+ + l^-$  as (where all particles are treated massless):

$$d\sigma(q + \bar{q} \rightarrow l^+ + l^-) = \frac{1}{2M^2} |\mathcal{M}(q\bar{q} \rightarrow l^+ l^-)|^2 \frac{d^4 k_1}{(2\pi)^3} \frac{d^4 k_2}{(2\pi)^3} (2\pi)^4 \delta^4(p_1 + p_2 - k_1 - k_2) \quad (7.10)$$

$$\begin{aligned} &= \frac{1}{2M^2} |\mathcal{M}(q\bar{q} \rightarrow \gamma^*)|^2 d^4 q \delta^4(p_1 + p_2 - q) \frac{1}{Q^4} |\mathcal{M}(\gamma^* \rightarrow l^+ l^-)|^2 \\ &\quad \times \frac{d^4 k_1}{(2\pi)^3} \frac{d^4 k_2}{(2\pi)^3} (2\pi)^4 \delta^4(q - k_1 - k_2) \\ &= \frac{1}{2M^2} |\mathcal{M}(q\bar{q} \rightarrow \gamma^*)|^2 d^4 q \delta^4(p_1 + p_2 - q) \frac{1}{Q^4} |\mathcal{M}(\gamma^* \rightarrow l^+ l^-)|^2 \frac{d\Omega}{32\pi^2} \\ &= \frac{1}{2M^2} \frac{4\pi\alpha}{3} M^2 e_q^2 d^4 q \delta^4(p_1 + p_2 - q) \frac{1}{Q^4} \frac{16\pi\alpha}{3} Q^2 \frac{d\Omega}{32\pi^2} \\ &= \frac{1}{2M^2} \frac{4\pi\alpha}{3} M^2 e_q^2 d^4 q \delta^4(p_1 + p_2 - q) 2\pi \frac{\alpha}{3\pi M^2} \quad (7.11) \end{aligned}$$



This can be written as a cross section differential in  $M^2$  as:

$$\frac{d\sigma}{dM^2} = \frac{4\pi^2\alpha e_q^2}{3} \times \frac{\alpha}{3\pi M^2} \delta(Q^2 - M^2) \quad (7.12)$$

$$= \frac{4\pi^2\alpha^2 e_q^2}{9M^2} \delta(Q^2 - M^2) \quad (7.13)$$

where we recovered in the last line again eq.(7.3).

Applying the factorization of production and decay, one only needs to calculate the production cross sections for:

$$\begin{aligned} pp &\rightarrow Z_0 + X \\ pp &\rightarrow \gamma^* + X \\ pp &\rightarrow W^\pm + X \\ pp &\rightarrow H + X \end{aligned}$$

where  $H$  stands for the Higgs boson, while applying the decay separately.

### 7.1.2 Factorization of transverse momenta in Drell Yan processes

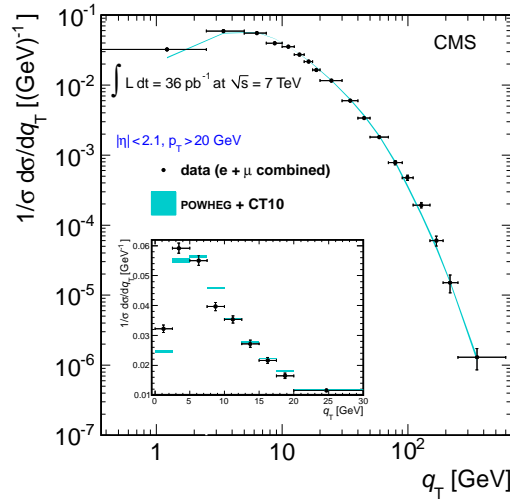


Figure 7.4: The transverse momentum of the  $Z_0$  boson as measured by [67].

A crucial assumption of Bjorken scaling is, that the amplitude of a process is suppressed, when the virtuality of the partons becomes larger than a typical hadronic mass scale (see discussion in [24][p 304]). This assumption is equivalent to the requirement that the partons can have only limited transverse momenta with respect to the direction of the beam hadron. We can generalize the parton distribution function to take into account also transverse momenta (please note, in comparison to the discussion on Transverse Momentum Dependent PDFs in Section 6, we treat here only the intrinsic transverse momentum, not the one coming from parton evolution)

$$d\xi f(\xi) \rightarrow d^2\vec{k}_T d\xi P(k_T, \xi) \text{ with } \int d^2\vec{k}_T P(\vec{k}_T, \xi) = f(\xi)$$

where  $\vec{k}_T$  is a 2-dimensional vector.

For a hard scattering in an inclusive process (where we do not investigate observables sensitive to  $k_T$ ) one can make the assumption:

$$P(\vec{k}_T, \xi) = \delta(\vec{k}_T) f(\xi)$$

and neglect all transverse momenta (as was done in the discussion of the DGLAP PDFs). If the transverse momentum of the partons is zero, then also the DY pair has zero transverse momentum, which is in contrast to what is observed in measurements [67] (Fig. 7.4).

Assuming a distribution function  $P(\vec{k}_T, \xi)$  with:

$$\begin{aligned} P(\vec{k}_T, \xi) &= h(\vec{k}_T) f(\xi) \\ h(\vec{k}_T) &= \frac{b}{\pi} \exp(-b\vec{k}_T^2) \end{aligned}$$

we obtain:

$$\frac{1}{\sigma} \frac{d\sigma}{dp_t} = \int d^2\vec{k}_{T1} d^2\vec{k}_{T2} \delta^{(2)}(\vec{k}_{T1} + \vec{k}_{T2} - \vec{p}_t) h(\vec{k}_{T1}) h(\vec{k}_{T2}) \quad (7.14)$$

$$= \int d^2\vec{k}_{T1} h(\vec{k}_{T1}) h(\vec{p}_t - \vec{k}_{T1}) \quad (7.15)$$

Applying the substitution<sup>1</sup>  $\vec{k} = \frac{1}{2}\vec{p}_t - \vec{k}_{T1}$  we obtain (using  $d^2\vec{k}_T = dk_T^2 \frac{d\phi}{2}$ ):

$$\frac{1}{\sigma} \frac{d\sigma}{dp_t} = \frac{b^2}{\pi^2} \int d^2\vec{k} h\left(\frac{1}{2}\vec{p}_t - \vec{k}\right) h\left(\vec{k} + \frac{1}{2}\vec{p}_t\right) \quad (7.16)$$

$$= \frac{b^2}{\pi^2} \int d^2\vec{k} \exp\left(-\frac{b}{2}p_t^2 - 2bk^2\right) \quad (7.17)$$

$$= \frac{b^2}{\pi} \exp\left(-\frac{b}{2}p_t^2\right) \int_0^\infty dk^2 \exp(-2bk^2) \quad (7.18)$$

$$= \frac{b}{2\pi} \exp\left(-\frac{b}{2}p_t^2\right) \quad (7.19)$$

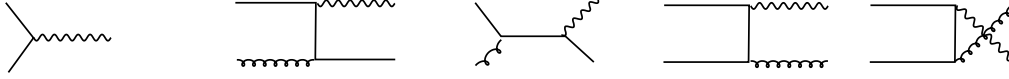
Another way to solve the integral is shown in Appendix A.5

At low  $p_t$  the measurements are well described by this expression, however a tail towards high  $p_t$  is observed (see Fig. 7.4), which cannot be described by the (limited) intrinsic transverse momentum of partons inside the hadrons.

### 7.1.3 $\mathcal{O}(\alpha_s)$ contributions to Drell Yan production

From the early measurements of the transverse momentum spectrum of Drell Yan production (for a measurement from LHC see Fig. 7.4) it became clear, that the naive parton model is incomplete: the tail of large  $p_t$  could not be described assuming that the intrinsic  $k_T$  of the partons inside the hadrons is small. Already by comparing the measured cross section of Drell Yan production with the prediction based on the parton model, the so called  $K$ -factor, defined as

$$K = \frac{\sigma^{\text{measured}}}{\sigma^{\text{calculated}}(LO)},$$

Figure 7.5: Diagrams contributing to Drell Yan production up to  $\mathcal{O}(\alpha_s)$ .

was found to be large, of the order of 2 – 3, indicating that important contributions to the cross section were not included in the lowest order (LO) calculation.

The  $\mathcal{O}(\alpha_s)$  contributions to Drell Yan production can be calculated using the same matrix elements, which have been used for the  $\mathcal{O}(\alpha_s)$  corrections to DIS (see section 3.4). The LO and  $\mathcal{O}(\alpha_s)$  diagrams are shown in Fig. 7.5, which are similar to the diagrams from DIS but with exchanged initial and final particles.

The matrix element for  $q\bar{q} \rightarrow \gamma^* g$  is given by:

$$|\mathcal{M}|^2 = 16\pi^2\alpha_s\alpha \frac{8}{9} \left[ \frac{\hat{u}}{\hat{t}} + \frac{\hat{t}}{\hat{u}} + \frac{2(M^2\hat{s})}{\hat{u}\hat{t}} \right] \quad (7.20)$$

$$= 16\pi^2\alpha_s\alpha \frac{8}{9} \left[ \left( \frac{1+z^2}{1-z} \right) \left( \frac{-\hat{s}}{\hat{t}} + \frac{-\hat{s}}{\hat{u}} \right) - 2 \right] \quad (7.21)$$

$$= 16\pi^2\alpha_s\alpha \frac{2}{3} \left[ P_{qq}(z) \left( \frac{-\hat{s}}{\hat{t}} + \frac{-\hat{s}}{\hat{u}} \right) - 2 \right] \quad (7.22)$$

where we have used  $z = \frac{M^2}{\hat{s}}$  and  $\hat{u} + \hat{t} = M^2 - \hat{s} = -\hat{s}(1-z)$ . We have also introduced the splitting function (known from DIS):

$$P_{qq} = \frac{4}{3} \frac{1+z^2}{1-z}$$

Similarly, we obtain for  $qg \rightarrow \gamma^* q$ :

$$|\mathcal{M}|^2 = 16\pi^2\alpha_s\alpha \frac{1}{3} \left[ -\frac{\hat{t}}{\hat{s}} - \frac{\hat{s}}{\hat{t}} - \frac{2(M^2\hat{u})}{\hat{s}\hat{t}} \right] \quad (7.23)$$

$$= 16\pi^2\alpha_s\alpha \frac{1}{3} [(z^2 + (1-z)^2) \times \dots] \quad (7.24)$$

$$= 16\pi^2\alpha_s\alpha \frac{2}{3} [P_{qg}(z) \times \dots] \quad (7.25)$$

with the splitting function

$$P_{qg}(z) = \frac{1}{2}(z^2 + (1-z)^2)$$

We can now calculate the cross section for Drell Yan production up to  $\mathcal{O}(\alpha_s)$  using the relation for  $p_t$  as given in eq.(A.42) in the Appendix-section A.4.2 with the Jacobean

$$dp_t^2 = d\hat{t} \frac{u-t}{s} = (1-z)d\hat{t}.$$

In order to simplify the calculation we again consider only the leading contribution at small transverse momenta (taking the small  $\hat{t}$  approximation, as done in the DIS case). We see, that we obtain

<sup>1</sup>Thanks to Radek Zlebcik for pointing out this elegant solution

a similar behavior of the cross section:

$$\begin{aligned}\frac{d\sigma}{dp_t^2} &= \frac{1}{1-z} \frac{d\sigma}{d\hat{t}} \\ &\propto \frac{1}{16\pi^2 \hat{s}} \frac{1}{1-z} P_{qq}(z) \hat{s} \left( \frac{-1}{t} + \dots \right) \\ &\propto \frac{1}{\hat{s}} P_{qq}(z) \frac{1}{p_t^2}\end{aligned}$$

We observe the same behavior as in DIS. The cross section is divergent if we perform the integral over  $p_t$  from zero, and we have to apply the same renormalization procedure as in the DIS case. We also observe, that the renormalization is the same as in DIS, as we obtained the same splitting functions. This is one of the important results of the QCD improved parton model: the parton densities, including the renormalization of the bare parton densities, are the same in DIS lepton proton scattering as in  $pp$  or  $p\bar{p}$  scattering: this is a consequence of factorization.

## 7.2 The $p_t$ spectrum of Drell Yan production

The complete calculation of the transverse momentum spectrum of Drell Yan production becomes complicated, because of the integration over the longitudinal and transverse components of the interaction partons. The original papers on this are very interesting [68,69]. Here we only consider the small  $p_t$  approximation and give the final result (without attempting to perform the calculation in detail, the full derivation can be found in [23]):

$$\begin{aligned}\frac{d\sigma}{dM^2 dy dp_t^2} &= \frac{8}{27} \frac{\alpha^2 \alpha_s}{s M^2} \frac{1}{p_T^2} \int_{x_a^{min}}^1 dx_a H(x_a, x_b, M^2) \\ &\quad \frac{x_a x_b}{x_a - x_1} \left( 1 + \frac{\tau^2}{(x_a x_b)^2} - \frac{x_T^2}{2x_a x_b} \right)\end{aligned}\tag{7.26}$$

$$\sim \frac{8}{27} \frac{\alpha^2 \alpha_s}{s M^2} \frac{2}{p_T^2} H(x_a, x_b, M^2) \log \frac{s}{p_t^2}\tag{7.27}$$

$$= \left( \frac{d\sigma}{dM^2 dy} \right)_{Born} \times \left( \frac{4\alpha_s}{3\pi} \frac{1}{p_t^2} \log \frac{s}{p_t^2} \right)\tag{7.28}$$

with the product of the parton densities defined by:

$$H(x_a, x_b, Q^2) = \sum_q e_q^2 (q_i(x_a, Q^2) \bar{q}_i(x_b, Q^2) + \bar{q}_i(x_a, Q^2) q_i(x_b, Q^2))$$

and the lowest order ( $\mathcal{O}(\alpha_s^0)$ ) Born cross section given in eq.(7.8):

$$\left( \frac{d\sigma}{dM^2 dy} \right)_{Born} = \frac{4\pi\alpha^2}{9sM^2} H_q(x_a, x_b, M^2)\tag{7.29}$$

As we know already from the discussion of DIS, the divergent behavior is absorbed by virtual corrections, for example when the emitted gluons become reabsorbed. As in the DIS case, we can calculate the virtual corrections explicitly, or argue on the basis of unitarity (and knowing that the final state configuration of a virtual correction is the same as the lower order process).

### Heuristic approach to describe the small $p_t$ region

We use here a heuristic argument to obtain the behavior of the cross section at small  $p_t$ , by assuming that the virtual and the non-branching corrections will compensate the divergent behavior of the real emission cross section. We write:

$$\int_0^s \frac{d\sigma}{dM^2 dy dp_t^2} dp_t^2 = \left( \frac{d\sigma}{dM^2 dy} \right)_{Born} + \mathcal{O}(\alpha_s) \quad (7.30)$$

We rearrange the integral:

$$\int_0^s \frac{d\sigma}{dM^2 dy dp_t^2} dp_t^2 = \int_0^{p_t^2} \frac{d\sigma}{dM^2 dy dp_t'^2} dp_t'^2 + \int_{p_t^2}^s \frac{d\sigma}{dM^2 dy dp_t'^2} dp_t'^2 \quad (7.31)$$

giving:

$$\int_0^{p_t^2} \frac{d\sigma}{dM^2 dy dp_t'^2} dp_t'^2 = \int_0^s \frac{d\sigma}{dM^2 dy dp_t'^2} dp_t'^2 - \int_{p_t^2}^s \frac{d\sigma}{dM^2 dy dp_t'^2} dp_t'^2 \quad (7.32)$$

Assuming that the total cross section is the Born cross section multiplied with a  $k$ -factor  $k$  (which we will neglect) we can write:

$$\int_0^{p_t^2} \frac{d\sigma}{dM^2 dy dp_t'^2} dp_t'^2 = \left( \frac{d\sigma}{dM^2 dy} \right)_{Born} (1 + k) - \int_{p_t^2}^s \frac{d\sigma}{dM^2 dy dp_t'^2} dp_t'^2 \quad (7.33)$$

$$= \left( \frac{d\sigma}{dM^2 dy} \right)_{Born} \left( 1 - \frac{4\alpha_s}{3\pi} \int_{p_t^2}^s \frac{\log \frac{s}{p_t'^2}}{p_t'^2} dp_t'^2 \right) \quad (7.34)$$

$$= \left( \frac{d\sigma}{dM^2 dy} \right)_{Born} \left( 1 - \frac{2\alpha_s}{3\pi} \left( \log \frac{s}{p_t^2} \right)^2 \right) \quad (7.35)$$

This form suggests for an extension to higher orders in  $\alpha_s$ , and we assume that the corrections in the bracket will exponentiate:

$$1 + a + \frac{a^2}{2!} + \frac{a^3}{3!} + \dots = \exp a$$

and we write for the cross section:

$$\rightsquigarrow \int_0^{p_t^2} \frac{d\sigma}{dM^2 dy dp_t'^2} dp_t'^2 = \left( \frac{d\sigma}{dM^2 dy} \right)_{Born} \exp \left( -\frac{2\alpha_s}{3\pi} \log^2 \frac{s}{p_t^2} \right) \quad (7.36)$$

Thus we have obtained an integrated cross section which, with the assumption that the  $\alpha_s$  corrections exponentiate, is finite over the whole range in  $p_t$ . To obtain the differential cross section as a function of  $p_t^2$ , we differentiate eq.(7.36) with respect to  $p_t^2$  and obtain:

$$\frac{d\sigma}{dM^2 dy dp_t^2} = \left( \frac{d\sigma}{dM^2 dy} \right)_{Born} \frac{4\alpha_s}{3\pi} \frac{1}{p_t^2} \log \frac{s}{p_t^2} \exp \left( -\frac{2\alpha_s}{3\pi} \log^2 \frac{s}{p_t^2} \right) \quad (7.37)$$

We see, that the cross section for  $p_t \rightarrow 0$  vanishes. This is the effect of the all order resummation of soft gluon emissions. A similar effect we have already observed in the discussion of the Sudakov form factor in section 4.3.2, where we found that the probability for no branching from one scale to another is very small: only if there is no resolvable branching, the  $p_t$  of the Drell Yan pair is zero (except if the emitted partons all compensate each other in transverse momentum).

### A formal approach to small $p_t$

A more detailed discussion and calculation of the Drell Yan  $p_t$  spectrum can be found in [70], here we just sketch the basic idea. We start from a general equation for multiparton emissions  $q\bar{q} \rightarrow \gamma^* + N$  (where  $N$  gives the number of emitted gluons):

$$\frac{1}{\sigma} \frac{d\sigma^{(N)}}{dp_t^2} \sim \prod_{i=1}^N \left[ \int d^2 k_{ti} dx_i \mathcal{M}^{(N)} \right] \delta \left( \sum \vec{k}_{ti} + \vec{p}_t \right) \quad (7.38)$$

where  $\mathcal{M}^{(N)}$  is the matrix element for the emission of  $N$  gluons. In the limit of small emission angles we can write:

$$\mathcal{M}^{(N)} \sim \prod_{i=1}^N \frac{\alpha_s}{k_{ti}^2} \log \frac{s}{k_{ti}^2} \quad (7.39)$$

and obtain:

$$\frac{1}{\sigma} \frac{d\sigma^{(N)}}{dp_t^2} \sim \prod_{i=1}^N \left[ \int \frac{d^2 k_{ti}}{k_{ti}^2} \log \frac{s}{k_{ti}^2} \right] \delta \left( \sum \vec{k}_{ti} + \vec{p}_t \right) \quad (7.40)$$

In the limit of strong ordering of the transverse momenta of the emitted gluons  $k_{t1}^2 \ll k_{t2}^2 \ll k_{t3}^2 \ll \dots \ll s$ , with  $s$  being the center-of-mass energy, the delta-function acts only on the last emitted gluon (the one with the largest  $k_T$ ):

$$\begin{aligned} \frac{1}{\sigma} \frac{d\sigma^{(N)}}{dp_t^2} &\sim \prod_{i=1}^N \left[ \int \frac{d^2 k_{ti}}{k_{ti}^2} \log \frac{s}{k_{ti}^2} \right] \delta \left( \vec{k}_{t \text{ last}} + \vec{p}_t \right) \\ &\sim \frac{1}{p_t^2} \log \frac{s}{p_t^2} \int \frac{d^2 k_{t,N-1}}{k_{t,N-1}^2} \log \frac{s}{k_{t,N-1}^2} \int \frac{d^2 k_{t,N-2}}{k_{t,N-2}^2} \log \frac{s}{k_{t,N-2}^2} \dots \end{aligned} \quad (7.41)$$

Using

$$\int \frac{dk_T^2}{k_T^2} \log^N \frac{s}{k_T^2} = \frac{\left( \log \frac{s}{k_T^2} \right)^{N+1}}{N+1} \quad (7.42)$$

we can integrate the equation term by term:

$$\begin{aligned} \frac{d\sigma^{(1)}}{dp_t^2} &\simeq \frac{1}{p_t^2} \log \frac{s}{p_t^2} = A \\ \frac{d\sigma^{(2)}}{dp_t^2} &\simeq A \int \frac{d^2 k_t}{k_t^2} \log \frac{s}{k_t^2} = A \frac{1}{2} \log^2 \frac{s}{k_t^2} \\ \frac{d\sigma^{(3)}}{dp_t^2} &\simeq \int \frac{d^2 k_t}{k_t^2} \log \frac{s}{k_t^2} \frac{d\sigma^{(2)}}{dp_t^2} = A \frac{1}{2} \int \frac{d^2 k_t}{k_t^2} \log^3 \frac{s}{k_t^2} = A \frac{1}{2} \left( \frac{1}{2} \log^2 \frac{s}{k_t^2} \right)^2 \\ \frac{d\sigma^{(4)}}{dp_t^2} &\simeq \int \frac{d^2 k_t}{k_t^2} \log \frac{s}{k_t^2} \frac{d\sigma^{(3)}}{dp_t^2} = A \frac{1}{2} \frac{1}{4} \int \frac{d^2 k_t}{k_t^2} \log^5 \frac{s}{k_t^2} = A \frac{1}{2} \frac{1}{3} \left( \frac{1}{2} \log^2 \frac{s}{k_t^2} \right)^3 \\ \frac{d\sigma^{(N)}}{dp_t^2} &\simeq A \frac{1}{(N-1)!} \left( \frac{1}{2} \log^2 \frac{s}{k_t^2} \right)^{N-1} \end{aligned}$$

We obtain for the cross section including the emission of  $N$  gluons:

$$\begin{aligned} \frac{d\sigma}{dp_t^2} &= \sum_i \frac{d\sigma^{(i)}}{dp_t^2} \simeq A \sum_i \frac{1}{(i-1)!} \left( \frac{1}{2} \log^2 \frac{s}{p_t^2} \right)^{i-1} \\ &\simeq A \exp \left[ \frac{1}{2} \log^2 \frac{s}{p_t^2} \right] \end{aligned}$$

Summing up everything, we finally obtain again eq.(7.37):

$$\frac{d\sigma}{dM^2 dy dp_t^2} = \left( \frac{d\sigma}{dM^2 dy} \right)_{Born} \frac{4\alpha_s}{3\pi} \frac{1}{p_t^2} \log \frac{s}{p_t^2} \exp \left( -\frac{2\alpha_s}{3\pi} \log^2 \frac{s}{p_t^2} \right) \quad (7.43)$$

The essential ingredients to obtain this formula was the application of eq.(7.42) and the strong ordering of the transverse momenta. Only under these conditions the delta function applies only to the hardest (last) emission and the product of integrals can be written as nested integrals, meaning that soft and collinear gluons are treated independently.

In order to obtain a full expression for the  $p_t$  spectrum, the strong ordering condition has to be relaxed, meaning that energy-momentum conservation has to be included for every single emission, which will result in additional contributions. Such calculations are difficult to be performed, and usually a Fourier transform to impact parameter space is performed. A full description is given in the original CSS (Collins-Soper-Sterman) paper [71] and in [72]:

$$\begin{aligned} \frac{d\sigma}{dM^2 dy dp_t^2} &= \sum_q \sigma_0^{qq} \frac{d}{dp_t^2} ([q(x_a, p_t)q(x_b, p_t) + a \leftrightarrow b]) \\ &\times \exp \left( - \int_{p_t^2}^{M^2} \frac{d\mu^2}{\mu^2} [A \log(M^2/\mu^2) + B] \right) \end{aligned}$$

The terms  $A$  and  $B$  have again a perturbative expansion in  $\alpha_s$ . This is also the form of the DY cross section in TMD factorization, which has received quite some attention in recent years.

### 7.2.1 The DY cross section and PB TMD distributions

The exponential appearing in eq.(7.43) can be interpreted as a Sudakov form factor, describing the probability for no emission. In the discussion on parton density functions an in particular in the discussion of TMD distributions, Sudakov form factors appeared.

In eq.(5.2) the splitting functions are given explicitly including virtual terms. We start writing down the DGLAP evolution equation (see also [53]):

$$\mu^2 \frac{\partial f_a(x, \mu^2)}{\partial \mu^2} = \sum_b \int_x^1 \frac{dz}{z} P_{ab}(z) f_b\left(\frac{x}{z}, \mu^2\right) \quad (7.44)$$

$$= \sum_b \int_0^1 \frac{dz}{z} \left( D_{ab} \delta(1-z) + K_{ab} \frac{1}{(1-z)_+} + R_{ab}(z) \right) f_b\left(\frac{x}{z}\right) \quad (7.45)$$

$$\begin{aligned} &= \sum_b \int_0^1 \frac{dz}{z} \left( \frac{K_{ab}}{1-z} + R_{ab}(z) \right) f_b\left(\frac{x}{z}\right) \\ &\quad - f_a(z) \int_0^1 dz \left( \frac{k_a}{(1-z)} - d_a \delta(1-z) \right) \end{aligned} \quad (7.46)$$

$$(7.47)$$

The Sudakov form factor  $\Delta_S(\mu^2)$  is now defined as:

$$\Delta_a^S(\mu^2) = \exp \left( - \int_{\mu_0^2}^{\mu^2} \frac{d\mu'^2}{\mu'^2} \int_0^{1-\epsilon} dz \left[ \frac{k_a}{(1-z)} - d_a \delta(1-z) \right] \right), \quad (7.48)$$

Considering only  $P_{qq}$  from eq.(4.24) at lowest order we obtain:

$$\begin{aligned} \Delta^S(z_M, \mu_0, \mu) &= \exp \left( - \frac{\alpha_s}{2\pi} \left[ \int_{\mu_0^2}^{\mu^2} \frac{d\mu'^2}{\mu'^2} \int_0^{z_M} dz P(z) + \frac{3}{2} \right] \right) \\ &\sim \exp \left( - \frac{\alpha_s}{2\pi} \left[ \int_{\mu_0^2}^{\mu^2} \frac{d\mu'^2}{\mu'^2} \int_0^{1-\frac{\mu'}{\mu}} dz \left[ \frac{2}{1-z} \right] + \frac{3}{2} \right] \right) \\ &= \exp \left( - \frac{\alpha_s}{2\pi} \left[ \int_{\mu_0^2}^{\mu^2} \frac{d\mu'^2}{\mu'^2} 2 \log \frac{\mu^2}{\mu'^2} + \frac{3}{2} \right] \right) \end{aligned} \quad (7.49)$$

where we have assumed angular ordering as well as taking the limit  $z \rightarrow 1$  (see also [73,74])

We observe that the form of the Sudakov form factor obtained with the PB method is the same as the one obtained with from CSS [75] in eq.(7.44) provided the angular ordering conditions are used.



### 7.3 Exercises: Boson Production

8. Calculate  $\sigma(p + p \rightarrow h)$  (Higgs production via gluon fusion) in lowest order. Take  $\sqrt{s} = 7000$  GeV. Calculate the total cross section, and plot  $x_1$ ,  $x_2$  and  $y_h$ . Require  $120 < m_h < 130$  GeV. Plot the transverse momenta of the incoming partons. Use for simplicity parton density of the form  $xg(x) = 3(1 - x)^5$ .

The Higgs cross section is:

$$\sigma(g + g \rightarrow h) = \alpha_s^2 \frac{\sqrt{2}}{\pi} \frac{G_F}{576}$$

with  $G_F = 1.166 \cdot 10^{-5} \text{ GeV}^{-2}$  and  $\alpha_s = 0.1$ .

Use a Breit-Wigner form for the Higgs:

$$P(m) = \frac{1}{2\pi} \frac{\Gamma_h}{(m - m_h)^2 + \Gamma_h^2/4}$$

with  $m_h = 125$  GeV and  $\Gamma_h = 0.4$  GeV. Calculate the cross section.

Include in the calculation a small intrinsic transverse momentum from both of the incoming partons. Assume  $h(k_T) = \exp(-bk_T^2)$ . Using  $b = 1$  corresponds to a gauss distribution with  $\mu = 0$  and  $\sigma \sim 0.7$ . Plot the transverse momentum  $k_T$  and the transverse momentum squared  $k_T^2$  of both incoming partons and the resulting  $h$ .

Write the code in a modular way, such that it can be used for the last exercise.

9. Use the evolved pdf (from previous exercise) to calculate higgs production from above. Set the scale  $t = 10000 \text{ GeV}^2$ . Use for simplicity the a gluon density  $xg(x) = 3(1-x)^5$  as a starting distribution and use  $P_{gg}$ . Calculate the transverse momentum of the incoming partons and calculate the transverse momentum of the Higgs. Plot the  $x$ -values of the incoming partons and the transverse momenta.

## 7.4 Exercise: Boson Production - Solutions

### 7.4.1 Calculate the x-section for $p p \rightarrow \text{Higgs} + X$

Plot the distribution in  $p_t$  and rapidity  $y$

Authors: H. Jung, S. Taheri Monfared, P. L.S. Connor, R. Zlebick

```
[1]: # Import what is necessary
import numpy as np
import matplotlib.pyplot as plt
from math import sqrt, log, log10, pi, exp, sin, cos

[2]: # Define 4-vector operations
# px, py, pz, E
# dot product of 4-vectors
def pdot(a, b):
    return a[3]*b[3] - a[0]*b[0] - a[1]*b[1] - a[2]*b[2]
# Define addition of 4-vectors
def padd(a, b):
    return a[0]+b[0], a[1]+b[1], a[2]+b[2], a[3]+b[3]
# Define mass**2 of 4-vector
def pmass2(a):
    return a[3]*a[3] - a[0]*a[0] - a[1]*a[1] - a[2]*a[2]
# Define mass of 4-vector
def pmass(a):
    return sqrt(max(0., a[3]*a[3] - a[0]*a[0] - a[1]*a[1] - a[2]*a[2]))
# Define pT
def pT(a):
    return sqrt(max(0., a[0]*a[0] + a[1]*a[1]))
# Define Rapidity
def pRapidity(a):
    arg = a[3]-a[2]
    if arg == 0:
        rap = -999999.
    else:
        rap = 0.5*log((a[3]+a[2])/(a[3]-a[2]))
    return rap
```

The cross section of the Higgs

```
[3]: def sigma(m2):
    # calculate partonic x-section
    #
    # calculate sigma0 (qq -> gamma^*)
    # double aem=1./137.;
    # result = 4.*pi*pi*aem/3.;
    #
    # calculate sigma0(qq->H)
    # sigma0 = as^2/pi /576 * GF * sqrt(2)*Delta(1.-tau)
    aS = 0.1 # alphaS
    GF = 1.166e-5 # Fermi constant
    result = aS**2 * sqrt(2.) * GF /pi / 576.
    return result
```

Function to get randomly 2D Gaussian distribution

```
[4]: def gauss2D(sigma):
    kT = sigma * sqrt(-2.*log(rng.random()));
    phi = 2.*pi * rng.random()
    kx, ky = kT*cos(phi), kT*sin(phi)
    return (kx, ky)
```

Get the four-momentum of the parton according to the parton density

```
[5]: def getpdf(q2):
    xmin = 0.00001
    xmax = 0.999
    x = xmin*pow(xmax/xmin, rng.random())
    weightx = x*log(xmax/xmin)
    # this is for the simple case
    pdf = 3.*pow((1-x),5)/x
    # now generate intrinsic kt according to a gauss distribution
    kx, ky = gauss2D(0.7)
    En = sqrt(kx**2 + ky**2 + (x*Eb)**2)
    pvec=kx, ky, x*Eb, En
    return pvec, weightx * pdf
```

```
[6]: # initialise random number generator:
rng = np.random.default_rng(1234) # initialise random number generator PCG-64
print(rng)
```

Generator(PCG64)

```
[7]: s = 7000*7000 # center of mass energy
Eb = sqrt(s)/2 # Beam energy

# Scale of the process and the mass window

q2 = 125.**2
mass_min = 0.
mass_max = 200.

m_higgs = 125.
Gamma = 0.4
```

Loop over MC events

```
[8]: sum0 = sum00 = 0.
nacc = 0
npoints = 100000

Weight_x1=[]
Weight_x2=[]
x1_log10=[]
x2_log10=[]
pA_pT=[]
pB_pT=[]

pH_pT=[]
pH_Rapidity=[]
pH_Mass=[]
Weight_ff=[]

for n1 in range(npoints):
    # generate p4 of incoming parton 1
    pA, weightx1 = getpdf(q2)
    # generate p4 of incoming parton 2
    pB, weightx2 = getpdf(q2)
    pB=pB[0], pB[1], -pB[2], pB[3]

    x1 = abs(pA[2]) / Eb
    x2 = abs(pB[2]) / Eb
    # plot dxg(x)/dlogx *Jacobian, Jacobian dlogx/dx = 1/x
    x1_log10.append(log10(x1))
    x2_log10.append(log10(x2))
    Weight_x1.append(weightx1)
    Weight_x2.append(weightx2)
    pA_pT.append(ppT(pA))
    pB_pT.append(ppT(pB))

    pH = padd(pA,pB)
    mass = pmass(pH)
    if mass < mass_min or mass > mass_max:
        continue
    # note, pdfs are already included in weightx

    Hx1x2 = weightx1*weightx2* sigma(mass**2)
    # multiply with a Breit Wigner resonance
    Hx1x2 = Hx1x2 * Gamma/(pow((mass-m_higgs),2) + pow(Gamma,2)/4)/2./pi

    # Change units to nb
    gev2nb = 0.3893857E+6
    ff = Hx1x2 * gev2nb

    nacc += 1
    sum0 += ff
    sum00 += ff**2
    # weighting with 1/x0:
    # plot dxg(x)/dlogx *Jacobian, Jacobian dlogx/dx = 1/x
    pH_pT.append(ppT(pH))
    # calculate rapidity of Higgs
    pH_Rapidity.append(pRapidity(pH))
    pH_Mass.append(mass)
    Weight_ff.append(ff)
```

Normalization and evaluation of the error

```
[9]: sum0 /= npoints
sum00 /= npoints
sigma2 = sum00 - sum0*sum0
error = sqrt(sigma2/npoints)
print (" nr of events accepted: ", nacc )
print (" integral for Higgs xsection is [pb]: ", sum0 * 1000., " +/- " , error*1000.)
```

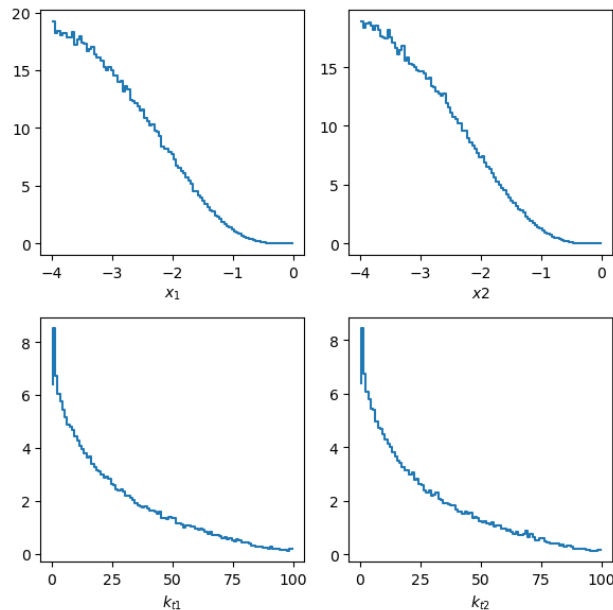
```
nr of events accepted: 80767
integral for Higgs xsection is [pb]: 0.016933846009681064 +/-
0.001885949913159124
```

Plotting of  $x_1$ ,  $x_2$  and  $k_{T1}$  and  $k_{T2}$

```
[10]: fig, axs = plt.subplots(figsize=(6, 6),nrows=2, ncols=2,sharey=False, tight_layout=False)
histo1,bin_edge = np.histogram(x1_log10, bins=100, range=[-4,0],weights=Weight_x1, density=False)
xcenters = (bin_edge[:-1] + bin_edge[1:]) / 2
bin_width= (bin_edge[1:] - bin_edge[:-1])
# normalize histo with log(10) and bin_width
histo1 = histo1/log(10)/bin_width/npoints
# use step (instead plot) to plot histogram style
axs[0,0].step(xcenters, histo1)
axs[0,0].set_xlabel(r'$x_1$')
histo2,bin_edge = np.histogram(x2_log10, bins=100, range=[-4,0],weights=Weight_x2, density=False)
xcenters = (bin_edge[:-1] + bin_edge[1:]) / 2.
bin_width= (bin_edge[1:] - bin_edge[:-1])
histo2 = histo2/log(10)/bin_width/npoints
axs[0,1].step(xcenters, histo2)
axs[0,1].set_xlabel(r'$x_2$')

histo3,bin_edge = np.histogram(pA_pT, bins=100, range=[0,10],weights=Weight_x1, density=False)
xcenters = (bin_edge[:-1] + bin_edge[1:]) / 2.
bin_width= (bin_edge[1:] - bin_edge[:-1])
histo3 = histo3/bin_width/npoints
axs[1,0].step(xcenters, histo3)
axs[1,0].set_xlabel(r'$k_{t1}$')
histo4,bin_edge = np.histogram(pB_pT, bins=100, range=[0,10],weights=Weight_x2, density=False)
xcenters = (bin_edge[:-1] + bin_edge[1:]) / 2.
bin_width= (bin_edge[1:] - bin_edge[:-1])
histo4 = histo4/bin_width/npoints
axs[1,1].step(xcenters, histo4)
axs[1,1].set_xlabel(r'$k_{t2}$')
#axs[1,1].set_xscale('log')
```

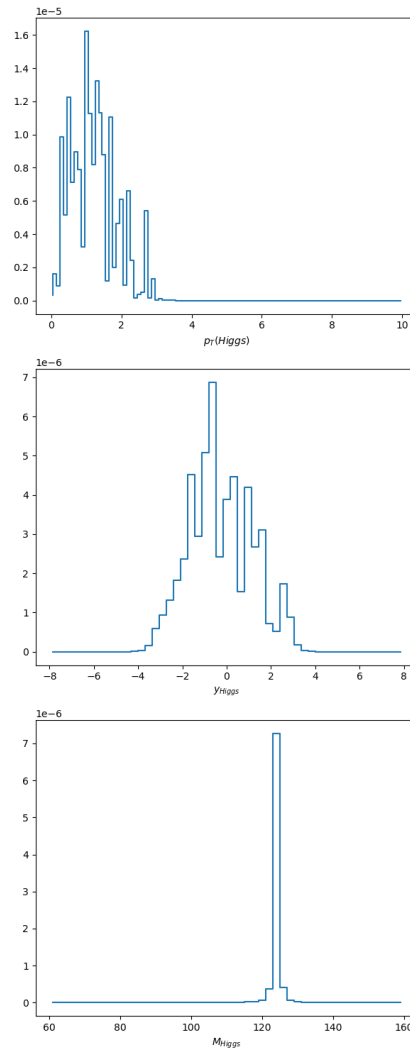
```
[10]: Text(0.5, 0, '$k_{t2}$')
```



Draw the  $p_T$ ,  $\eta$  and mass of the Higgs boson

```
[11]: fig, axs = plt.subplots(figsize=(6, 15), nrows=3, ncols=1, sharey=False, tight_layout=False)
histo5, bin_edge = np.histogram(pH_pT, bins=100, range=[0,10], weights=Weight_ff, density=False)
xcenters = (bin_edge[:-1] + bin_edge[1:]) / 2
bin_width = (bin_edge[1:] - bin_edge[:-1])
# normalize histo with log(10) and bin_width
histo5 = histo5/bin_width/npoints
# use step (instead plot) to plot histogram style
axs[0].step(xcenters, histo5)
axs[0].set_xlabel(r'$p_{T, T}(\text{Higgs})$')
histo6, bin_edge = np.histogram(pH_Rapidity, bins=50, range=[-8,8], weights=Weight_ff, density=False)
xcenters = (bin_edge[:-1] + bin_edge[1:]) / 2
bin_width = (bin_edge[1:] - bin_edge[:-1])
histo6 = histo6/bin_width/npoints
axs[1].step(xcenters, histo6)
axs[1].set_xlabel(r'$y_{T, T}(\text{Higgs})$')
histo7, bin_edge = np.histogram(pH_Mass, bins=50, range=[60,160], weights=Weight_ff, density=False)
xcenters = (bin_edge[:-1] + bin_edge[1:]) / 2
bin_width = (bin_edge[1:] - bin_edge[:-1])
histo7 = histo7/bin_width/npoints
axs[2].step(xcenters, histo7)
axs[2].set_xlabel(r'$M_{T, T}(\text{Higgs})$')
```

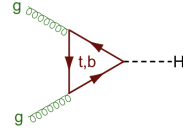
```
[11]: Text(0.5, 0, '$M_{T, T}(\text{Higgs})$')
```



### 7.4.2 Calculation of the Higgs cross section using Monte Carlo integration.

We calculate the x-section for  $p p \rightarrow \text{Higgs} + X$  and plot the distribution in  $p_t$  and rapidity  $y$

We use our own evolved pdf.



**Authors: H. Jung, S. Taheri Monfared, P. L.S. Connor, R. Zlebcik**

```
[1]: # Import what is necessary

import numpy as np
import matplotlib.pyplot as plt
from math import sqrt, log, log10, pi, exp, sin, cos
```

We make use of the code from example-8

```
[2]: # Define 4-vector operations
# px, py, pz, E
# dot product of 4-vectors
def pdot(a, b):
    return a[3]*b[3] - a[0]*b[0] - a[1]*b[1] - a[2]*b[2]
# Define addition of 4-vectors
def padd(a, b):
    return a[0]+b[0], a[1]+b[1], a[2]+b[2], a[3]+b[3]
# Define mass**2 of 4-vector
def pmass2(a):
    return a[3]*a[3] - a[0]*a[0] - a[1]*a[1] - a[2]*a[2]
# Define mass of 4-vector
def pmass(a):
    return sqrt(max(0., a[3]*a[3] - a[0]*a[0] - a[1]*a[1] - a[2]*a[2]))
# Define pT
def ppT(a):
    return sqrt(max(0., a[0]*a[0] + a[1]*a[1]))
# Define Rapidity
def pRapidity(a):
    arg = a[3]-a[2]
    if arg == 0:
        rap = -99999.
    else:
        rap = 0.5*log((a[3]+a[2])/(a[3]-a[2]))
    return rap
```

```
[3]: def sigma(m2):
    # calculate partonic x-section
    #
    # calculate sigma0 (qq -> gamma*)
    # double aem=1./137.;
    # result = 4.*pi*pi*aem/3.;
    #
    # calculate sigma0 (gg->H)
    # sigma0 = as^2/pi /576 * GF * sqrt(2)*\Delta(1.-tau)
    aS = 0.1 # alphaS
    GF = 1.166e-5 # Fermi constant
    result = aS**2 * sqrt(2.) * GF /pi / 576.
    return result
```

here we use the evolution code from example-7

```
[4]: def gauss2D(sigma):
    kT = sigma * sqrt(-2.*log(rng.random()));
    phi = 2.*pi * rng.random()
    kx, ky = kT*cos(phi), kT*sin(phi)
    return (kx, ky)

# Get PDF at the scale $q^2$ (currently no dependence on $q^2$)

def get_starting_pdf(q2):
    xmin = 0.00001
    xmax = 0.999
    # get x value according to g(x)\sim 1/x
    x = xmin * (xmax/xmin)**rng.random()
    weightx = x*log(xmax/xmin)
    # use: xg(x) = 3 (1-x)**5
    pdf = 3.*pow((1-x),5.)/x

    # now generate intrinsic kt according to a gauss distribution
```

```

kx, ky = gauss2D(0.7)
En = sqrt(kx**2 + ky**2 + (x*Eb)**2)
pvec=kx, ky, x*Eb, En
return pvec, weightx * pdf

# Calculate Sudakov form factor

def sudakov(t0):
    # here we calculate from the sudakov form factor the next t > t0
    epsilon = 0.1
    as2pi = 0.1/(2.*pi)
    Ca = 3.
    # for Pgg use fact = 2*Ca
    fac = 2.*Ca
    # use fixed alphas and only the 1/(1-z) term of the splitting fct

    r1 = rng.random()
    Pint=log((1.-epsilon)/epsilon) # for 1/(1-z) splitting fct
    t2 = -log(r1)/fac/as2pi/Pint
    t2 = t0 * exp(t2)
    assert(t2 >= t0)
    return t2

# The splitting function which is needed to get the z on the branching point

def splitting():
    epsilon = 0.1

    as2pi = 0.1/2./pi

    # here we calculate the splitting variable z for 1/z and 1/(1-z)
    # use Pgg=6(1/z + 1/(1-z)) // for large z we use z -> 1-z

    g0 = 6.*as2pi * log((1.-epsilon)/epsilon)
    g1 = 6.*as2pi * log((1.-epsilon)/epsilon)
    gtot = g0 + g1

    zmin = epsilon
    zmax = 1.-epsilon

    r1 = rng.random()
    r2 = rng.random()

    z = zmin * (zmax/zmin)**r2
    if r1 > g0/gtot:
        z = 1. - z
    weightz = 1.
    return z

# Evolve the PDF between scales $q^2_0$ and $q^2$, the kinematics of the parton in the beginning is_
# described by four-vector p0

def evolve_pdf(q20, q2, p0):
    x = p0[2]/Eb
    kx = p0[0]
    ky = p0[1]
    # print(" evolve0 kx,ky ",kx,ky)
    weightx = 1.
    t1 = q20
    tcut = q2
    while t1 < tcut:
        # here we do now the evolution
        # first we generate t
        t0 = t1
        t1 = sudakov(t0)

        # now we generate z
        z = splitting()
        # since the sudakov involves only the 1/(1-z) part
        # of the splitting fct, we need to weight each branching
        # by the ratio of the integral of the full and
        # approximate splitting fct
        # print(" z ",z)
        ratio_splitting = 2 # for using Pgg

        if t1 < tcut:
            x = x*z
            weightx = weightx *ratio_splitting
            # use here the angular ordering condition: sqrt(t1) = qt/(1-z)

```

```

        # and apply this also to the propagator gluons
        #
        phi = 2.*pi*rng.random()
        kx += sqrt(t1)*cos(phi)*(1.-z)
        ky += sqrt(t1)*sin(phi)*(1.-z)
        #   kx += sqrt(t1)*cos(phi)
        #   ky += sqrt(t1)*sin(phi)
        #   print(" evolve kx,ky ",kx,ky)

    En = sqrt(kx**2 + ky**2 + (x*Eb)**2)
    k=kx, ky, x*Eb, En
    return k, weightx

```

get parton distribution

```

[5]: def getpdf(q2):
    # generate starting distribution in x and kt
    q20 = 1
    k0, weightx0 = get_starting_pdf(q20)
    x0 = k0[2]/Eb
    #   print(" k0 ", k0)

    # now do the evolution
    k, weightxf = evolve_pdf(q20, q2, k0)
    xf = k[2]/Eb
    #   print(" k ", k)

    weightx = weightx0 * weightxf
    momsum0 = x0*weightx0
    momsum = xf*weightx

    return k, weightx

[6]: # initialise random number generator:
rng = np.random.default_rng(1234) # initialise random number generator PCG-64
print(rng)

```

Generator (PCG64)

```

[7]: s=4*3500.*3500 # center of mass energy
Eb = sqrt(s)/2 # Beam energy

print( " sqrt(s) = " , sqrt(s) )

sqrt(s) = 7000.0

[8]: # Scale of the process and the mass window

q2 = 10000 # this gives reasonable results... remember we use simplifications
mass_min = 0.
mass_max = 200.

m_higgs = 125.
Gamma = 0.4

```

```

[9]: # Loop over MC events
sum0 = sum00 = 0.
nacc = 0
npoints = 1000000
#npoints=10

Weight_x1=[]
Weight_x2=[]
x1_log10=[]
x2_log10=[]
pA_pT=[]
pB_pT=[]

pH_pT=[]
pH_Rapidity=[]
pH_Mass=[]
Weight_ff=[]

for n1 in range(npoints):
    # generate p4 of incoming parton 1
    pA, weightx1 = getpdf(q2)
    # generate p4 of incoming parton 2
    pB, weightx2 = getpdf(q2)

```



```

pB=pB[0], pB[1], -pB[2], pB[3]

x1 = abs(pA[2]) / Eb
x2 = abs(pB[2]) / Eb
# plot dxg(x)/dlogx *Jacobian, Jacobian dlogx/dx = 1/x
x1_log10.append(log10(x1))
x2_log10.append(log10(x2))
Weight_x1.append(weightx1)
Weight_x2.append(weightx2)
pA_pT.append(ppT(pA))
pB_pT.append(ppT(pB))

# print(" pA =", pA,pmass(pA))
# print(" pB =", pB,pmass(pB))
pH = padd(pA,pB)
mass = pmass(pH)
# print(" pH =", pH,pmass(pH))
if mass < mass_min or mass > mass_max:
    continue
# note, pdfs are already included in weightx
Hx1x2 = weightx1*weightx2* sigma(mass**2)
# multiply with a Breit Wigner resonance
Hx1x2 = Hx1x2 * Gamma/(pow((mass-m_higgs),2) + pow(Gamma,2)/4)/2./pi

# Change units to nb
gev2nb = 0.3893857E+6
ff = Hx1x2 * gev2nb

nacc += 1
sum0 += ff
sum00 += ff**2
# weighting with 1/x0:
# plot dxg(x)/dlogx *Jacobian, Jacobian dlogx/dx = 1/x
pH_pT.append(ppT(pH))
# calculate rapidity of Higgs
pH_Rapidity.append(pRapidity(pH))
pH_Mass.append(mass)
Weight_ff.append(ff)

```

Normalization and evaluation of the error

```

[10]: sum0 /= npoints
sum00 /= npoints
sigma2 = sum00 - sum0*sum0
error = sqrt(sigma2/npoints)
print(" nr of events accepted: ", nacc )
print(" integral for Higgs xsection is [pb]: " , sum0 * 1000., " +/- " , error*1000.)

```

```

nr of events accepted: 894569
integral for Higgs xsection is [pb]: 0.7426023013610623 +/-
0.0932402479901271

```

Plotting of x1, x2 and kT1 and kT2

```

[11]: fig, axs = plt.subplots(figsize=(6, 6),nrows=2, ncols=2,sharey=False, tight_layout=False)
histo1,bin_edge = np.histogram(x1_log10, bins=100, range=[-4,0],weights=Weight_x1, density=False)
xcenters = (bin_edge[:-1] + bin_edge[1:]) / 2
bin_width= (bin_edge[1:] - bin_edge[:-1])
# normalize histo with log(10) and bin_width
histo1 = histo1/log(10)/bin_width/npoints
# use step (instead plot) to plot histogram style
axs[0,0].step(xcenters, histo1)
axs[0,0].set_xlabel(r'$x_{1}$')
histo2,bin_edge = np.histogram(x2_log10, bins=100, range=[-4,0],weights=Weight_x2, density=False)
xcenters = (bin_edge[:-1] + bin_edge[1:]) / 2.
bin_width= (bin_edge[1:] - bin_edge[:-1])
histo2 = histo2/log(10)/bin_width/npoints
axs[0,1].step(xcenters, histo2)
axs[0,1].set_xlabel(r'$x_{2}$')

histo3,bin_edge = np.histogram(pA_pT, bins=100, range=[0,100],weights=Weight_x1, density=False)
xcenters = (bin_edge[:-1] + bin_edge[1:]) / 2.
bin_width= (bin_edge[1:] - bin_edge[:-1])
histo3 = histo3/bin_width/npoints
axs[1,0].step(xcenters, histo3)
axs[1,0].set_xlabel(r'$k_{t1}$')
histo4,bin_edge = np.histogram(pB_pT, bins=100, range=[0,100],weights=Weight_x2, density=False)
xcenters = (bin_edge[:-1] + bin_edge[1:]) / 2.
bin_width= (bin_edge[1:] - bin_edge[:-1])
histo4 = histo4/bin_width/npoints

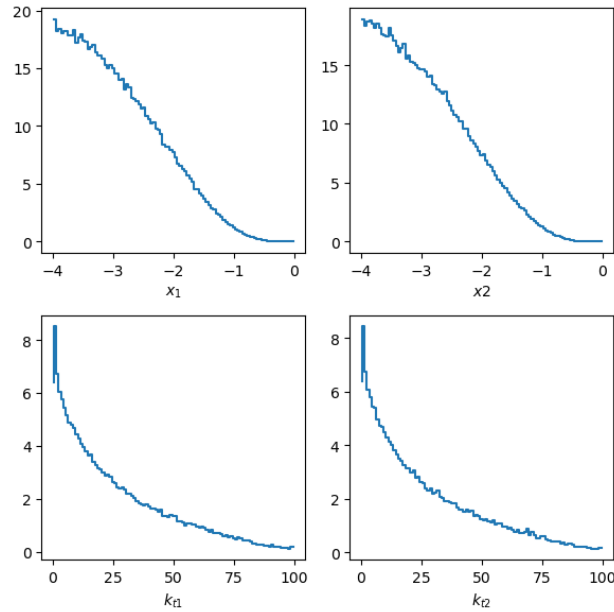
```

```

axs[1,1].step(xcenters, histo4)
axs[1,1].set_xlabel(r'$k_{t2}$')
#axs[1,1].set_xscale('log')

```

```
[11]: Text(0.5, 0, '$k_{t2}$')
```



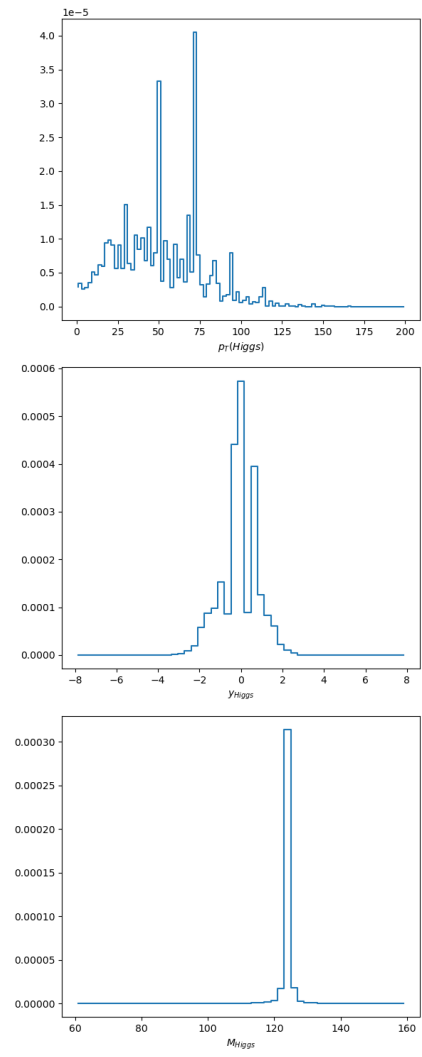
Draw the pT, eta and mass of the Higgs boson

```

[12]: fig, axs = plt.subplots(figsize=(6, 15),nrows=3, ncols=1,sharey=False, tight_layout=False)
histo5,bin_edge = np.histogram(pH_pT, bins=100, range=[0,200],weights=Weight_ff, density=False)
xcenters = (bin_edge[:-1] + bin_edge[1:]) / 2
bin_width= (bin_edge[1:] - bin_edge[:-1])
# normalize histo with log(10) and bin_width
histo5 = histo5/bin_width/npoints
# use step (instead plot) to plot histogram style
axs[0].step(xcenters, histo5)
axs[0].set_xlabel(r'$p_T$ (Higgs)')
histo6,bin_edge = np.histogram(pH_Rapidity, bins=50, range=[-8,8],weights=Weight_ff, density=False)
xcenters = (bin_edge[:-1] + bin_edge[1:]) / 2.
bin_width= (bin_edge[1:] - bin_edge[:-1])
histo6 = histo6/bin_width/npoints
axs[1].step(xcenters, histo6)
axs[1].set_xlabel(r'$y_{Higgs}$')
histo7,bin_edge = np.histogram(pH_Mass, bins=50, range=[60,160],weights=Weight_ff, density=False)
xcenters = (bin_edge[:-1] + bin_edge[1:]) / 2.
bin_width= (bin_edge[1:] - bin_edge[:-1])
histo7 = histo7/bin_width/npoints
axs[2].step(xcenters, histo7)
axs[2].set_xlabel(r'$M_{Higgs}$')

```

```
[12]: Text(0.5, 0, '$M_{Higgs}$')
```





## Chapter 8

# Generalization of Splitting Functions for all Standard Model particles

At energies in the multi-TeV range (much larger than the masses of known particles of  $\mathcal{O}(100)$  GeV), mass effects of the particles become negligible and eventually they can be neglected. In this energy range even the "heavy" gauge bosons (like the Z, the W boson and the H boson) can be treated similarly to the massless photon  $\gamma$ .

Already in the discussion about the Superconducting Super Collider (SSC) [76,77] in the 1980's there were proposals for treating the W and Z boson as part of the parton densities [78–80], like ordinary particles. The concept of an *effective W, Z approximation* is described briefly in [81][Section 8.11]. Recently collinear parton densities including electroweak bosons are discussed in a more complete approach [82–85].

At the LHC, measurements of jets and electroweak bosons [86,87] support the picture, that at high energies the radiation of massive electroweak bosons from light quarks [88] can be treated similarly as those of massless photons or gluons. Although the electroweak bosons are treated as massless particles, their mass threshold must be respected. Such a picture offers new possibilities to also understand the so-called dead cone effect [89–92], which describes a region devoid of energy due to the emission from or off a heavy particle in a parton shower cascade.

### 8.1 Extraction of General Splitting Functions

In previous chapters we have extracted the DGLAP splitting functions for strong interacting partons using lowest order and higher order processes in DIS, as well as DY production processes. It is the triumph of collinear factorization, that the splitting functions obtained in DIS agree with those obtained in DY production in pp collisions.

We now turn to calculate splitting functions for all particles and gauge bosons within the standard model, which would be valid at highest energies, when the masses of the particles can be neglected. We can apply the same techniques as in DIS to obtain the splitting functions, the only difference in the processes is the coupling. In order to obtain the relevant effective couplings, we calculate the processes  $q\bar{q} \rightarrow \gamma^*$ ,  $q\bar{q} \rightarrow Z$  and  $q_i\bar{q}_j \rightarrow W$ . The matrix elements are given by (see also

eq.(7.9) ):

$$\mathcal{M}(q\bar{q} \rightarrow \gamma^*) = -ie\delta_{ij}\bar{q}_i(p_2)\gamma^\mu q_j(p_1)\epsilon_\mu^{(\gamma)} \quad (8.1)$$

$$\mathcal{M}(u\bar{u} \rightarrow Z) = -ig_Z\delta_{ij}\bar{q}_i(p_2)\gamma^\mu \frac{v_f - \gamma_5 v_a}{2} q_j(p_1)\epsilon_\mu^{(Z)} \quad (8.2)$$

$$\mathcal{M}(u\bar{d} \rightarrow W) = -\frac{iV_{ud}g_W\delta_{ij}}{\sqrt{2}}\bar{d}_i(p_2)\gamma^\mu \frac{1 - \gamma_5}{2} u_j(p_1)\epsilon_\mu^{(W)}. \quad (8.3)$$

The weak coupling is related at leading order to the electromagnetic coupling  $e^2 = 4\pi\alpha_{em}$  via:

$$g_W^2 = 4\sqrt{2}G_F m_W^2 = \frac{e^2}{\sin^2 \theta_W} = \frac{4\pi\alpha_{em}}{\sin^2 \theta_W} \quad (8.4)$$

$$g_Z^2 = \frac{g_W^2}{4\cos^2 \theta_W} \quad (8.5)$$

The sine of the Weinberg angle

$$\sin \theta_W \sim 0.23, \quad (8.6)$$

and the Fermi constant

$$G_F \sim 1.166 \cdot 10^{-5} \text{GeV}^{-2}. \quad (8.7)$$

The mass  $m_Z$  is related to  $m_W$  by:

$$m_Z^2 = \frac{m_W^2}{\cos^2 \theta_W} \quad (8.8)$$

With this we obtain the following squared matrix elements (after summing and averaging over colors, which gives an overall factor of 1/6):

$$|\mathcal{M}|^2(q\bar{q} \rightarrow \gamma^*) = \frac{1}{3}4\pi\alpha_{em}e_q^2 m_{DY}^2 \quad (8.9)$$

$$|\mathcal{M}|^2(q\bar{q} \rightarrow Z) = \frac{1}{3}m_Z^2 g_Z^2 (V_f^2 + A_f^2) = \frac{1}{3}m_Z^2 \frac{2G_F}{\sqrt{2}} m_Z^2 (V_f^2 + A_f^2) \quad (8.10)$$

$$|\mathcal{M}|^2(q_i\bar{q}_j \rightarrow W) = \frac{1}{12}m_W^2 g_W^2 |V_{qq}|^2 = \frac{1}{3} \frac{2|V_{qq}|^2 G_F m_W^4}{\sqrt{2}} \quad (8.11)$$

with  $V_f, A_f$  being the vector and axial couplings,  $|V_{qq}|$  being the Kobayashi-Maskawa Matrix. The total cross sections for these processes are:

$$\sigma(q\bar{q} \rightarrow \gamma^*) = \frac{1}{3} \frac{\pi}{m_{DY}^2} [4\pi\alpha_{em} m_{DY}^2] = \frac{1}{3} \pi [4\pi\alpha_{em}] \quad (8.12)$$

$$\sigma(q\bar{q} \rightarrow Z) = \frac{1}{3} \frac{\pi}{m_Z^2} \left[ \frac{2G_F}{\sqrt{2}} m_Z^4 (V_f^2 + A_f^2) \right] = \frac{1}{3} \pi \left[ \sqrt{2} G_F m_Z^2 (V_f^2 + A_f^2) \right] \quad (8.13)$$

$$\sigma(q_i\bar{q}_j \rightarrow W) = \frac{1}{3} \frac{\pi}{m_W^2} \left[ \frac{2|V_{qq}|^2 G_F m_W^4}{\sqrt{2}} \right] = \frac{1}{3} \pi \left[ \sqrt{2} G_F m_W^2 |V_{qq}|^2 \right] \quad (8.14)$$

With the following relations we can transform to a scheme, where we have only  $\alpha_{em}$ ,  $\theta_W$ , and  $m_Z$ :

$$\frac{G_F}{\sqrt{2}} = \frac{4\pi\alpha_{em}}{\sin^2 \theta_W} \frac{1}{8m_W^2} \quad (8.15)$$

$$m_Z^2 = \frac{m_W^2}{\cos^2 \theta_W} \quad (8.16)$$

Thus we obtain the cross sections by replacing the coupling in  $\alpha_{em}$  in  $\sigma(q\bar{q} \rightarrow \gamma^*)$  by an effective coupling  $\alpha_{eff}$ :

$$Z : \alpha_{eff} = \frac{\alpha_{em}}{4 \sin^2 \theta_W \cos^2 \theta_W} (V_f^2 + A_f^2) \quad (8.17)$$

$$W : \alpha_{eff} = \frac{\alpha_{em} |V_{qq}|^2}{4 \sin^2 \theta_W} \quad (8.18)$$

In Fig. 8.1 generic diagrams are shown where in addition to quarks and gluons also other gauge bosons are interacting (the blue line in Fig. 8.1 can be a gluon, a photon, a W or a Z boson).

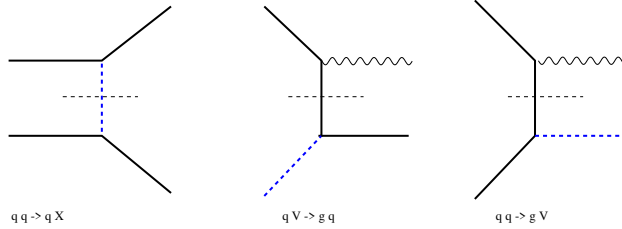


Figure 8.1: Schematic diagrams to illustrate extraction of splitting functions

We are now ready to write down the splitting functions including electroweak bosons, by simply replacing the coupling (as well as color factors) in the standard QCD DGLAP splitting functions. The so-called equivalent W-approximation was first calculated in Refs. [78,79,93].

For example for  $P_{qq}$  at leading order we obtain (see also Ref. [88]):

$$P_{qq}(z) = \frac{\alpha_{eff}}{2\pi} \frac{1+z^2}{1-z} \quad (8.19)$$

$$\alpha_{eff} = C_F \alpha_s \quad \text{for } q \rightarrow qg \quad (8.20)$$

$$\alpha_{eff} = \alpha_{em} \quad \text{for } q \rightarrow q\gamma \quad (8.21)$$

$$\alpha_{eff} = \frac{\alpha_{em}}{4 \sin^2 \theta_W \cos^2 \theta_W} (V_f^2 + A_f^2) \quad \text{for } q \rightarrow qZ \quad (8.22)$$

$$\alpha_{eff} = \frac{\alpha_{em} |V_{qq}|^2}{4 \sin^2 \theta_W} \quad \text{for } q \rightarrow qZ \quad (8.23)$$

In Tab. 8.1 we give an overview over the splitting functions at leading order. A full account including different polarization states is given in Refs. [82,84,85,94,95]. A very concise derivation of the equivalent vectorboson approximation is given in Ref. [96].

## 8.2 Photon and Heavy Boson Parton Densities

Photon radiation from quarks can happen, similarly to gluon radiation from quarks. The splitting functions are the same as in the QCD case, only with different color factors as given in Tab. 8.1, and except the self-coupling process, which does not exist for photons.

The evolution equation in terms of Sudakov form factors  $\Delta_a^S(z_M, \mu^2)$  is given by eq.(5.17):

$$xf_a(x, \mu^2) = \Delta_a^S(\mu^2) xf_a(x, \mu_0^2) + \sum_b \int_{\mu_0^2}^{\mu^2} \frac{d\mu'^2}{\mu'^2} \frac{\Delta_a^S(\mu'^2)}{\Delta_a^S(\mu^2)} \int_x^{z_M} dz \frac{\alpha_{eff}}{2\pi} \hat{P}_{ab}(z) \frac{x}{z} f_b\left(\frac{x}{z}, \mu'^2\right), \quad (8.24)$$





Splitting function	Diagram	$V = g$	$V = \gamma$	$V = Z$	$V = W$
$P_{qq}(z) = \frac{\alpha_{eff}}{2\pi} \frac{1+z^2}{1-z}$		$C_F \alpha_s$	$\alpha_{em}$	$\frac{\alpha_{em}(V_f^2 + A_f^2)}{4 \sin^2 \theta_W \cos^2 \theta_W}$	$\frac{\alpha_{em} V_{qq} ^2}{4 \sin^2 \theta_W}$
$P_{qV}(z) = \frac{\alpha_{eff}}{2\pi} (z^2 + (1-z)^2)$		$T_R \alpha_s$	$\alpha_{em}$	$\frac{\alpha_{em}(V_f^2 + A_f^2)}{4 \sin^2 \theta_W \cos^2 \theta_W}$	$\frac{\alpha_{em} V_{qq} ^2}{4 \sin^2 \theta_W}$
$P_{Vq}(z) = \frac{\alpha_{eff}}{2\pi} \frac{1+(1-z)^2}{z}$		$C_F \alpha_s$	$\alpha_{em}$	$\frac{\alpha_{em}(V_f^2 + A_f^2)}{4 \sin^2 \theta_W \cos^2 \theta_W}$	$\frac{\alpha_{em} V_{qq} ^2}{4 \sin^2 \theta_W}$
$P_{VV'}(z) = \frac{\alpha_{eff}}{2\pi} 2 \left( \frac{1-z}{z} + \frac{z}{1-z} + z(1-z) \right)$		$C_A \alpha_s$	0	$4\pi \alpha_{em} \cot \theta_W$	

Table 8.1: Splitting functions at lowest order and  $\alpha_{eff}$  for QCD and electroweak processes with the color factors  $C_F = 4/3$ ,  $C_A = 3$  and  $T_R = 1/2$ .

with the coupling  $\alpha_{eff}$  as given in Tab. 8.1, and  $a$  and  $b$  including now also the photon.

Given that we have obtained effective splitting functions also for the Z and W bosons, this equation is easily extended to include also the heavy vector-bosons.

### 8.2.1 Photon densities

The calculation of collinear photon densities has been discussed quite extensively in literature, see e.g. Refs. [97–104]. For a complete description of the photon density, also an intrinsic distribution of photons inside the hadron must be included, which is relevant at smaller scales  $\mu^2$ , while at large scales the dominant contribution comes from photon radiation off the quarks. Since the quark distribution changes when photon radiation is included, new fits of the starting distributions must be performed.

In Ref. [97] the collinear and TMD density of photons has been determined from anew fit to DIS inclusive measurements. Since the contribution from photon is small, the fit quality is unchanged. In [97] only the perturbative contribution is included, the intrinsic photon density is entirely neglected (also because the same approach is intended to be applied for Z and W, discussed below).

In Fig. 8.2 the collinear photon density as a function of  $x$  is shown for different values of the evolution scales  $\mu$  (from Ref. [97]). For comparison also the prediction from CT14qed-proton [99] is shown.

In Fig. the TMD density of photons is shown (from Ref. [97]).



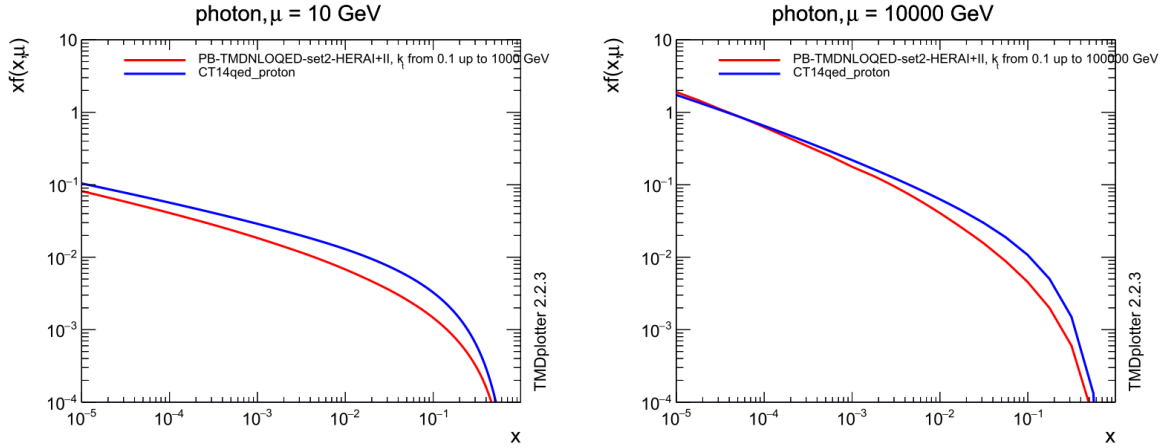


Figure 8.2: The collinear photon density at  $\mu = 10$  GeV and  $\mu = 100$  GeV as a function of  $x$ . For comparison also shown is the prediction from CT14qed-proton [99]. Plot from [97].

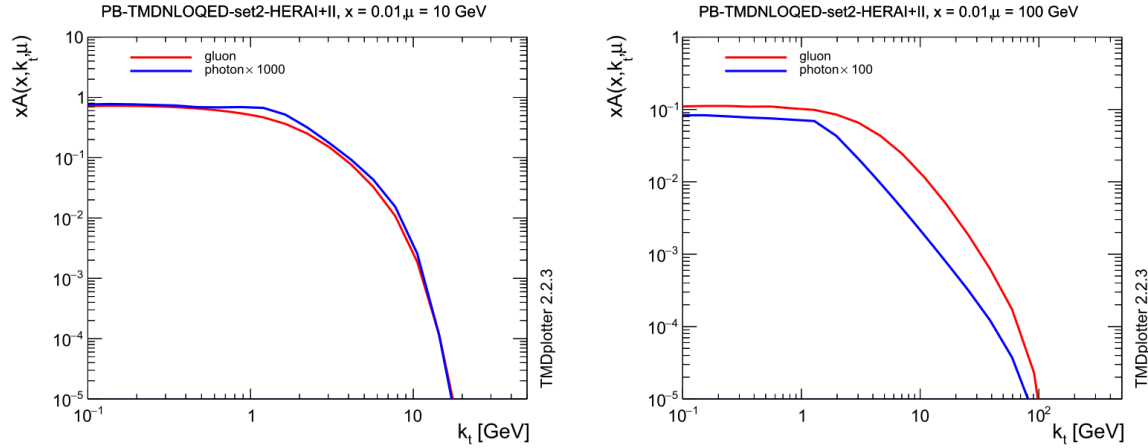


Figure 8.3: The TMD photon density at  $\mu = 10$  GeV and  $\mu = 100$  GeV as a function of  $k_T$ . For comparison also shown is the gluon density. Plot from [97].

### 8.2.2 Heavy Boson densities

The determination of effective W densities has been discussed already in Refs. [78–80, 93, 105–109]. In recent years, this ideas has been picked up again in Refs. [82–84, 94, 95].

The approach to determine the photon densities within the PB-method can be easily extended to determine the collinear and TMD densities of Z and W making use of the effective couplings in Tab.. 8.1. The straight forward application of the method give the collinear and TMD densities as shown in Figs., compared also to the photon density.

The heavy vector-boson density vanished (in the approach applied here) for scales  $\mu < m_W$  therefore the densities are only shown for larger scales. One can see very nicely, that for higher scales, the photon and W densities approach each other, as it should.

In the transverse momentum distribution, one can observe the similarity of photon and W densities at large  $k_T$ , while significant differences are visible at smaller  $k_T$ .

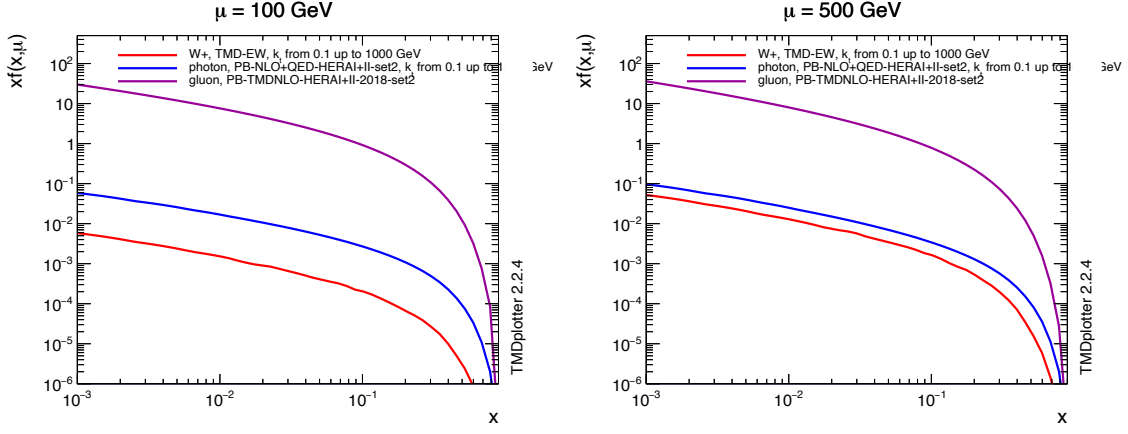


Figure 8.4: The collinear vectorboson density at  $\mu = 100$  GeV and  $\mu = 500$  GeV as a function of  $x$ .

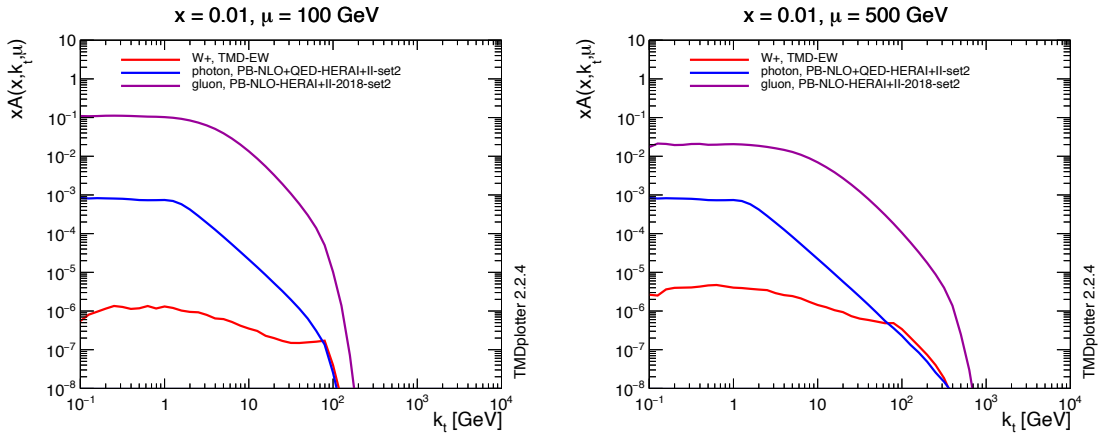


Figure 8.5: The TMD vectorboson density at  $\mu = 100$  GeV and  $\mu = 500$  GeV as a function of  $x$ .

## Appendix A

# Kinematics and Cross Section definition

### A.1 Four-Vector Kinematics

Four-vectors are used to characterize fully the state and the motion of a particle.

$$(E, \mathbf{p}) \stackrel{\text{def}}{=} (p^0, p^1, p^2, p^3) = p^\mu \stackrel{\text{def}}{=} p \quad (\text{A.1})$$

A four-vector is defined in a specific frame. Boost (or Lorentz-) invariant quantities can be defined from four-vectors. The simplest example is the invariant mass of a particle defined as:

$$E^2 - \mathbf{p}^2 = m^2 \quad (\text{A.2})$$

Products of four-vectors are Lorentz invariant. The four-vector product is defined as:

$$A.B \stackrel{\text{def}}{=} A^0 B^0 - \mathbf{A}\mathbf{B} \quad (\text{A.3})$$

In the collision of two particles,  $p_1$  and  $p_2$  the invariant mass of the system is given by:

$$\begin{aligned} s &= (P_1 + P_2)^2 = P_1^2 + P_2^2 + 2P_1.P_2 \\ &= M_1^2 + M_2^2 + 2(E_1 E_2 - \vec{P}_1 \vec{P}_2) \end{aligned} \quad (\text{A.4})$$

In the center-of-mass of the two colliding particles we have  $|\vec{P}_1| = |\vec{P}_2|$ . Assuming  $M_1 = M_2$  we get:

$$s = (P_1 + P_2)^2 = 2M^2 + 2(E^2 + P^2) \quad (\text{A.5})$$

with  $M = M_1 = M_2$ ,  $E = E_1 = E_2$  and  $P = |\vec{p}_1| = |\vec{p}_2|$ . In the case of  $E \gg M$ , we obtain:

$$s = (P_1 + P_2)^2 = 4E_b^2 = E_{cm}^2 \quad (\text{A.6})$$

with  $E_b$  being the beam energy and  $E_{cm}$  being the center-of-mass energy.

At LHC the energy of the colliding protons was increasing from a start up value of  $E_b = 450$  GeV, giving a center-of-mass energy of  $\sqrt{s} = 900$  GeV, to the design energy for each proton beam of  $E_b = 3500$  GeV giving a center-of-mass energy of  $\sqrt{s} = 13$  TeV, the highest energy achieved in a collider.

If one of the colliding particles is at rest ( $P_2 = (M, \vec{0})$ ), in a so-called *fixed-target* experiment, the energy available in the collision is (assuming the mass of the other particle to be small  $M_1 = 0$ ):

$$s = (P_1 + P_2)^2 = M^2 + 2E \cdot M \quad (\text{A.7})$$

In a *fixed-target* experiment with a muon beam of  $E = 280$  GeV colliding with protons at rest, the available center-of-mass energy squared was  $s = (P_1 + P_2)^2 \approx 560 \text{ GeV}^2$  which gives  $\sqrt{s} = 24$  GeV. At HERA, a electron-proton collider at DESY, electrons with an energy of  $E_e = 27$  GeV were collided with protons of energy of  $E_p = 920$  GeV yielding  $\sqrt{s} \approx 315$  GeV.

## A.2 Light Cone Variables

Some calculations become easier and the results are easier understood when so-called *light-cone* variables instead of the Cartesian variables are used (see for a description and discussion [110]). Any four-vector, defined as:

$$V = (V^0, V^1, V^2, V^3) = (V^0, V_\perp, V^3)$$

with  $V_\perp$  being a two-component vector, can be changed to its lightcone representation:

$$V^+ = \frac{1}{\sqrt{2}} (V^0 + V^3) \quad (\text{A.8})$$

$$V^- = \frac{1}{\sqrt{2}} (V^0 - V^3) \quad (\text{A.9})$$

$$V_\perp = (V^1, V^2) \quad (\text{A.10})$$

We also have:

$$V^0 = \frac{1}{\sqrt{2}} (V^+ + V^-) \quad (\text{A.11})$$

$$V^3 = \frac{1}{\sqrt{2}} (V^+ - V^-) \quad (\text{A.12})$$

From the definition of a four-vector product in eq.(A.3) we obtain the four-products of two four-vectors  $V$  and  $W$  in light-cone representation:

$$V \cdot W = V^+ W^- + V^- W^+ - V_\perp W_\perp \quad (\text{A.13})$$

$$V \cdot V = 2V^+ V^- - V_\perp^2 \quad (\text{A.14})$$

The light-cone components transform simpler under boosts along the  $z$ -axis: only the  $V^\pm$  components are affected under the boost. When a vector is highly boosted, the light-cone variables show easily the large and small components.

Sometimes, the light-cone variables are used to define the *Sudakov* decomposition:  $p = p^+ + p^- + k_T$  where here  $p^\pm$  and  $k_T$  have four components. Let us consider the following example to calculate the invariant mass of two colliding particles with momenta  $p_1 = \mathbf{p}_1^+ + \mathbf{p}_1^- + k_{t1}$  and  $p_2 = \mathbf{p}_2^+ + \mathbf{p}_2^- + k_{t2}$  with

$$\begin{aligned} \mathbf{p}_1^+ &= (p_1^+, 0^-, \vec{0}) \\ \mathbf{p}_1^- &= (0^+, p_1^-, \vec{0}) \\ k_{t1} &= (0^+, 0^-, \vec{k}_{T1}) \end{aligned}$$

and analogously for  $\mathbf{p}_2$ . The invariant mass  $s = (p_1 + p_2)^2$  is then :

$$\begin{aligned} s &= (\mathbf{p}_1^+ + \mathbf{p}_2^+ + \mathbf{p}_1^- + \mathbf{p}_2^- + k_{t1} + k_{t2})^2 \\ &= 2(\mathbf{p}_1^+ + \mathbf{p}_2^+)(\mathbf{p}_1^- + \mathbf{p}_2^-) + (k_{t1} + k_{t2})^2 \\ &= 2p_1^+ p_2^- \end{aligned}$$

where the last line was obtained since  $p_1^- = p_2^+ = 0$  and  $\vec{k}_{T1} = -\vec{k}_{T2}$ .

Lorentz boost appear very simple in terms of lightcone variables. The boosted vector  $V'^0$  and  $V'^3$  are defined as (with a boost along the  $z$  axis with velocity  $v$ ) :

$$V'^0 = \frac{V^0 + vV^3}{\sqrt{1 - v^2}} \quad (\text{A.15})$$

$$V'^3 = \frac{vV^0 + V^3}{\sqrt{1 - v^2}} \quad (\text{A.16})$$

$$V'^1 = V^1 \quad (\text{A.17})$$

$$V'^2 = V^2 \quad (\text{A.18})$$

Then we can calculate the boosted lightcone components:

$$V'^+ = \frac{1}{\sqrt{2}} \frac{V^0 + vV^3 + vV^0 + V^3}{\sqrt{1 - v^2}} \quad (\text{A.19})$$

$$= \frac{1}{\sqrt{2}} \frac{(V^0 + V^3)(1 + v)}{\sqrt{1 - v^2}} \quad (\text{A.20})$$

$$= \frac{1}{\sqrt{2}} \sqrt{\frac{(1 + v)(1 + v)}{(1 - v)(1 + v)}} (V^0 + V^3) \quad (\text{A.21})$$

$$= \frac{1}{\sqrt{2}} \sqrt{\frac{(1 + v)}{(1 - v)}} (V^0 + V^3) \quad (\text{A.22})$$

and similarly for  $V'^-$  with

$$V'^- = \frac{1}{\sqrt{2}} \sqrt{\frac{(1 - v)}{(1 + v)}} (V^0 - V^3) \quad (\text{A.23})$$

Defining

$$\psi = \frac{1}{2} \log \frac{1 + v}{1 - v}$$

one obtains

$$e^\psi = e^{\frac{1}{2} \log \frac{1+v}{1-v}} = \sqrt{\frac{1 + v}{1 - v}}$$

and thus

$$V'^+ = V^+ e^\psi \quad (\text{A.24})$$

$$V'^- = V^- e^{-\psi} \quad (\text{A.25})$$

Consider a particle at rest with

$$p^{rest} = \left( \frac{m}{\sqrt{2}}, \frac{m}{\sqrt{2}}, 0 \right)$$

which is obtained from  $p = (m, 0, 0)$  in Cartesian coordinates. In a moving frame the momentum becomes:

$$p' = (p'^+, p'^-, 0) = \left( \frac{m}{\sqrt{2}} e^\psi, \frac{m}{\sqrt{2}} e^{-\psi}, 0 \right)$$

with

$$\begin{aligned} \frac{p'^+}{p'^-} &= e^{2\psi} \\ \leadsto \log \frac{p'^+}{p'^-} &= 2\psi \end{aligned}$$

we obtain the expression for rapidity:

$$\psi = y = \frac{1}{2} \log \frac{p'^+}{p'^-} \quad (\text{A.26})$$

### A.3 Cross Section definition

In general, the cross section of the scattering of two particles  $p_1$  and  $p_2$  with masses  $m_1$  and  $m_2$  into any number of final state particles  $p_i$  is defined as:

$$d\sigma = \frac{1}{flux} \cdot dLips \cdot |M|^2$$

where  $|M|^2$  is the squared matrix element, which contains the physics,  $flux$  is the flux of the incoming particles defined as:

$$flux = 4\sqrt{(p_1 p_2)^2 - m_1^2 m_2^2} \quad (\text{A.27})$$

and  $dLips$  is the *Lorentz-invariant-phase-space* defined as

$$dLips = (2\pi)^4 \delta^4 \left( -p_1 - p_2 + \sum_i p_i \right) \prod_{i>2} \frac{d^4 p_i}{(2\pi)^3} \delta(p_i^2 - m_i^2) \quad (\text{A.28})$$

$$= (2\pi)^4 \delta^4 \left( -p_1 - p_2 + \sum_i p_i \right) \prod_{i>2} \frac{d^3 p_i}{(2\pi)^3 2E_i} \quad (\text{A.29})$$

$$= (2\pi)^4 \delta^4 \left( -p_1 - p_2 + \sum_i p_i \right) \prod_{i>2} \frac{1}{(2\pi)^3} \frac{dp_i^+}{p_i^+} d^2 p_{t\ i} \quad (\text{A.30})$$

The cross section for a  $2 \rightarrow 2$  process of  $p_1 + p_2 \rightarrow p_3 + p_4$  can be written as (assuming massless incoming particles) :

$$\frac{d\sigma}{dt} = \frac{1}{16\pi} \frac{1}{s^2} |M|^2 \quad (\text{A.31})$$

If one particle has mass, like the virtual photon with virtual mass  $Q^2$ , then the formula is modified to (for  $p_1^2 = -Q^2$ ) :

$$\frac{d\sigma}{dt} = \frac{1}{16\pi} \frac{1}{s + Q^2} \frac{1}{s} |M|^2 \quad (\text{A.32})$$

with  $s, t$  being the Mandelstam variables:

$$s = (p_1 + p_2)^2 = (p_3 + p_4)^2 \quad (\text{A.33})$$

$$t = (p_1 - p_3)^2 = (p_2 - p_4)^2 \quad (\text{A.34})$$

$$u = (p_1 - p_4)^2 = (p_2 - p_3)^2 \quad (\text{A.35})$$

$$s + t + u = m_1^2 + m_2^2 + m_3^2 + m_4^2 \quad (\text{A.36})$$

## A.4 Kinematics for DIS and pp

In a  $2 \rightarrow 2$  process we can relate the Mandelstam variable  $\hat{t}$  to the transverse momentum of the  $\hat{t}$ -propagator.

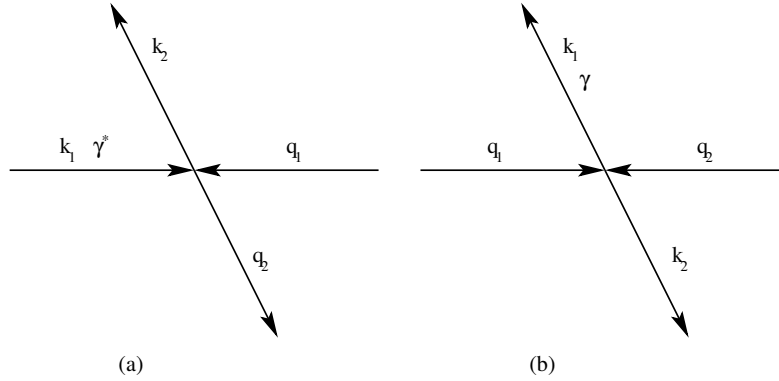


Figure A.1: Schematic drawing of  $\gamma^* + g \rightarrow q\bar{q}$  (a) and  $g + g \rightarrow q\bar{q}$  (b) scattering..

### A.4.1 $ep$ - case

In the center of mass frame of the parton process  $\gamma^*(k_1)q(q_1) \rightarrow q(q_2)g(k_2)$  the four-vectors of the incoming and outgoing particles are (see Fig. A.1(a)) :

$$\begin{aligned} k_1 &= (\sqrt{\vec{k}^2 - Q^2}, 0, 0, k) \\ q_1 &= (k, 0, 0, -k) \\ q_2 &= (q, -q \sin \theta, 0, -q \cos \theta) \\ k_2 &= (q, q \sin \theta, 0, q \cos \theta) \end{aligned}$$

with  $k_1^2 = -Q^2$ . From this we obtain

$$\begin{aligned} \hat{s} &= (k_2 + q_2)^2 = 4q^2 \\ \hat{t} &= (k_1 - q_2)^2 = (q_1 - k_2)^2 = -2(kq + kq \cos \theta) = -2kq(1 + \cos \theta) \\ \hat{u} &= (q_1 - q_2)^2 = -2(kq - kq \cos \theta) = -2kq(1 - \cos \theta) \\ \hat{s}\hat{t}\hat{u} &= 4q^2 4(qk)^2 (1 + \cos \theta)(1 - \cos \theta) = (4kq)^2 q^2 \sin^2 \theta \\ \hat{t} + \hat{u} &= -\hat{s} - Q^2 = -2kq(1 + \cos \theta) - 2kq(1 - \cos \theta) = -4kq \end{aligned}$$

With this we obtain:

$$p_t^2 = q^2 \sin^2 \theta \quad (\text{A.37})$$

$$= \frac{\hat{t}\hat{u}\hat{s}}{(\hat{s} + Q^2)^2} \quad (\text{A.38})$$

In the small  $t$  limit we obtain from  $\hat{t} + \hat{u} + \hat{s} = -Q^2 \rightsquigarrow \hat{u} = -Q^2 - \hat{s}$ . Using  $z = \frac{Q^2}{2k_1 \cdot q_1}$  and  $\hat{s} = -Q^2 + Q^2/z$  we obtain:

$$p_t^2 = -\frac{\hat{t}\hat{s}}{\hat{s} + Q^2} \quad (\text{A.39})$$

$$= -\hat{t}(1 - z) \quad (\text{A.40})$$

#### A.4.2 $pp$ - case

Here we calculate the relation between the transverse momentum  $p_t$  of a final state parton in a  $2 \rightarrow 2$  process, like  $q(q_1)\bar{q}(q_2) \rightarrow \gamma^*(k_1)g(k_2)$  with the four-vectors indicated in the brackets. The four-vectors are given by (see Fig. A.1(b)):

$$\begin{aligned} q_1 &= (q, 0, 0, q) \\ q_2 &= (q, 0, 0, -q) \\ k_1 &= (\sqrt{M^2 + \vec{k}^2}, -k \sin \theta, 0, -k \cos \theta) \\ k_2 &= (k, k \sin \theta, 0, k \cos \theta) \end{aligned}$$

with  $k_1^2 = M^2$ . From this we obtain

$$\begin{aligned} \hat{s} &= (q_1 + q_2)^2 = 4k_1 k_2 = 4q^2 \\ \hat{t} &= (q_1 - k_1)^2 = (q_2 - k_2)^2 = -2(qk + qk \cos \theta) = -2qk(1 + \cos \theta) \\ \hat{u} &= (q_1 - k_2)^2 = -2(qk - qk \cos \theta) = -2qk(1 - \cos \theta) \\ \hat{t}\hat{u} &= 4(qk)^2(1 - \cos \theta)(1 + \cos \theta) = 4(qk)^2 \sin^2 \theta \end{aligned}$$

With this we obtain:

$$p_t^2 = k^2 \sin^2 \theta \quad (\text{A.41})$$

$$= \frac{\hat{t}\hat{u}}{\hat{s}} \quad (\text{A.42})$$

Please note that this is different compare to the DIS case (eq.(A.38)), where we obtained:

$$p_t^2 = \frac{\hat{t}\hat{u}\hat{s}}{(\hat{s} + Q^2)^2}$$

However, performing the small  $t$  limit and using  $\hat{s} + \hat{t} + \hat{u} = M^2$  together with  $z = M^2/\hat{s}$  we obtain:

$$p_t^2 = \frac{\hat{t}\hat{u}}{\hat{s}} \quad (\text{A.43})$$

$$\rightsquigarrow p_t^2 = \frac{\hat{t}(\hat{s} - M^2)}{\hat{s}} \quad (\text{A.44})$$

$$= -\hat{t}(1 - z) \quad (\text{A.45})$$

which agrees with what is obtained in the DIS case.



## A.5 Calculation of transverse momentum of Drell Yan pair

Starting from eq.(7.15) we obtain:

$$\frac{1}{\sigma} \frac{d\sigma}{dp_t} = \int d^2\vec{k}_{T1} d^2\vec{k}_{T2} \delta^{(2)}(\vec{k}_{T1} + \vec{k}_{T2} - \vec{p}_t) h(\vec{k}_{T1}) h(\vec{k}_{T2}) \quad (\text{A.46})$$

$$= \int d^2\vec{k}_{T1} h(\vec{k}_{T1}) h(\vec{p}_t - \vec{k}_{T1}) \quad (\text{A.47})$$

$$= \frac{1}{2} \int_0^\infty dk_{t1}^2 \int d\phi \frac{b^2}{\pi^2} \exp(-2bk_{t1}^2) \exp(-bp_t^2) \exp(2bp_t k_{t1} \cos \phi) \quad (\text{A.48})$$

$$= \frac{b^2}{2\pi^2} \exp(-bp_t^2) \int dk_{t1}^2 \exp(-2bk_{t1}^2) 2\pi I_0(2bp_t k_{t1}) \quad (\text{A.49})$$

$$= \frac{b}{2\pi} \exp\left(-\frac{1}{2}bp_t^2\right) \quad (\text{A.50})$$

where we have used the expression for the modified Bessel function:

$$\int_0^{2\pi} d\phi \exp(z \cos \phi) = 2\pi I_0(z)$$

with:

$$I_0(z) = \sum_n \frac{\left(\frac{1}{4}z^2\right)^n}{(n!)^2} \quad (\text{A.51})$$

and have integrated this expression term by term<sup>1</sup>. Using eq.(A.49):

$$\begin{aligned} \frac{1}{\sigma} \frac{d\sigma}{dp_t} &= \int d^2\vec{k}_{T1} d^2\vec{k}_{T2} \delta^{(2)}(\vec{k}_{T1} + \vec{k}_{T2} - \vec{p}_t) h(\vec{k}_{T1}) h(\vec{k}_{T2}) \\ &= \frac{b^2}{2\pi^2} \exp(-bp_t^2) \int dk_{t1}^2 \exp(-2bk_{t1}^2) 2\pi I_0(2bp_t k_{t1}) \end{aligned}$$

together with eq.(A.51):

$$I_0(z) = \sum_n \frac{\left(\frac{1}{4}z^2\right)^n}{(n!)^2}$$

gives:

$$\frac{1}{\sigma} \frac{d\sigma}{dp_t} = \frac{b^2}{2\pi^2} \exp(-bp_t^2) \int dk_{t1}^2 \exp(-2bk_{t1}^2) 2\pi \sum_{n=0}^{n=\infty} \frac{\left(\frac{1}{4}(2bp_t k_{t1})^2\right)^n}{(n!)^2}$$

and we can perform the integration term by term giving:

$$\begin{aligned} S &= \frac{1}{\sigma} \frac{d\sigma}{dp_t} \\ &= \sum_{n=0}^{n=\infty} S_n \end{aligned}$$

---

<sup>1</sup>Courtesy of K. Kutak, who showed how to perform the integral

with:

$$\begin{aligned}
S_0 &= \frac{b^2}{2\pi^2} \exp(-bp_t^2) \int dk_{t1}^2 2\pi \exp(-2bk_{t1}^2) \\
&= \frac{b^2}{\pi} \exp(-bp_t^2) \frac{1}{2b} \\
&= \frac{b}{2\pi} \exp(-bp_t^2) \\
S_1 &= \frac{b^2}{2\pi^2} \exp(-bp_t^2) \int dk_{t1}^2 2\pi \exp(-2bk_{t1}^2) \frac{1}{4} (2bp_t k_{t1})^2 \\
&= \frac{b^2}{\pi} \exp(-bp_t^2) \frac{1}{4} 4b^2 p_t^2 \int dk_{t1}^2 \pi \exp(-2bk_{t1}^2) k_{t1}^2 \\
&= \frac{b}{2\pi} \exp(-bp_t^2) \frac{b}{2} p_t^2 \\
S_2 &= \frac{b^2}{2\pi^2} \exp(-bp_t^2) \int dk_{t1}^2 2\pi \exp(-2bk_{t1}^2) \frac{\frac{1}{4} (4b^2 k_{t1}^2 p_t^2)^2}{4} \\
&= \frac{b^2}{2\pi} \exp(-bp_t^2) \frac{1}{2} b^4 p_t^4 \int dk_{t1}^2 \pi \exp(-2bk_{t1}^2) k_{t1}^4 \\
&= \frac{b}{2\pi} \exp(-bp_t^2) \frac{b^2}{8} p_t^4 \\
&\vdots
\end{aligned}$$

Summing up all terms gives:

$$\begin{aligned}
S &= S_0 + S_1 + S_2 + \dots \\
&= \frac{b}{2\pi} \exp(-bp_t^2) \left( 1 + \frac{b}{2} p_t^2 + \frac{1}{8} b^2 p_t^4 + \dots \right) \\
&= \frac{b}{2\pi} \exp(-bp_t^2) \left( 1 + \frac{1}{1!} \frac{bp_t^2}{2} + \frac{1}{2!} \left( \frac{bp_t^2}{2} \right)^2 + \dots \right) \\
&= \frac{b}{2\pi} \exp\left(-\frac{1}{2} bp_t^2\right)
\end{aligned}$$

# Bibliography

- [1] “United Nations Charter”, 26 June, 1945.
- [2] W. O. Lock, “A History of the Collaboration Between the European Organization for Nuclear Research (CERN) and the Joint Institute for Nuclear Research (JINR), and with Soviet Research Institutes in the USSR, 1955-1970”. CERN Yellow Report 75-7, 1975.
- [3] CERN, “Science for Peace”.
- [4] CMS Collaboration, “The CMS HCAL and Russian Navy Shells”, Nov, 2011.
- [5] H. Schopper, “Science For Peace? More than ever!”. CERN Courier, 2022.
- [6] M. Albrecht et al., “Beyond a Year of Sanctions in Science”, 2023. [arXiv:2311.02141](#).
- [7] H. Jung, “Science needs cooperation, not exclusion”. CERN Courier, 2024.
- [8] A. Ali et al., “A Science4Peace initiative: Alleviating the consequences of sanctions in international scientific cooperation”, [arXiv:2403.07833](#).
- [9] R. Brun and F. Rademakers, “ROOT: An object oriented data analysis framework”, *Nucl. Instrum. Meth. A* **389** (1997) 81–86.
- [10] Random.Org, “True Random Number Service”. <http://www.random.org/>.
- [11] ID QUANTIQUE SA, “Quantique random number generator”. <http://www.idquantique.com/true-random-number-generator/products-overview.html>.
- [12] S. Weinzierl, “Introduction to Monte Carlo methods”, [arXiv:hep-ph/0006269](#).
- [13] G. Cowan, “Statistical data analysis”. Oxford, UK: Clarendon (1998) 197 p.
- [14] D. E. Knuth, “The Art of Computer Programming Volumes 1-3 Boxed Set”. Addison-Wesley Longman Publishing Co., Inc., Boston, MA, USA, 1998.
- [15] F. James, “RANLUX: A FORTRAN implementation of the high quality pseudorandom number generator of Luscher”, *Comput.Phys.Commun.* **79** (1994) 111–114.
- [16] M. Luscher, “A Portable high quality random number generator for lattice field theory simulations”, *Comput. Phys. Commun.* **79** (1994) 100–110, [arXiv:hep-lat/9309020](#).
- [17] M. Luscher, “A Portable high quality random number generator for lattice field theory simulations”. <http://luscher.web.cern.ch/luscher/ranlux/index.html> C++ code.

- [18] M. E. O'Neill, "PCG: A Family of Simple Fast Space-Efficient Statistically Good Algorithms for Random Number Generation", Technical Report A-Random, Harvey Mudd College, Claremont, CA, Sep, 2014.
- [19] V. Blobel and E. Lohrmann, "Statistische und numerische Methoden der Datenanalyse", volume 54. Teubner, 1998.
- [20] G. Bohm and G. Zech, "Introduction to statistics and measurement analysis for physicists". Hamburg, Germany: DESY (2005) 331 p.
- [21] F. James, "Monte Carlo Theory and Practice", *Rept.Prog.Phys.* **43** (1980) 1145.
- [22] F. Halzen and A. D. Martin, "Quarks and Leptons: An introductory course in modern particle physics". 1984. New York, USA: Wiley ( 1984) 396p.
- [23] R. D. Field, "Applications of Perturbative QCD". Addison-Wesley Longman Publishing Co., Inc., 1989.
- [24] R. K. Ellis, W. J. Stirling, and B. R. Webber, "QCD and collider physics", *Camb. Monogr. Part. Phys. Nucl. Phys. Cosmol.* **8** (1996) 1.
- [25] Y. L. Dokshitzer, V. A. Khoze, A. H. Mueller, and S. I. Troian, "Basics of perturbative QCD". Gif-sur-Yvette, France: Ed. Frontieres (1991) 274 p.
- [26] J. Bjorken and E. A. Paschos, "Inelastic Electron Proton and gamma Proton Scattering, and the Structure of the Nucleon", *Phys.Rev.* **185** (1969) 1975–1982.
- [27] H1 and ZEUS Collaboration, "Combination of measurements of inclusive deep inelastic  $e^\pm p$  scattering cross sections and QCD analysis of HERA data", *Eur. Phys. J. C* **75** (2015) 580, [arXiv:1506.06042](https://arxiv.org/abs/1506.06042).
- [28] V. N. Gribov and L. N. Lipatov, "Deep inelastic  $ep$  scattering in perturbation theory", *Sov. J. Nucl. Phys.* **15** (1972) 438. [*Yad. Fiz.*15,781(1972)].
- [29] L. N. Lipatov, "The parton model and perturbation theory", *Sov. J. Nucl. Phys.* **20** (1975) 94. [*Yad. Fiz.*20,181(1974)].
- [30] G. Altarelli and G. Parisi, "Asymptotic freedom in parton language", *Nucl. Phys. B* **126** (1977) 298.
- [31] Y. L. Dokshitzer, "Calculation of the structure functions for Deep Inelastic Scattering and  $e^+e^-$  annihilation by perturbation theory in Quantum Chromodynamics.", *Sov. Phys. JETP* **46** (1977) 641. [*Zh. Eksp. Teor. Fiz.*73,1216(1977)].
- [32] G. Altarelli, "Partons in Quantum Chromodynamics", *Phys. Rept.* **81** (1982) 1.
- [33] CTEQ Collaboration, "Handbook of perturbative QCD: Version 1.0", *Rev.Mod.Phys.* **67** (1995) 157–248.
- [34] J. C. Collins, D. E. Soper, and G. F. Sterman, "Factorization of Hard Processes in QCD", *Adv.Ser.Direct.High Energy Phys.* **5** (1988) 1–91, [arXiv:hep-ph/0409313](https://arxiv.org/abs/hep-ph/0409313). To be publ. in 'Perturbative QCD' (A.H. Mueller, ed.) (World Scientific Publ., 1989).
- [35] CTEQ Collaboration, "Global QCD analysis of parton structure of the nucleon: CTEQ5 parton distributions", *Eur. Phys. J. C* **12** (2000) 375, [arXiv:hep-ph/9903282](https://arxiv.org/abs/hep-ph/9903282).

- [36] N. A. Abdulov et al., “TMDlib2 and TMDplotter: a platform for 3D hadron structure studies”, *Eur. Phys. J. C* **81** (2021) 752, [arXiv:2103.09741](#).
- [37] F. Hautmann et al., “TMDlib and TMDplotter: library and plotting tools for transverse-momentum-dependent parton distributions”, *Eur. Phys. J. C* **74** (2014), no. 12, 3220, [arXiv:1408.3015](#).
- [38] F. Hautmann et al., “Collinear and TMD quark and gluon densities from Parton Branching solution of QCD evolution equations”, *JHEP* **01** (2018) 070, [arXiv:1708.03279](#).
- [39] F. Hautmann et al., “Soft-gluon resolution scale in QCD evolution equations”, *Phys. Lett. B* **772** (2017) 446, [arXiv:1704.01757](#).
- [40] M. Bengtsson, T. Sjostrand, and M. van Zijl, “Initial state radiation effects on W and jet production”, *Z. Phys. C* **32** (1986) 67.
- [41] S. Gieseke, P. Stephens, and B. Webber, “New formalism for QCD parton showers”, *JHEP* **12** (2003) 045, [arXiv:hep-ph/0310083](#).
- [42] T. Sjöstrand and P. Z. Skands, “Transverse-momentum-ordered showers and interleaved multiple interactions”, *Eur. Phys. J.* **C39** (2005) 129–154, [arXiv:hep-ph/0408302](#).
- [43] G. Marchesini and B. R. Webber, “Simulation of QCD initial state radiation at small  $x$ ”, *Nucl. Phys.* **B349** (1991) 617–634.
- [44] G. Marchesini and B. R. Webber, “Final states in heavy quark lepton production at small  $x$ ”, *Nucl. Phys. B* **386** (1992) 215–235.
- [45] F. Hautmann, H. Jung, and S. T. Monfared, “The CCFM uPDF evolution uPDFevolv”, *Eur. Phys. J. C* **74** (2014) 3082, [arXiv:1407.5935](#).
- [46] M. Botje, “QCDNUM: fast QCD evolution and convolution”, *Comput.Phys.Commun.* **182** (2011) 490, [arXiv:1005.1481](#).
- [47] K. J. Golec-Biernat et al., “Markovian Monte Carlo solutions of the one-loop CCFM equations”, *Acta Phys. Polon.* **B38** (2007) 3149–3168, [arXiv:hep-ph/0703317](#).
- [48] K. J. Golec-Biernat, S. Jadach, W. Placzek, and M. Skrzypek, “Markovian Monte Carlo solutions of the NLO QCD evolution equations”, *Acta Phys. Polon.* **B37** (2006) 1785–1832, [arXiv:hep-ph/0603031](#).
- [49] S. Jadach et al., “Constrained MC for QCD evolution with rapidity ordering and minimum  $k_T^*$ ”, *Comput. Phys. Commun.* **180** (2009) 675–698, [arXiv:hep-ph/0703281](#).
- [50] S. Jadach and M. Skrzypek, “QCD evolution in the fully unintegrated form”, *Acta Phys. Polon. B* **40** (2009) 2071–2096, [arXiv:0905.1399](#).
- [51] S. Jadach and M. Skrzypek, “Exact solutions of the QCD evolution equations using Monte Carlo method”, *Acta Phys. Polon.* **B35** (2004) 745, [arXiv:hep-ph/0312355](#).
- [52] A. Bermudez Martinez et al., “Collinear and TMD parton densities from fits to precision DIS measurements in the parton branching method”, *Phys. Rev. D* **99** (2019) 074008, [arXiv:1804.11152](#).
- [53] M. Mendizabal, F. Guzman, H. Jung, and S. Taheri Monfared, “On the role of soft gluons in collinear parton densities”, [arXiv:2309.11802](#).

- [54] R. Angeles-Martinez et al., “Transverse Momentum Dependent (TMD) parton distribution functions: status and prospects”, *Acta Phys. Polon. B* **46** (2015), no. 12, 2501, [arXiv:1507.05267](#).
- [55] T. Sjöstrand, S. Mrenna, and P. Skands, “PYTHIA 6.4 physics and manual”, *JHEP* **05** (2006) 026, [arXiv:hep-ph/0603175](#).
- [56] T. Sjöstrand, S. Mrenna, and P. Z. Skands, “A brief introduction to PYTHIA 8.1”, *Comput. Phys. Commun.* **178** (2008) 852–867, [arXiv:0710.3820](#).
- [57] G. Marchesini et al., “HERWIG: A Monte Carlo event generator for simulating hadron emission reactions with interfering gluons. Version 5.1 - April 1991”, *Comput. Phys. Commun.* **67** (1992) 465.
- [58] G. Corcella et al., “HERWIG 6.5 release note”, [arXiv:hep-ph/0210213](#).
- [59] M. Bahr et al., “Herwig++: physics and manual”, *Eur. Phys. J. C* **58** (2008) 639–707, [arXiv:0803.0883](#).
- [60] H. Jung, “Hard diffractive scattering in high-energy  $ep$  collisions and the Monte Carlo generator RAPGAP”, *Comp. Phys. Commun.* **86** (1995) 147.
- [61] H. Jung, “The RAPGAP Monte Carlo version 3.2”. <http://projects.hepforge.org/rapgap/>, Nov., 2011.
- [62] F. Von Samson-Himmelstjerna, “Determination of parton density functions using Monte Carlo event generators”, Master’s thesis, [/afs/desy.de/group/h1/psfiles/theses/h1th-516.pdf](#), 2009.
- [63] J. Pumplin et al., “New generation of parton distributions with uncertainties from global QCD analysis”, *JHEP* **0207** (2002) 012, [arXiv:hep-ph/0201195](#).
- [64] J. Collins and H. Jung, “Need for fully unintegrated parton densities”, [arXiv:hep-ph/0508280](#).
- [65] S. Drell and T.-M. Yan, “Massive Lepton Pair Production in Hadron-Hadron Collisions at High-Energies”, *Phys. Rev. Lett.* **25** (1970) 316.
- [66] J. M. Campbell, J. W. Huston, and W. J. Stirling, “Hard Interactions of Quarks and Gluons: A Primer for LHC Physics”, *Rept. Prog. Phys.* **70** (2007) 89, [arXiv:hep-ph/0611148](#).
- [67] CMS Collaboration, “Measurement of the rapidity and transverse momentum distributions of  $Z$  Bosons in  $pp$  collisions at  $\sqrt{s} = 7$  TeV”, *Phys.Rev.* **D85** (2012) 032002, [arXiv:1110.4973](#).
- [68] Y. L. Dokshitzer, D. Diakonov, and S. I. Troian, “On the Transverse Momentum Distribution of Massive Lepton Pairs”, *Phys. Lett. B* **79** (1978) 269.
- [69] G. Parisi and R. Petronzio, “Small Transverse Momentum Distributions in Hard Processes”, *Nucl. Phys.* **B154** (1979) 427.
- [70] S. D. Ellis, N. Fleishon, and W. J. Stirling, “Logarithmic approximations, quark form-factors and Quantum Chromodynamics”, *Phys. Rev. D* **24** (1981) 1386.
- [71] J. C. Collins, D. E. Soper, and G. F. Sterman, “Transverse Momentum Distribution in Drell-Yan Pair and W and Z Boson production”, *Nucl. Phys. B* **250** (1985) 199.

- [72] C. T. H. Davies, B. R. Webber, and W. J. Stirling, “Drell-Yan Cross-Sections at Small Transverse Momentum”, *Nucl. Phys.* **B256** (1985) 413. [1,I.95(1984)].
- [73] A. Lelek, “Determination of TMD parton densities from HERA data and application to pp processes”. PhD thesis, 2018.
- [74] M. Pavlov, “Study of transverse momentum dependent formalisms”, Master’s thesis, University Antwerp, 2020.
- [75] J. Collins, “Foundations of perturbative QCD”, volume 32. Cambridge monographs on particle physics, nuclear physics and cosmology., 2011.
- [76] V. Lüth, “Summary of experiments”, *AIP Conf. Proc.* **302** (1994) 727–741.
- [77] [Wikipedia](#), “[Superconducting Super Collider](#)”.
- [78] S. Dawson, “The Effective  $W$  Approximation”, *Nucl. Phys. B* **249** (1985) 42.
- [79] G. L. Kane, W. Repko, and W. Rolnick, “The Effective  $W^{+-}$ ,  $Z^0$  Approximation for High-Energy Collisions”, *Phys. Lett. B* **148** (1984) 367.
- [80] Z. Kunszt and D. E. Soper, “On the Validity of the Effective  $W$  Approximation”, *Nucl. Phys. B* **296** (1988) 253.
- [81] V. D. Barger and R. J. N. Phillips, “COLLIDER PHYSICS”. 1987.
- [82] B. Fornal, A. V. Manohar, and W. J. Waalewijn, “Electroweak Gauge Boson Parton Distribution Functions”, *JHEP* **05** (2018) 106, [arXiv:1803.06347](#).
- [83] C. W. Bauer, N. Ferland, and B. R. Webber, “Combining initial-state resummation with fixed-order calculations of electroweak corrections”, *JHEP* **04** (2018) 125, [arXiv:1712.07147](#).
- [84] C. W. Bauer, N. Ferland, and B. R. Webber, “Standard Model Parton Distributions at Very High Energies”, *JHEP* **08** (2017) 036, [arXiv:1703.08562](#).
- [85] J. Chen, T. Han, and B. Tweedie, “Electroweak Splitting Functions and High Energy Showering”, *JHEP* **11** (2017) 093, [arXiv:1611.00788](#).
- [86] [M. Mendizabal Morentin](#), “[Z boson production in association with jets: measurement and phenomenology](#)”. PhD thesis, Hamburg University, 2024.
- [87] [ATLAS Collaboration Collaboration](#), “[Measurements of the production cross section of a  \$Z\$  boson in association with high transverse momentum jets in  \$pp\$  collisions at  \$\sqrt{s} = 13\$  TeV with the ATLAS detector](#)”, technical report, CERN, Geneva, Jul, 2021. All figures including auxiliary figures are available at <https://atlas.web.cern.ch/Atlas/GROUPS/PHYSICS/CONFNOTES/ATLAS-CONF-2021-033>.
- [88] J. R. Christiansen and T. Sjöstrand, “Weak Gauge Boson Radiation in Parton Showers”, *JHEP* **04** (2014) 115, [arXiv:1401.5238](#).
- [89] S. Kluth, W. Ochs, and R. Perez-Ramos, “Dead cone effect in charm and bottom quark jets”, in *26th High-Energy Physics International Conference in QCD*. 9, 2023. [arXiv:2309.01708](#).



- [90] ALICE Collaboration, “Direct observation of the dead-cone effect in quantum chromodynamics”, *Nature* **605** (2022) 440, [arXiv:2106.05713](#). [Erratum: *Nature* 607, E22 (2022)].
- [91] F. Maltoni, M. Selvaggi, and J. Thaler, “Exposing the dead cone effect with jet substructure techniques”, *Phys. Rev. D* **94** (2016), no. 5, 054015, [arXiv:1606.03449](#).
- [92] Y. L. Dokshitzer, V. A. Khoze, and S. I. Troian, “Particle spectra in light and heavy quark jets”, *J. Phys. G* **17** (1991) 1481–1492.
- [93] M. S. Chanowitz and M. K. Gaillard, “The TeV Physics of Strongly Interacting W’s and Z’s”, *Nucl. Phys. B* **261** (1985) 379–431.
- [94] P. Ciafaloni, G. Co’, D. Colferai, and D. Comelli, “Electroweak Evolution Equations and Isospin Conservation”, [arXiv:2403.08583](#).
- [95] P. Ciafaloni and D. Comelli, “Electroweak evolution equations”, *JHEP* **11** (2005) 022, [arXiv:hep-ph/0505047](#).
- [96] I. Alikhanov, “The equivalent vector boson approximation at threshold energies”, [arXiv:1812.05578](#).
- [97] H. Jung, S. T. Monfared, and T. Wening, “Determination of collinear and TMD photon densities using the Parton Branching method”, *Physics Letters B* **817** (2021) 136299, [arXiv:2102.01494](#).
- [98] A. V. Manohar, P. Nason, G. P. Salam, and G. Zanderighi, “The Photon Content of the Proton”, *JHEP* **12** (2017) 046, [arXiv:1708.01256](#).
- [99] C. Schmidt, J. Pumplin, D. Stump, and C. P. Yuan, “CT14QED parton distribution functions from isolated photon production in deep inelastic scattering”, *Phys. Rev. D* **93** (2016), no. 11, 114015, [arXiv:1509.02905](#).
- [100] A. Manohar, P. Nason, G. P. Salam, and G. Zanderighi, “How bright is the proton? A precise determination of the photon parton distribution function”, *Phys. Rev. Lett.* **117** (2016), no. 24, 242002, [arXiv:1607.04266](#).
- [101] NNPDF Collaboration, “Parton distributions with QED corrections”, *Nucl. Phys. B* **877** (2013) 290–320, [arXiv:1308.0598](#).
- [102] A. D. Martin, R. G. Roberts, W. J. Stirling, and R. S. Thorne, “Parton distributions incorporating QED contributions”, *Eur. Phys. J.* **C39** (2005) 155–161, [arXiv:hep-ph/0411040](#).
- [103] M. Roth and S. Weinzierl, “QED corrections to the evolution of parton distributions”, *Phys.Lett.B* **590** (2004) 190–198, [arXiv:hep-ph/0403200](#).
- [104] M. Gluck, C. Pisano, and E. Reya, “The Polarized and unpolarized photon content of the nucleon”, *Phys. Lett. B* **540** (2002) 75–80, [arXiv:hep-ph/0206126](#).
- [105] J. Lindfors, “Distribution Functions for Heavy Vector Bosons Inside Colliding Particle Beams”, *Z. Phys. C* **28** (1985) 427.
- [106] R. N. Cahn, “Production of Heavy Higgs Bosons: Comparisons of Exact and Approximate Results”, *Nucl. Phys. B* **255** (1985) 341. [Erratum: *Nucl.Phys.B* 262, 744 (1985)].



- [107] R. Kleiss and W. J. Stirling, “Anomalous High-energy Behavior in Boson Fusion”, *Phys. Lett. B* **182** (1986) 75.
- [108] S. Dawson and S. S. D. Willenbrock, “Heavy Fermion Production in the Effective  $W$  Approximation”, *Nucl. Phys. B* **284** (1987) 449.
- [109] G. Altarelli, B. Mele, and F. Pitolli, “Heavy Higgs Production at Future Colliders”, *Nucl. Phys. B* **287** (1987) 205–224.
- [110] J. C. Collins, “Light cone variables, rapidity and all that”, [arXiv:hep-ph/9705393](https://arxiv.org/abs/hep-ph/9705393).